Using genetic resources to identify favourable alleles for ammonium and nitrate transporter genes that contribute to nitrogen uptake efficiency in wheat

Dissertation

zur Erlangung des

Doktogrades der Naturwisseschaften (Dr. rer. nat.)

der

Naturwissenschaftlichen Fakultät I

-Biowissenschaften-

der Martin-Luther-Universität

Halle-Wittenberg

Vorgelegt

von Herr Bijal Thakkar

geb. 06.08.1988 in Kadi, India

Gutachter

1. Prof. Dr. Nicolaus von Wirén
2. Prof. Dr. Edgar Peiter
3. Prof. Dr. Gerd Patrick Bienert

Halle (Saale), den 18.11.2022

For my beloved mother,

My father

Table of contents

List of Figures

Supplementary Figures

List of Tables

Supplementary Table

Abbreviations

%	Percent
µl	Microliter
µm	Micrometer
µmol	Micromoles
ABA	Abscisic acid
AMT	Ammonium transporters
ATAF	*Arabidopsis thaliana* transcription factors
AXR	Auxin resistance
B	Boron
BLAST	Basic Local Alignment Sequencing Tool
BLASTp	Protein-protein BLAST
bp	basepair
BR	Brassinosteroids
BSK	Brassinosteroid Signalling Kinase
C	Carbon
cDNA	Complementary DNA
CHL	Chloroplastic lipocalin
cm	Centimeter
Cu	Copper
CUC	Cup Shaped Cotyledon
DMSO	Dimethyl sulfoxide
DNA	Deoxyribonucleic acid
dNTP	Deoxyribonucleotide triphosphate
dpi	Dots per inch
DW	Dry weight
FAO	Food and Agricultural Organisation
FP	Forward primer
FW	Fresh weight
GA	Gibberellic acid
ha	Hectares

HATS High Affinity Transport System

HF High fidelity

HLB Hydrophilic lipophilic balanced

HN High nitrogen

Hv Hordeum vulgare

IAA Indole acetic acid

IRMS Isotope ratio mass spectrometry

K Potassium

kg/ha Kilogram per hectare

LATS Low affinity transport system

LB Luria broth

LN Low nitrogen

LRL Lateral root length

LRN Lateral root number

MEGA Molecular evolutionary genetics analysis

mg Milligram

min Minute (s)

ml Milliliter

mM Millimolar

MMT Million metric tons

Mo Molybdenum

MRI Magnetic resonance imaging

MUSCLE Multiple sequence comparison by log- expectation

N Nitrogen

NAC derived from NAM, ATAF, CUC

NAM No apical meristem

ng/mg Nanogram per milligram

NLP Nodule inception-like protein

NPF Nitrate transporter/peptide transporter

NRT Nitrate transporter

NUE Nitrogen use efficiency

NUpE Nitrogen uptake efficiency

NUtE Nitrogen utilization efficiency

ºC Celsius

Os Oryza sativa

P Phosphorus

PCR Polymerase chain reaction

pEPP.CKX Expressed protein cytokinin oxidase

qRT-PCR Quantitative real time polymerase chain reaction

QTL Quantitative trait locus

RDW Root dry weight

RNA Ribonucleic acid

RSA Root system architecture

S Sulfur

SDW Shoot dry weight

Sd Standard deviation

SNP Single nucleotide polymorphism

SPE Solid phase extraction

SRL Seminal root length

SRN Seminal root number

Ta Triticum aestivum

TAE Tris-acetate-EDTA

TAR Tryptophan aminotransferase-related protein

TM Transmembrane helices

TMHMM Transmembrane helices; hidden Markov model

uv Ultraviolet

v/v Volume by volume

Zm Zea mays

Zn Zinc

Summary

Nitrogen (N) is the quantitatively most relevant mineral element for crops, and it is the most important nutrient-related yield-limiting factor worldwide. N is important for plant growth and development, therefore N fertilization is a dominant factor in crop nutrition. The excess use of N fertilizers creates serious problems by N losses to water bodies and the environment, threatening water quality and biodiversity. To overcome this problem, it is mandatory to improve N fertilization management by decreasing N inputs and increasing N use efficiency in agricultural plant production. As winter wheat is a highly N-demanding crop, efficient N uptake, especially during the early vegetative growth phase before winter, is an important trait when breeding for N-efficient winter wheat cultivars.

To exploit the genetic variation in early N uptake efficiency of winter wheat accessions hosted by the IPK genebank and to assess the breeding progress made for this trait during the past decades, a dual approach has been used: In the first step, two winter wheat panels, one comprising 100 recent elite lines (adapted lines) and another comprising 100 cultivars released before the 'green revolution' (unadapted lines), were used to measure N uptake rates. Determining the uptake capacity of double-labeled $^{15}NH_4{}^{15}NO_3$ in hydroponically grown plants allowed distinguishing contrasting lines with lower and higher uptake capacity in both gene pools, varying in N uptake rates by approx. twofold. Examining NH_4^+ and NO_3^- uptake rates separately at micromolar or millimolar N concentrations and under adequate or low N supply, showed that best-performing genotypes differed in dependence of the applied N form and concentration range, making the selection of N uptake-efficient lines more complicated. While ammonium or nitrate uptake rates in the unadapted lines were always in the same range as in the adapted lines, they showed larger biological variation, which may have been caused by lower homogeneity of the seed material in the unadapted lines. Among the adapted lines, the line Tobak showed consistently higher uptake rates than Rockefeller for ammonium under all conditions and for nitrate uptake in the low-affinity range. Quantitative assessment of root traits, incl. the number and average length of seminal and lateral roots, showed that these two lines didn't differ significantly, indicating that physiological rather than morphological root traits were responsible for the superior N uptake capacity in the elite cultivar Tobak.

Since AMT-type ammonium transporters and NRT-type nitrate transporters are known to determine the uptake efficiency for NH_4^+ and NO_3^-, respectively, allelic variation in AMT and NRT genes was assumed to be responsible for the variation in two winter wheat populations. Consequently, 9-12 lines from each panel, consisting of lines with contrasting nitrate and ammonium uptake capacities, were used to re-sequence *AMT1.1*, *AMT1.2* and *NRT1.1*. Using cluster analysis to search for allelic variations causing amino acid substitutions in the coding region allowed identifying up to 16 amino acid substitutions in each of the three genes, whereby the two *AMT1* sequences were more conserved than *NRT1.1*. Based on these amino acid substitutions, haplotype groups were formed and compared for their NH_4^+ or NO_3^- uptake capacity determined before. However, except for the V439I substitution in NRT1.1 that

coincided with higher nitrate uptake capacity, no further relations were found. In an alternative approach for the two AMTs, homology modelling was employed to predict their protein structure, indicating that in some lines AMT1.2 forms an additional beta-sheet. Interestingly, formation of this beta-sheet coincided significantly with an elevated high-affinity uptake capacity for ammonium.

To test the hypothesis that differential expression of *AMT1.1* and *AMT1.2* or *NRT1.1* may have caused differences in ammonium uptake, transcript levels of these genes were determined in a separate experiment. Unexpectedly, all three genes responded weakly to N deficiency and only *AMT1.1* transcript levels in elite lines were slightly upregulated under low N. However, no significant correlation was found that could support a role of *AMT1.1* and *AMT1.2* or *NRT1.1* transcript levels in the uptake efficiency of the corresponding N forms.

In long-term and short-term influx studies, Tobak showed consistently higher N uptake rates than Rockefeller. This advantage of Tobak was neither caused by an altered response of root biomass or architectural traits to N deficiency nor by an altered N nutritional status. While homology-based structural modelling of the AMT proteins showed no difference for AMT1.1, AMT1.2 in Tobak was predicted to form an additional beta-sheet, which coincided with higher ammonium uptake rates across all tested wheat lines. However, transcript levels of both of these transporter genes were not upregulated under N deficiency.

AMT3-type transporter genes were initially not considered of relevance for the ammonium uptake capacity under low N conditions. Unexpectedly, roots of both wheat lines upregulated *AMT3.1* and *AMT3.2* mRNA levels by up to 20-fold after 4 days of N deficiency. In N-adequate roots of both lines, transcript levels were highly similar, whereas with progressing N deficiency upregulation of both genes was significantly higher in Tobak, indicating a higher responsiveness of *AMT3.1* and *AMT3.2* in Tobak. Since transcript levels of both genes correlated significantly with uptake rates, AMT3.1 and AMT3.2 are promising candidates to contribute to a superior uptake efficiency for ammonium under increasing N deficiency. With these newly characterized traits, the present findings contribute to an improved knowledge on genotypical differences in the N uptake capacity of adapted and unadapted wheat lines. They also point to a hidden potential especially in one unadapted wheat line, which exhibited exceptionally high ammonium and nitrate uptake rates, to exploit allelic variation when breeding for N uptake efficiency.

1. Introduction

1.1 Nitrogen fertilization and its effect on planetary boundaries

Nitrogen (N) is essential for life, the main mineral nutrient for crops, and the most important crop yield-limiting factor in the world. It is an essential element for plant growth and development, therefore meeting the crop N demand by N fertilization is mandatory to sustain food production. The world N demand was 110.02 million tons in 2015, with an average annual growth of 1.9%. It is expected to reach more than 118.76 million tons by the end of 2020, whereas the world N fertilizer consumption increased from 112.5 million tons in 2015 to 118.2 million tons in 2019 (FAO, 2016). There are a few countries in the European Union where the average nitrogen use per area of cropland is more than 80 kg/ha; these include Germany (FAO, 2019) (Figure 1.1).

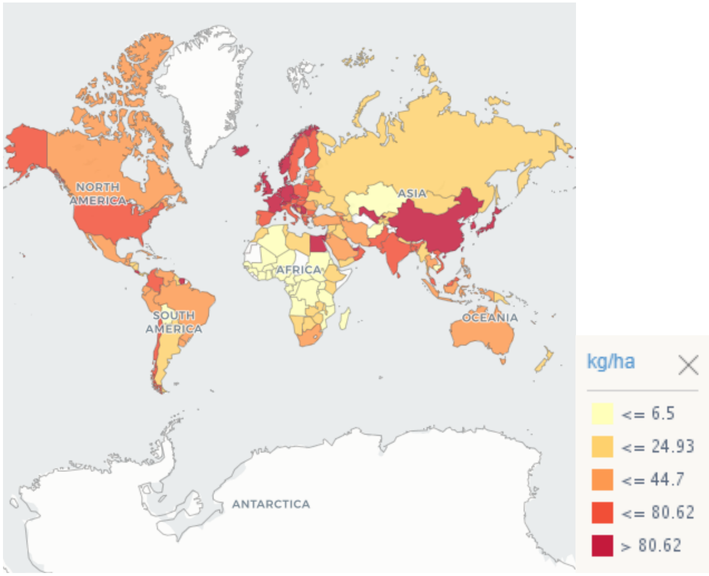

Figure 1.1. Global comparison of the average use of nitrogen per area of cropland (in kg/ha). Figure based on (FAO, 2019).

Generally, ammonium (NH_4^+) and nitrate (NO_3^-) are the major inorganic N sources present in most soils, and besides urea, they also represent the main N forms in fertilizers. while N is taken up throughout the plant's lifecycle, N fertilization at an early growth stage is particularly important for the canopy formation required and high grain yield and at later stages to increase grain protein content (Fueki et al., 2015). When supplied with a N source containing 25% NH_4^+, the N uptake capacity in wheat increased by 35% when compared with all N being supplied as NO_3^- (Raun & Johnson, 1999)

Furthermore, because of its lower potential to cause leaching or denitrification losses and its higher stability when adsorbed to the soil matrix, NH_4^+ is also a favourable N source for uptake during the plant's reproductive phase, i.e. anthesis and grain filling (McGuire et al., 1998). Due to its reduced oxidation state, the assimilation of NH_4^+ in plants requires only 25% of the total energy consumed during nitrate assimilation. The energy saved during this process may lead to a higher biomass of the plant when the plants are solely supplied with NH_4^+ (Bloom et al., 1992).

High fertilizer inputs provoke cereal crops with long stems and large grain biomass that are more susceptible to lodging. To overcome the issue of lodging, wheat breeders developed cultivars with short and stiff straw, which are better adapted to intensive agriculture. The application of N fertilizers has increased drastically after the Green Revolution because high-yielding cultivars respond to elevated N supplies with elevated grain yield (Hawkesford, 2014). In Middle Europe, it is estimated that approx. 150 kg/ha of N fertilizer is required to produce 6 to 9 tons/ha of high-quality yield. Although wheat is having a large demand for N, an estimate from a global report suggests that only 33% of applied N fertilizers are harvested with the grain, which represents a huge waste of valuable resources (Raun & Johnson, 1999).

The effect of excess fertilizer use and emission of reative N into the environment along with other factors is having a serious impact on planetary boundaries. The planetary boundary concept relates to earth system processes, which are restricted by natural or environmental boundaries. According to the model proposed by Rockström (2009) crossing one or more planetary boundaries may be deleterious or even catastrophic due to the risk of crossing critical thresholds, which trigger a non-linear, abrupt environmental changes at a continental or planetary scale. The planetary boundary framework provides a paradigm from science-based analysis of the risk that human perturbation will destabilize the earth system at a planetary scale. As of today, four out of nine planetary boundaries have already been crossed because of human activity, which includes climate change, loss of biosphere integrity, land system change, and altered biogeochemical cycles, including those of P and N.

The major anthropogenic perturbation of the N cycle arises from fertilizer production and application, as regions with higher N application rates are the leading contributors for the transgression of the biogeochemical cycle boundary (Kahiluoto et al., 2014). Nitrogen emissions in the form of ammonia, nitrogen oxide, and nitrous oxide contribute to a large extent to global climate change. Excess nitrate runoff from agricultural soils, from industries as well as intentional biological N fixation contribute to eutrophication of aquatic systems and may result in oxygen depletion of the water bodies. In EU legislation, the maximal acceptable NO_3^- level in freshwater is 50 µg/l, which isn't achieved in many agricultural areas in Middle Europe, often because of excess organic manure inputs and N-containing disposal from animal farming industry. To overcome this problem it is highly needed to improve N use management by decreasing N inputs and increasing nitrogen use efficiency (NUE) in agricultural production systems, by developing and using wheat genotypes with higher NUE.

1.2 Wheat production and its economic importance

In the world, wheat (*Triticum aestivum* L) is the second most widely grown crop with an estimated surface of over 200 million ha. It is one of the most domesticated cereal crops and serves as a major staple food. Wheat grain is rich in carbohydrates and has a higher protein content than many other cereal crops like maize, rice, fox millet, and barley combining a substantial level of minerals (e.g. Zn, Fe) and vitamins, making it a good source of nutrition (Hawkesford, 2014, 2017). Approx. 40% of produced wheat is used to feed poultry and livestock whilst wheat grains account for 19% of the calories in the global human diet (Zörb et al., 2018). Regarding the global wheat production by countries, European Union member countries are the largest producer over the last 10 years, between 2019 and 2020 more than 154.5 million metric tons of wheat has been yielded (Shahbandeh, 2021). Approximately 95% of the global wheat crop is hexaploid bread wheat (*Triticum aestivum* L.; genomic constitution AABBDD), whereas the remaining includes tetraploid durum wheat (*Triticum turgidum* L. AABB) and other wheat types of smaller economic importance.

1.3 Unadapted and adapted wheat germplasm

The IPK genebank has over thousands of wheat accessions, including unadapted lines (released before the 'Green Revolution') and adapted lines (elite lines representing modern cultivars mostly released after the 'Green Revolution'). The improved breeding process within the Green Revolution was initiated after the 1960s and achieved higher grain yield by the introduction of dwarf alleles (*rht* lines) (Peng et al., 1999; Hedden, 2003; Saville et al., 2012). Varieties carrying the *rht* gene locus are shorter in height (Figure 1.2) and utilize large inputs of applied nitrogen much better. Most of these *rht* loci represent mutations in transcription factors that target components of the gibberellin acid (GA) signalling pathway, which regulates the GA response. GA is a tetracyclic diterpenoid acid that acts as a hormone for the onset of flowering and pollen development, as well as a key determinant of cell elongation and therefore plant height. Reduced height (*rht*) loci extremely boosted assimilate partition to growing spikes of wheat (Abbate et al., 1998; Fischer, 2007; Foulkes et al., 2007). In this time, grain yield traits were extensively enhanced due to more assimilates being designated to the spikes (Fischer, 2011; Foulkes et al., 2011a). This leads to wheat plants that are shorter in height and have a higher harvest index. The Green Revolution led to a doubling of worldwide produced grain within a few decades, while it took almost 1000 years for humans to achieve such a doubling before.

Figure 1.2. Tall unadapted wheat lines before the “Green Revolution” (left) and adapted high-yielding lines after the ‘Green Revolution’ (right). Figure based on (Voss-Fels et al., 2019).

Over several decades of observations, breeders selected best-adapted lines based on their productivity, uniformity, and quality. In recent days, adapted lines became more differentiated with respect to disease resistance, fertilizer use efficiency, and grain quality or yield potential (Foulkes et al., 2011b; Hawkesford, 2017; Zetzsche et al., 2020). Unadapted lines are stored in several genebanks to safeguard the rare alleles that will be useful for crop plant improvement (Hao et al., 2020). The option of utilizing rare alleles from unadapted germplasm is required to avoid intensive and time-consuming selection of uneconomically large breeding populations (Reynolds et al., 2021). Potential linkage drags can be broken using QTL mapping or marker-based selection. Such approaches have been largely expanded for hexaploid wheat (X. Q. Huang et al., 2003, 2004; S. Liu et al., 2006), rice (Xiao et al., 1998), and tomato (Tanksley et al., 1996).

1.4 Ways to improve nitrogen use efficiency without compromising grain yield

Nitrogen use efficiency is defined in various ways, based on the applied situation. NUE is defined as the ratio of dry shoot biomass or grain biomass to the total amount of N being available in the soil (Moll et al., 1982; Weih et al., 2018). NUE comprises of two key components: N uptake efficiency (NUpE), which defines the amount of N taken up by the plant relative to the amount of N available in the soil, and N utilization efficiency (NUtE), which defines the shoot or grain biomass formed per unit N in the plant (Han et al., 2015). However, the above-stated definition needs to be modified in the case of unadapted wheat lines with a low harvest index, where the definition of total biomass production per unit of N taken up is more appropriate. Theoretically, improving NUE can be attained by improving either NUpE, NUtE, or both. NUE is an extremely complex trait with various interactions among genetic and environmental effects (Xu et al., 2012). Factors determining NUE may vary at each stage of plant development so that overall NUE represents an integration of all NUE-related processes during the course of plant development (Figure 1.3).

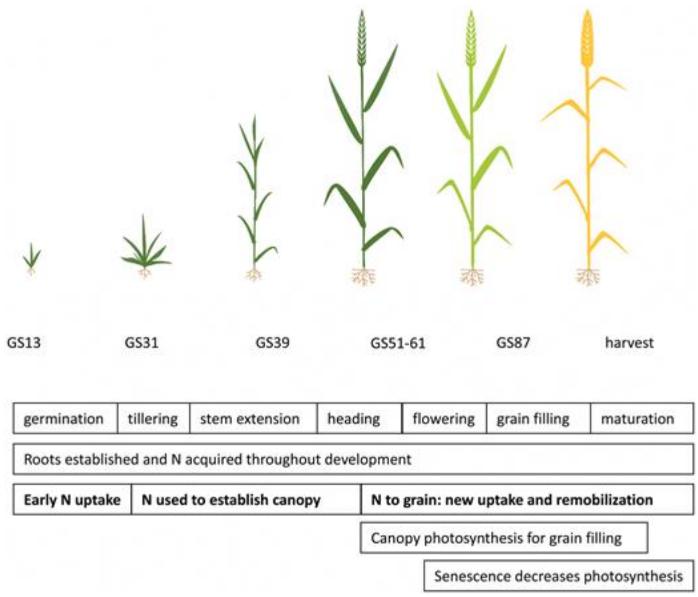

Figure 1.3. Nitrogen use efficiency key stages in the development of wheat. Critical processes for N acquisition and allocation from germination to maturation stage are mentioned in boxes. Figure based on (Zadoks et al., 1974).

Nowadays, the selection of NUE traits is mostly performed under high N inputs. However, this selection process may have lead to the loss of other relevant traits that gain importance under low N input. At a certain point, the application of higher N leads to a negative effect on grain yield and an incremental increase of N leaching, which decreases NUE (Figure 1.4; Hawkesford, 2012).

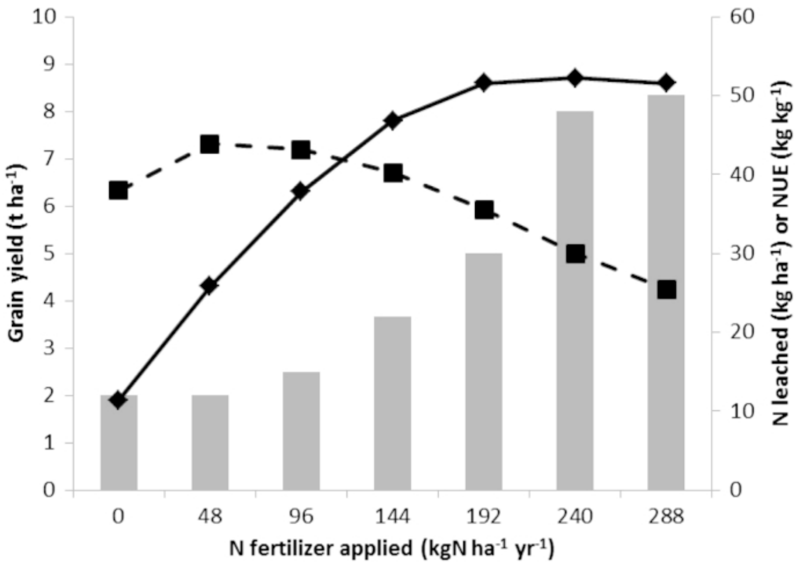

Figure 1.4. Response of grain yield and N leaching to increasing N fertilizer doses in winter wheat. Grain yield (solid line), N losses (bar chart), and grain nitrogen use efficiency (dashed line). Figure based on (Hawkesford, 2012).

Achieving higher yield without increasing the amount of applied N or by reducing the N requirements will enhance NUE. Higher yields with fewer N inputs can be achieved by optimizing individual plant traits. Although this may be a simplistic view, it is worth looking at the final impact of each trait on yield when breeding for NUE (Lammerts van Bueren & Struik, 2017).

1.5 Relevant traits for the improvement of nitrogen uptake efficiency

1.5.1 Root morphological traits and phenotyping

Plant roots are of key importance for grain productivity as they drive water and nutrient uptake (Ehdaie et al., 2012; Palta & Yang, 2014; Sharma et al., 2009; Shen et al., 2013). Hence, improving root morphological traits in breeding programs is a promising strategy to increase nutrient acquisition. The results of QTL studies for N uptake and root traits also suggest that breeding crops with efficient root systems can maximize N uptake, which is an important goal in breeding (Atkinson et al., 2015). In crop breeding programs, the selection of root morphological traits depends on various components of root system architecture (Lynch & Brown, 2012). RSA is composed of individual root traits, including root length, seminal root number, lateral root number or length, number and length of root hairs etc. Deep and narrow root systems provide opportunities to take up more N from deeper layers of the soil than those with small and shallow root systems (Garnett et al., 2009). Regarding the available N sources, the local availability of nitrate and ammonium appears to have complementary effects on lateral root development, because ammonium stimulates lateral root branching, whereas nitrate stimulates lateral root elongation (Jia et al., 2022) (Figure 1.5). In general, root depth depends on soil texture, structure, nutrition, and depth of available groundwater (Barraclough et al., 1991). Additionally, plants with higher root surface area (e.g. lateral roots and root hairs) can take up more N than plants with inadequate root systems (Gahoonia et al., 2007; Liao et al., 2004). To acquire sufficient N, plants advance root length density to seek for N in a greater soil volume and enhance N uptake (Liu et al., 2009), whereas deep rooting enables plants to take up residual N from the subsoil (Barraclough et al., 2010). Although RSA is crucial for nutrient and water uptake, there is only a limited number of studies conducted on root morphological traits and their spatial arrangement, which might be due to technical difficulties when studying below-ground plant traits including their interactions with the environment (Liu et al., 2018).

Wheat as a monocot species forms a root system that consists of seminal roots and adventitious or nodal roots. Depending on the genetic background and environmental conditions, there is high plasticity in the RSA of a plant (Giehl et al., 2014). In wheat root length and biomass have been shown to have a strong correlation with N uptake suggesting a major contribution of those two traits towards the efficiency of N uptake (Bowman et al., 2002; Brady et al., 1993).

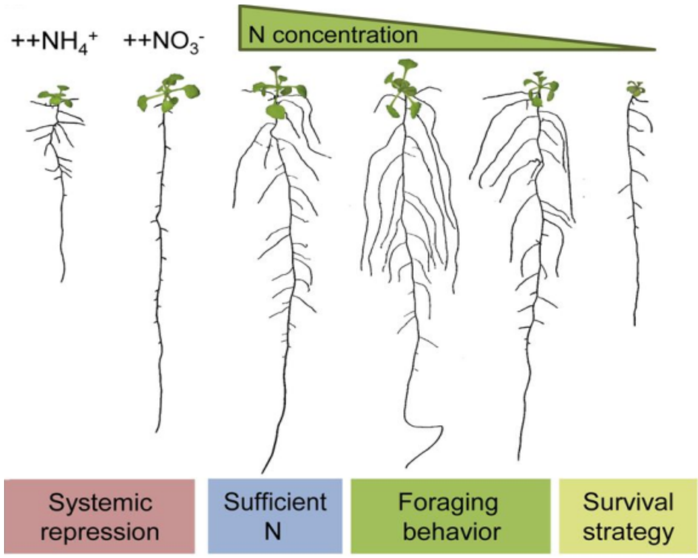

Figure 1.5. The development of root morphological traits is dependent on supplied nitrogen. Figure taken from (Giehl & von Wiren, 2014).

Current methodological developments to explore RSA have resulted in several different root phenotyping platforms that operate under various conditions such as laboratory, greenhouse, or field conditions (le Marié et al., 2019; Trachsel et al., 2011). RSA phenotyping systems require controlled growth conditions, automated root imaging systems, and software tools. The images of the root can be obtained with or without destruction of roots depending on the imaging technology and growth conditions that are used for the experimental purpose. Using agar gel-based growth conditions may give visible images, while the root behaviour cannot be directly compared to that of plants grown in soil. In contrast, the root systems of soil-grown plants cannot be accurately imaged as long as roots need to be uplifted and become destructed. Although there are techniques for nondestructive imaging of roots in soils, such as magnetic resonance imaging (MRI) or X-ray-based imaging platforms, these are quite expensive approaches that mostly deal with a lower number of replicate plants in small-scale experiments (Fiorani & Schurr, 2013). In this context, plants grown in hydroponic culture, in which the root system can be separated, imaged, and analyzed, are easier to monitor and subject to quantitative analysis of the RSA.

1.5.2 Nitrogen uptake capacity

Nitrogen uptake capacity is another key trait underpinning NUE. N uptake varies greatly among varieties depending on the forms of N used in the cropping system and the strategies used for N application in terms of timing and fertilizer doses. N uptake capacity also depends on crop development and plant age. In particular energy supply to roots is of utmost importance to sustain high N uptake capacities. While assimilate provision to roots is usually high during the vegetative growth phase, it decreases during generative plant growth. This makes post-anthesis N uptake a critical factor for overall NUpE (Kichey et al., 2007).

During plant growth, roots take up N from agricultural soils mainly in the form of nitrate and ammonium and to some extent as organic N in the form of urea or amino acids.

Since N forms vary greatly in the soil, plants have developed a large variety of sensing mechanisms and uptake systems to bring these different N forms into root cells (Dechorgnat et al., 2011; Masclaux-Daubresse et al., 2010). Uptake of almost every different N form is catalyzed by one of the more isoforms of membrane transporters that reside in the plasma membrane and belong to separate protein families (Garnett et al., 2013; Williams & Miller, 2001).

1.6 High- and low-affinity transport systems for ammonium and nitrate

In agricultural and most natural soils, the soluble N forms ammonium (NH_4^+) and nitrate (NO_3^-) are the major N sources for root uptake. The ammonium ion (NH_4^+) deprotonates in alkaline solutions to volatile ammonia (NH_3) with a pKa = 9.25. Thus, the ratio of ammonium to ammonia in solutions depends on the pH value (Figure 1.6). In plant cells, the ammonium cation dominates because of the neutral pH in the cytosol (Schjoerring et al., 2002). Indeed, the roots of most plants prefer to take up ammonium compared to nitrate when supplied at the same concentrations (Eppley et al., 1969).

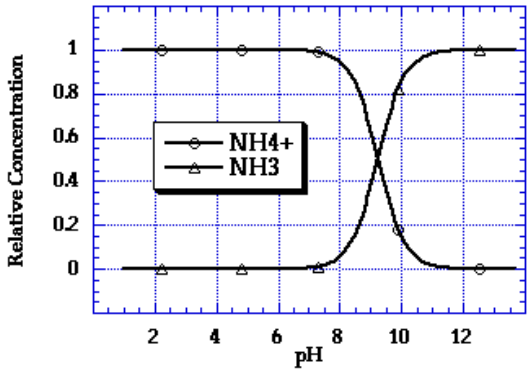

Figure 1.6. The relative concentration of ammonium and ammonia is dependent on pH. In acidic solutions, ammonium ion is the predominant species, whereas ammonia is dominant at alkaline pH. Figure based on (McCarty, 1978).

In roots, ammonium acquisition is mediated by at least two transport systems, i.e. high-affinity and low-affinity transport systems (HATS, LATS; Kronzucker et al., 1996). The contribution of each system depends on the external ammonium concentration. NH_4^+ ions are absorbed through membrane-bound proteins of the ammonium transporter (AMT) family (Figure 1.7). They constitute the high-affinity transport system that operates under low N conditions, with a Km in the µM range whilst a low-affinity transport system (LATS) is predominant when N concentrations in the medium are high, with an affinity (Km value) in the mM range (Loqué and von Wirén, 2004).

Also, nitrate is transported across cellular membranes by specific membrane proteins (Figure 1.7). Nitrate uptake into the root cells is proton-coupled, so H^+-ATPases are required to provide the energy for nitrate transport (Crawford & Glass, 1998; Forde, 2000, 2002). In roots, several distinct types of nitrate transport systems have been identified, including inducible and constitutive high-affinity transport systems (iHATS and cHATS) for nitrate as part of the high-affinity transport system (Forde, 2000; Thornton, 2004).

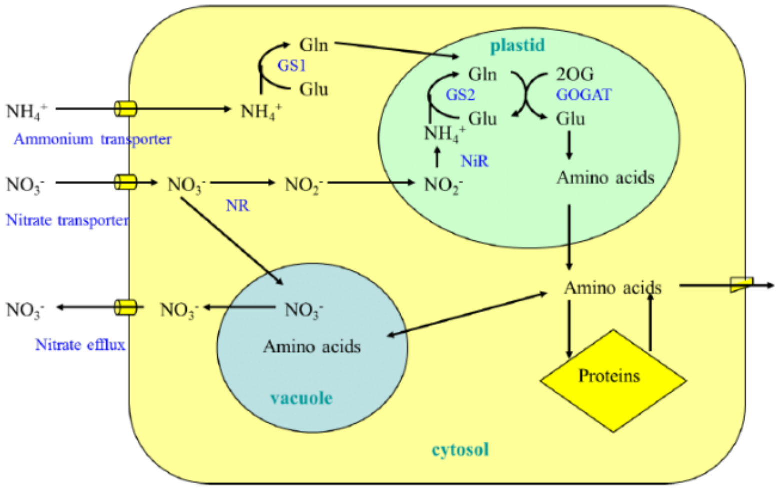

Figure 1.7. Simplified scheme for the absorption and metabolism of ammonium and nitrate in the plant cell. Figure based on (Ohyama et al., 2013).

1.6.1 High- and low-affinity transporters of ammonium

Ammonium is an important N nutrient. At low dosages it promotes plant growth and root system architecture, whereas at high dosages it results in toxicity like stunted growth, leaf chlorosis, and poor root development (Y. Liu & von Wirén, 2017a).

Following the first identification of an ammonium transporter gene in *Saccharomyces cerevisiae*, AMT-type ammonium transporter genes were identified in several plant species including *Arabidopsis thaliana* (Ninnemann et al., 1994; Gazzarrini et al., 1999; Sohlenkamp et al., 2000, 2002; Loqué and von Wirén, 2004; Yuan et al., 2007, 2009) and wheat (T. Li et al., 2017). In general, AMT-type transporters mediate ammonium transport preferably at micromolar external ammonium concentrations, although there are two subfamilies with one or several AMT isoforms that can differ in their substrate affinity (Loqué and von Wirén, 2004; Yuan et al., 2007). At higher external concentrations, NH_4^+ uptake is mediated by non-selective cation channels or potassium (K^+) channels, such as AKT1 (Straub et al., 2017).

In Arabidopsis, five members of the *AMT1* and *AMT2* subfamilies have been found to be expressed in roots, among which AMT1;1, AMT1;3 and AMT1;5 are localized at the plasma membrane of epidermis cells including root hairs and cortex cells, whilst AMT1;2 is localized at the endodermis and in mature roots zones in cortex cells (Yuan et al., 2007a; Hao et al., 2020). These transporter isoforms differ in both, cell type-specific expression and transcriptional regulation, allowing to assign slightly different physiological functions in ammonium uptake (Duan et al., 2018). Ammonium enters the root cells via the symplastic route mainly mediated by AMT1;1, AMT1;3 and AMT1;5 which operate at different substrate affinities (Km ~50, 60 µM and 5 µM, resp.), whereas ammonium that bypasses these transporters through the apoplastic route may ultimately enter the root symplast via AMT1;2 that operates at lower affinity (Km ~230 µM) (Figure 1.8). Once in the root stele, ammonium can be loaded into the xylem by AMT2;1 which contributes to high ammonium availability in pericycle cells and in the xylem sap (Giehl et al., 2017).

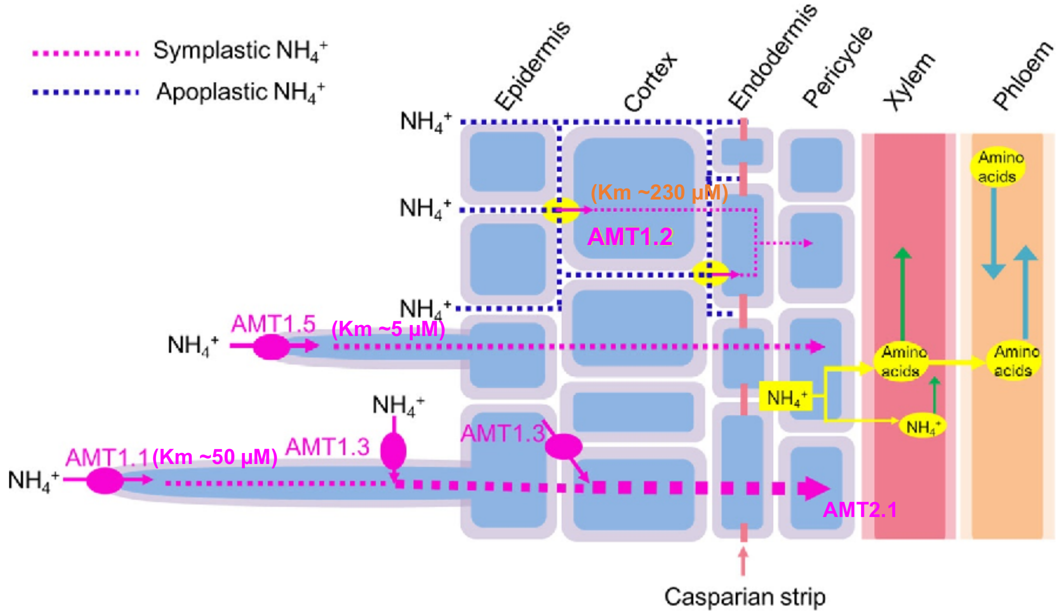

Figure 1.8. Model representation of the functions of AMT-type transporters in high-affinity ammonium uptake and xylem loading in plant roots. Figure based on (Yuan et al., 2007; Giehl et al., 2017).

AMTs are regulated at the transcriptional, post-transcriptional and post-translational levels. For instance, *AtAMT1;1* transcripts are subject to N-dependent mRNA degradation (Yuan et al., 2007). On the other hand, AMTs are regulated at the protein level by phosphorylation. In general, AMT1 transporter proteins form a trimeric complex in the plasma membrane (Loqué et al., 2007). In Arabidopsis, NH_4^+-mediated phosphorylation has been found to inhibit transporter activity by phosphorylation of T460 that is located in the cytosolic tail of AMT1;1 (Loqué et al., 2007; Lanquar et al., 2009). Considering physical interactions between AtAMT1;1 and AtAMT1;3, phosphorylation of one isoform can also trans-inactivate the other isoform as these two isoforms assemble in heterotrimeric complexes (Loqué et al., 2007; Yuan et al., 2013).

In rice, the expression of *AMT* genes also strongly depends on external N supply and the internal N status as e.g. *OsAMT1;1* and *OsAMT1;2* are up-regulated in response to NH_4^+, whereas *OsAMT1;3* is up-regulated by N deprivation (Kumar et al., 2003; Sonoda et al., 2003). Also, the overexpression of *AMT1;1* appeared to enhance NH_4^+ uptake under N-fertilized growth conditions (Ranathunge et al., 2014). In wheat, a large number of *AMT* genes has been identified, that appears closely associated with N starvation tolerance (Li et al., 2017), and a large number of genes are orthologous to rice, maize, barley, and Arabidopsis (Bajgain et al., 2018). Two wheat *AMT* genes, *TaAMT1.1*, *TaAMT1.2* have been confirmed to mediate the transport of ammonium (Søgaard et al., 2009).

1.6.2 High- and low-affinity transporters for nitrate

In higher plants, there are two types of nitrate transport systems (*NRT1* and *NRT2* families) that have been identified to take up nitrate from the soil and transport it to the plant (Daniel-Vedele et al., 1998; Tsay et al., 2007). The low-affinity transport system is encoded by transporters of the NRT1 protein family while the high-affinity system is encoded by the NRT2 protein family (Figure 1.9). Based on homologous sequences from dicots, several *NRT* gene family members have also been identified in monocots (Plett et al., 2010).

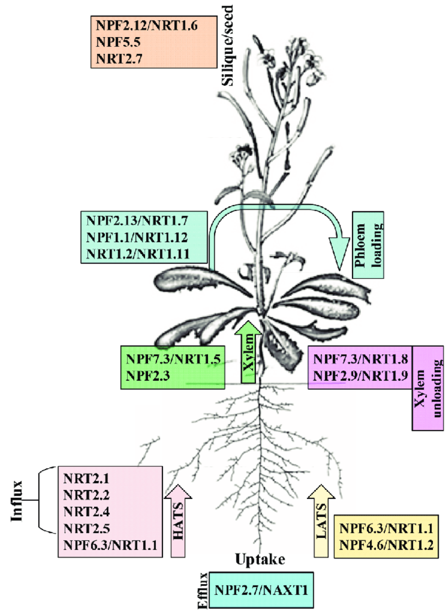

Figure 1.9. Nitrate transporters and their functions in uptake, transport, allocation, and seed development in Arabidopsis. Figure taken from (Iqbal et al., 2020).

In Arabidopsis, the *NRT1* family consists of 53 members, and the *NRT2* family contains 7 members. Among them, *AtNPF6.3/AtCHL1/AtNRT1.1*, a dual affinity transporter that participates in both low- and high-affinity nitrate uptake (Liu et al., 1999a) and also acts as a transceptor, additionally controls auxin accumulation in lateral root tips and regulates lateral root emergence under N starvation (Xuan et al., 2017). (Guo et al., 2003; Krouk et al., 2010) observed that *NRT1.1* does not transport only nitrate but also facilitates the auxin uptake and also supports stomatal opening. The dual action of *NRT1.1* is regulated by phosphorylation of threonine 101. It has been found that, when phosphorylated, NRT1.1 acts in the high-affinity mode but when de-phosphorylated acts as low-affinity transporter (Liu and Tsay, 2003). *NRT1.2* is a low-affinity transporter that is expressed mainly into the epidermis of young and mature roots and also in root hairs (Huang et al., 1999).

In Arabidopsis, the high-affinity nitrate transport system relies on the activity of the *NRT2* proteins, which operate when the external concentration of nitrate is low (Williams & Miller, 2001). *AtNRT2.1*, *AtNRT2.2*, and *AtNRT2.4* are involved in high-affinity nitrate uptake (Wang et al., 2012). *AtNRT2.4* is considered a very high-affinity transporter and its expression is stimulated by N starvation (Kiba et al., 2012). *NRT2.1* and *NRT2.2* are involved in nitrate import from the apoplast into cortex and endodermis cells (Iqbal et al., 2020) while *NRT2.5* and *NRT2.4* are expressed in shoots and help in phloem loading of nitrate (Lezhneva et al., 2014).

In rice, *OsNRT1* is the closest homolog to *AtNRT1.1*, and has been characterized as a low-affinity NO_3^- transporter which is expressed in the root epidermis (Lin et al., 2000). A single nucleotide polymorphism of *OsNRT1.1B* that differs between Indica and Japonica rice determines nitrate uptake capacity. Also, higher expression of

OsNRT1.1B enhances NUE by improving sensing, absorption, and accumulation of NO_3^- in the grains (Hu et al., 2015). Likewise, higher expression of *NRT2.1* under nitrogen starvation conditions impacted nitrate uptake capacity (Okamoto et al., 2003).

Homologous members to *OsNRT1* and *AtNRT1.1* also exist in wheat. Wheat NRT proteins are mainly divided into three subfamilies: NRT1, re-named as NPF (NRT1/PTR family), NRT2 (high-affinity transporters) and NRT3 (previously named as NAR (Bajgain et al., 2018). *TaNRT1* expression is strongly induced by NO_3^- provision while transcript levels of *TaNRT2.1* are upregulated in low N treatments but decrease with increasing NO_3^- supply (Yin et al., 2007). Another study in wheat by (He et al., 2015) has shown that TaNAC2-5A, a key transcription factor, regulates the expression of *TaNRT2.1* and controls N uptake in wheat. Overexpression of TaNAC2-5A increased growth, yield, and the N harvest index.

Apart from transporters, also transcription factors regulating the expression of nitrate and ammonium transporters play an important role in NUE. For instance, ZmNLP6 and ZmNLP8, which are maize homologs of AtNLP7, have been identified to play a vital role in nitrate signalling, promoting plant growth and yield under N-deficient conditions. This suggests that they are involved in NUE in maize (Cao et al., 2017). Also in wheat, TaNFYA1-6B, MYB-, and bZIP-type transcription factors have been identified, which are expressed in roots and shoots and stimulate lateral root branching, N uptake and promote higher grain yield (Zhang et al., 2012; Hu et al., 2015; Ma et al., 2020).

1.7 Nitrogen sensing and signalling

Ammonium and in particular nitrate have been shown to act as signalling molecules triggering a wide range of molecular, physiological, and developmental processes (Liu & von Wirén, 2017b; Vidal et al., 2020). The overall molecular signalling network includes transporters, transcription factors, calcium-sensing proteins, phosphatases and kinases that together regulate the expression of NRT genes or the activity of the corresponding proteins.

Several responses to N are mediated via calcineurin-B like interacting protein (CIPK), calcium binging proteins (CBL), and phytohormone signalling pathways, including gibberellins (GA), cytokinins, auxin (IAA), and ABA. For the regulation of *AMT1;1* and *AMT1;2*, CIPK23 plays an important role (Straub et al., 2017). Likewise, the interaction of CBLs and CIPK23 regulates nitrate uptake in plants (Ho et al., 2009). Publicly available transcriptome data (e.g., TAIR, Genevestigator) indicate that CIPK23 and CIPK15 are expressed in the same tissue where *AMT1;1* is expressed. This also holds true for *NRT1;1*. CIPK23 is the kinase that also modulates NRT1.1 affinity. At high nitrate concentrations, nitrate is imported by NRT1.1 in its non-phosphorylated state whilst at low concentration, When CBL1 or CBL9 is activated, it interacts with CIPK23 to phosphorylate NRT1.1 for high-affinity nitrate transport (Sun & Zheng, 2015).

1.8 The role of phytohormones in regulating root growth

Phytohormones like gibberellins (GA), cytokinin, auxin, and abscisic acid (ABA), regulate and influence plant growth, root system architecture, and the development of higher plants according to growth conditions. Decreased levels of GAs lead to dwarfism whilst exogenous GA treatment can restore normal plant growth of GA-dwarfed mutants (Chen et al., 2014; Plackett et al., 2012) and enhance N use efficiency under certain growth conditions (Bai et al., 2013). Plant growth can also be promoted by stimulating the degradation of DELLA proteins that repress growth via GA signalling (Harberd et al., 2009). Particularly dwarfism in rice and wheat was a major reason for boosted global food production during the “green revolution”.

Cytokinins (CK) regulate root system architecture (RSA) and the expression of N uptake- and assimilation-related genes. NO_3^- supply induces an increase in CK content in the xylem, due to the induction of a key gene in CK biosynthesis, adenosine phosphate-isopentenyl transferase (Sakakibara et al., 2006). CK also functions as a root-to-shoot long-distance signal in response to NO_3^- supply (Krouk et al., 2011; Ruffel et al., 2011). In Arabidopsis roots, external application of CK downregulates two *AtNRT2* genes (*AtNRT2.1* and *AtNRT2.3*) as well as three ammonium transporter (*AtAMT1;1, AtAMT1;2, AtAMT1;3*) (Brenner et al., 2005; Kiba et al., 2005; Sakakibara et al., 2006; Yokoyama et al., 2006).

Indole-3-acetic acid (IAA) influences the formation of primary and lateral roots, root apical meristem formation, root vascular differentiation, and the development of lateral roots. Importantly, IAA is necessary at all the stages of lateral root development, i.e., initiation, emergence and elongation (Jung & McCouch, 2013). Furthermore, there are reports from mutants or transgenic lines with higher IAA biosynthesis that have increased root branching (Shao et al., 2017). Depending on the N supply the auxin concentration varies in the plant. For instance, low nitrate availability increases shoot-to-root transport of IAA, which results in higher IAA concentrations in roots (Dong et al., 2018; W. Ma et al., 2014).

Besides auxin and cytokinin, brassinosteroids (BR) are a group of plant-specific steroid hormones that participate in root elongation under mild N deficiency (Jia et al., 2019) and additionally interact with other hormones such as auxin, cytokinin, and ethylene (Jia et al., 2022). Previous reports have suggested that the interaction between auxin and brassinosteroids is relevant for hypocotyl elongation, vascular bundle development, and root development (Tian et al., 2018). These examples show how hormones and related genes serve as endogenous mediators between internal or environmental signals and plant growth.

1.9 Aim of the thesis

The amendment of the German fertilizer regulation foresees a substantial decrease of the N surplus in a 3-years crop rotation. As rapeseed, which produces the largest N surplus in German crop rotations, is often the precedent crop to winter wheat, there will be an enhanced pressure on decreasing or omitting N fertilizer applications to winter wheat in autumn. Moreover, cutting N fertilization to crop residues after harvest will increase the risk of N immobilization, which additionally decreases N availability to winter wheat in the early growth period before winter. Therefore, efficient N uptake before winter, i.e. before and during tillering, will become an important trait when breeding for N-efficient winter wheat cultivars.

To exploit the genetic variation of the IPK genebank material in early N uptake efficiency a dual approach has been used. Since AMT-type ammonium transporters and NRT-type nitrate transporters are known to determine the uptake efficiency for NH_4^+ and NO_3^-, respectively, allelic variation in AMT and NRT genes has been explored in two winter wheat populations. One population represents elite (adapted) material, while the other represents IPK genebank material from the era before the "Green Revolution" (unadapted). From each population of approx. 100 lines, several genes of the AMT and NRT gene families have been cloned and sequenced for phylogenetic and cluster analysis to search for allelic variations causing amino acid substitutions in the coding region. Individual lines representing groups of allelic variation have been comparatively analysed for NH_4^+ and NO_3^- uptake efficiency using ^{15}N-labeled N forms in hydroponic experiments. This approach was inspired by the successful identification of allelic variations in the nitrate transporter NRT1.1 in rice, which significantly contributes to N uptake efficiency (Hu et al., 2015)

In the first part of the thesis, the two wheat populations have been screened for N uptake efficiency in hydroponics. Then, contrasting lines with comparable growth behaviour were subjected to refined short-term (6 min) and long-term (60 min) uptake studies, in which ^{15}N-labelled NH_4^+ or NO_3^- was supplied in the high-affinity (200 µM) or low-affinity (2 mM) range to plants precultured under adequate or deficient N supply. Since contrasting lines may not only differ in physiological traits relating here mostly to N uptake capacity but also to morphological traits, changes in root system architecture in dependence of the N preculture were also examined.

In the second part of the thesis, lines with different uptake capacities for nitrate or ammonium were compared for divergence in *AMT* and *NRT* gene sequences as well as in *AMT* and *NRT* gene expression levels. These analyses were built on a re-sequencing approach together with homology modelling of transport protein structures and on gene expression analyses.

2. Materials and methods

2.1 Plant material

In the frame of the GeneBank 2.0 project (website) 200 winter wheat (*Triticum aestivum* L.) lines were selected to generate two panels. One population represented elite material (adapted, dwarfed lines), while the other represented germplasm from the IPK Genebank originating or released from the era before the "Green Revolution" (non-adapted and non-dwarfed lines). The acquisition date and country of origin of all lines are listed in Supplementary Table 1.

2.2 Plant culture

Wheat seeds were surface sterilized using 0.1 % (v/v) Previcur®Energy (Bayer AG) and placed on a vertical plate covered by wet tissue paper to provide optimum moisture conditions. Seeds were stratified at 4°C in a dark climate-controlled room for 4 days. After stratification, seeds were transferred into plastic trays containing wet vermiculite and kept on the floor of a growth chamber. To reduce exposure to high light intensity, the trays were kept on the floor and everyday seeds were sprayed with water. After one week, uniformly germinated seedlings were washed under running tap water to remove vermiculite particles from roots.

Seedlings were pre-cultured for 2 days in half-strength nutrient solution and then placed on full-strength nutrient solution containing 1 mM NH_4NO_3, 0.5 mM K_2SO_4, 0.5 mM $MgCl_2$, 0.1mM KH_2PO_4, 2 mM $CaCl_2$, 1 µM H_3BO_3, 0.5 µM $MnSO_4$, 0.5 µM $ZnSO_4$, 0.2 µM $CuSO_4$, 0.01 µM $(NH_4)_6Mo_7O_{24}$, and 0.15 mM Fe-EDTA. Plants were grown hydroponically under non-sterile conditions for 10 days in a growth chamber under the following conditions: 16h of day and 8h of night; the light intensity of 250 µmol photons $m^{-2}\ s^{-1}$ at 20ºC during the day and 18ºC during the night; 70% relative humidity. The nutrient solution was aerated and changed after every other day.

2.3 Screening for nitrogen uptake-efficient lines

To determine the nitrogen uptake capacity, each wheat line was pre-cultured hydroponically for 10 days on a full nutrient solution and then transferred for 2 days on an N-deficient nutrient solution. For ^{15}N uptake studies, the whole root system was dipped first in 1 mM $CaSO_4$ solution for 1 min before plant roots were transferred to fresh N-free nutrient solution containing 200 µM double-labeled $^{15}NH_4{}^{15}NO_3$ (98 atom% ^{15}N) for a period of 1 h. Then, roots were rinsed again in 1mM $CaSO_4$ solution for 1 min. Plants were separated into roots and whole shoots to record fresh weights and stored at -20ºC. All tissue samples were freeze-dried, weighed, and approx. 1.4 to 1.7 mg finely ground powdery material was used for ^{15}N determination by isotope ratio mass spectrometry (Horizon, NU instruments). The entire screening approach was divided into 7 experiments run under the same growth conditions and representative results are shown.

^{15}N uptake capacity and root-to-shoot translocation were calculated using the following formulas:

$$^{15}N \text{ uptake capacity} = \left(\frac{(^{15}N \text{ in root}) + (^{15}N \text{ in shoot})}{RDW \times 1h}\right)$$

$$\text{Root-to-shoot translocation capacity of N} = \left(\frac{^{15}N \text{ in shoot}}{RDW \times 1h}\right)$$

Unit = µmoles g^{-1} root DW h^{-1}

SDW indicates shoot dry weight, RDW indicates root dry weight.

2.4 $^{15}NH_4^+$ or $^{15}NO_3^-$ uptake analysis on N-sufficient or N-deficient plants

For determining ammonium and nitrate uptake capacity, 12 adapted and 10 non-adapted contrasting lines from the initial screening approach were pre-cultured hydroponically for 10 days on full nutrient solution. After 10 days, half of the plants from each line was continued to grow on full nutrient solution for 2 days, whereas the other half was transferred to N-deficient nutrient solution. N-deficient and N-sufficient plants were used to determine the high-affinity uptake capacity of ammonium (using 100 µM $^{15}(NH_4)_2SO_4$) or nitrate (using 200 µM $K^{15}NO_3$) and for low-affinity uptake capacity using either 1 mM $^{15}(NH_4)_2SO_4$ or 2 mM $K^{15}NO_3$, following the same protocol as described in 2.3.

2.5 Root system architecture

For determination of root system architectural traits, 6 contrasting wheat lines from the panel with the adapted lines were pre-cultured hydroponically for 10 days under high (1 mM NH_4NO_3) or low N (100 µM NH_4NO_3), and of each line and N treatment, 5 plants were analyzed. To monitor differences in root morphological traits, individual seminal roots were placed on a glass plate and combed with the help of floating water and forceps until lateral roots were separated from the main root axis and became distinguishable from one another. The combed roots were scanned using an Epson Expression 10000XL scanner (Seiko Epson) with a resolution of 400 dots per inch. Root length was quantified with the Smart root plugin into ImageJ software (https://imagej.nih.gov/ij/plugins/index.html#tools). Average values of 5 plants from 6 contrasting wheat lines were calculated for each root trait.

2.6 $^{15}NH_4^+$ uptake analysis in contrasting lines after N-deficient preculture

2 contrasting adapted lines (Rockefeller and Tobak) were pre-cultured hydroponically for 12 days in nutrient solution. After 12 days of pre-culture encompassing 0, 2 or 4 days of growth in absence of N (N-sufficient, 2 days -N and, 4 days -N), short-term (6 min) ammonium uptake capacity was determined using 100 µM $^{15}(NH_4)_2SO_4$ or 1 mM $(^{15}NH_4)_2SO_4$, following the same protocol as described in 2.3.

2.7 Identification and phylogenetic analysis of AMT and NRT gene families in wheat

Functionally characterized AMTs and NRTs family sequences were obtained through the Aramemnon database (http://aramemnon.uni-koeln.de/seq_view.ep?search=ammonium+transporter&term=1&cat=0&x=21&y=13). Protein sequences of AMTs from *Oryza sativa*, *Zea mays*, *Arabidopsis thaliana* were used as queries for BLASTP search against the Chinese spring wheat genome (https://webblast.ipk-gatersleben.de/wheat_ten_genomes/). For the protein sequence, BLAST algorithm parameters used were an expected threshold less than 1e-50, default word size of 3, maximum target sequences 50, BLOSUM62 comparison matrix, allow gaps (existence cost of 11 and extension cost of 1), and included a filter of low complexity regions. Sequences were accepted from BLAST results as long as they were not a series of small fragments and shared at least 70% identity.

Transmembrane helices in protein sequences were predicted using the TMHMM Server v. 2.0 (http://www.cbs.dtu.dk/services/TMHMM/). Sequences with at least 8 TM domains were compared with the reference sequences, and only the ones that had a maximum difference of 50 amino acids in length were selected for further analysis.

For phylogenetic analyses, each transporter family protein sequences from *Triticum aestivum* (A, B, and D genome), *Escherichia coli, Saccharomyces cerevisiae, Arabidopsis thaliana, Oryza sativa, Glycine max, Zea mays, Brachypodium distachyon, Sorghum bicolor, Setaria italica, Brassica rapa, Populus trichocarpa, Physcomitrella patens* were included. Sequences were aligned using MUSCLE aligner, which allowed to generate neighbor-joining trees based on distance matrices. The resampling method was bootstrapping and consisted of 1000 replications. All procedures were run using MEGA software (https://www.megasoftware.net/). Phylogenies were rooted using Triticum sequences belonging to another family as an outgroup.

2.8 PCR, Gene cloning, sequencing, and haplotype detection

A subset of SNPs and haplotypes were detected through molecular cloning and re-sequencing of genes in selected contrasting lines from both panels. The coding sequences of *AMT1.1, AMT1.2, NRT1.1* from the A, B, and D genomes were extracted via BLAST. To amplify the full sequence of a gene across the range of templates, gene-specific primer pairs were designed in primer3plus (http://www.bioinformatics.nl/cgi-bin/primer3plus/primer3plus.cgi) from a consensus sequence generated through multiple alignment comparisons.

The oligonucleotides used as primers were synthesized based on the data accessible in literature (Table 1) and purchased from Metabion International AG. PCR reactions were performed in an Eppendorf 5331 Mastercycler Gradient Thermal Cycler with a heated lid in the final volume of 25 µl using genomic DNA extracted from lines with contrasting nitrogen uptake capacities from the adapted and unadapted lines that were identified in the screening approach.

Table 1. Gene-specific primer sequences used to amplify AMT1.1, AMT1.2 and NRT1.1; FP, forward primer; RP reverse primer.

Genes	Forward and reverse primer sequences (5' – 3')	Expected cDNA fragment
AMT1.1	FP: ATGTCGGCGACGTGCGCGG RP: TTAGACCTGGCTGTTGGCCGC	1485 bp
AMT1.2	FP: ATGTCGACGTGCGCGGCGAG RP: CTAGACCGAGCTGCTCGGGGAC	1512 bp
NRT1.1	FP: ATGGGCTCGGTGCTGCCGGA RP: TCAGTGGCCGACGATCATGGCC	1812 bp

The single PCR reaction mixture contained 1x Phusion HF buffer (NEB, Inc.), 200 µM dNTP, 1 µM of each primer, <250 ng of cDNA, 0.5 unit of Phusion DNA polymerase (NEB, Inc.), and 3% of DMSO. After the initial temperature for 95 °C for 2 min, 35 cycles were performed, depending on the individual gene-specific primers, at the following temperatures:

AMT1.1	*AMT1.2*	*NRT1.1*	*NRT2.1*
95°C for 1 min	95°C for 1 min	95°C for 1 min	95°C for 1 min
57.5°C for 30 s	67°C for 30 s	66°C for 30 s	67°C for 30 s
72°C for 45 s	72°C for 45 s	72°C for 50 s	72°C for 45 s

The final DNA extension temperature was 72°C for 5 min and the final step was at 4°C.

The PCR product was separated in ethidium bromide-stained 1% (w/v) agarose gels run in 1x TAE buffer and exposed to UV light to visualize DNA fragments (UVP GelStudio PLUS, Analytik Jena).

The amplified fragments were purified with the GeneJET Gel Extraction Kit (ThermoFisher Scientific, USA) and cloned into pCR^{TM}-BluntII-TOPO (Invitrogen, San Diego, CA, USA). For plasmid ligation, the ligation mixture was used to transform *E. coli* strain DH5α competent cells and plated onto LB Agar with kanamycin (50 µg/mL). After overnight incubation at 37°C putative positive clones (white colonies) were picked. Plasmid DNA was extracted from positive clones, incubated overnight in liquid medium at 37°C (LB Broth and 50 µg/mL of kanamycin) using Plasmid Miniprep (Promega) and analyzed by restriction enzyme digest (*EcoRI*). Positive clones were subjected to DNA sequencing using vector-specific primers (4 clones for each region). Sequencing was performed on an Applied Biosystems DNA sequencer (Eurofins Genomics, Germany).

For each coding region, the different sequences were aligned with Clustal Omega (https://www.ebi.ac.uk/Tools/msa/clustalo/). From the translated protein sequences of AMT1.1, AMT1.2, NRT1.1 haplogroups were formed for all resequenced lines. Similarly, allelic variation of *AMT3;1* and *AMT3;2* sequences was analyzed in 2 highly contrasting adapted lines (Rockefeller and Tobak)using the same protocol.

Genes	Forward and reverse primer sequences (5’ – 3’)	Expected cDNA fragment
AMT3.1	FP: ATGTCGACGGCCGCGGATTA RP: CTAGACGTCCTGGGTGACGC	1479 bp
AMT3.2	FP: ATGTCGGTGCCGGTGGCGTA RP: TCACACCGGCACGACGGCGG	1413 bp

2.9 Protein structure template selection and *ab initio* homology modeling

The translated protein sequences of AMT1.1 and AMT1.2 were submitted to two protein modeling softwares, SWISS-MODEL (Waterhouse et al., 2018) and Phyre2 (Kelley et al., 2015). The full length of the AMT1.1 and AMT1.2 protein sequence was used as search template. Default options were used to build and evaluate the model in SWISS-MODEL, whereas in Phyre2 intensive modeling parameter is selected. Evaluated model is selected based on their structural identity and confidence interval. Generated models were visualized by the Pymol software (https://pymol.org/2/).

2.10 RNA extraction, cDNA synthesis, and real-time quantitative RT-PCR

About 50 mg fresh root biomass was subjected to RNA extraction, in 4 biological replications from each line. RNA was extracted using a Macherey-Nagel™ NucleoSpin™ RNA kit (MACHEREY-NAGEL GmbH & Co. KG, Germany) according to the manufacturer’s protocol. RNA was quantified using a NanoDrop ND-1000 Spectrophotometer (Peqlab, Erlangen, Germany) and the quality of extracted RNA was verified with a Bioanalyzer 2100 (Agilent Technologies, Santa Clara, CA, USA). First-strand cDNA synthesis was carried out with the RevertAid First Strand cDNA Synthesis kit (ThermoFisher Scientific, USA), using 1 µg of purified total RNA per 20 µL of reaction volume.

Real-Time qPCR runs were performed in a CFX384™ Real-Time PCR System (Bio-Rad USA). Two µL of cDNA was added to each PCR reaction mixture (10 µL), containing 100-500 nM of each primer and 5 µL of 2x iQ SYBR Green Supermix (Bio-Rad, USA). The following protocol was used: an initial enzyme activation/cDNA denaturation step 95°C for 3 min, followed by 40 cycles at 95°C for 15 sec, 60°C for 30 sec and 72°C for 15 sec, with a final standard dissociation protocol to obtain the melting profiles. Data were acquired using the CFX Manager software.

Table 2. List of primer sequences for qRT-PCR.

Genes	Forward and reverse primer sequences (5' – 3')
AMT1.1	FP: CGGCTTCGACTACAGCTTCT RP: AAGGAACGCCGAGTAGATGA
AMT1.2	FP: GAACATCATGCTCACCAACG RP: AAGAAGTGCTCCCCGATGAA
NRT1.1	FP: GCGCTTCTTCAACTGGTTCT RP: GCTTCTTGAACCGGTACTTCC
Actin	FP: CAATGTTCCTGCCATGTACG RP: AGCGAGATCCAAACGAAGAA
ADP-RF	FP: TCTCATGGTTGGTCTCGATG RP: GGATGGTGGTGACGATCTCT

Similarly, about 50 mg fresh root samples were collected from the experiment in chapter 2.6, in which gene expression was analyzed in Rockefeller and Tobak, collecting RNA from 10 biological replicates of each line and treatment.

Table 3. List of primer sequences for AMT-type ammonium transporter genes used in the qRT-PCR.

Genes	Forward and reverse primer sequences (5' – 3')
AMT1.1	FP: CGGCTTCGACTACAGCTTCT RP: AAGGAACGCCGAGTAGATGA
AMT1.2	FP: GAACATCATGCTCACCAACG RP: AAGAAGTGCTCCCCGATGAA
AMT3.1	FP: GTCACCTGGGGCTACAACAT RP: CCTTGAAGAAGTGGGTGGAC
AMT3.2	FP: TCCTTCCTGTCACCAACTCC RP: GACGCAGATAATGGACGTGA

2.11 Statistical analysis

For correlation analysis, the R function "cor. test()" was used. Phenotypic and physiological traits on various lines from both the panel were compared by one-way analysis of variance (ANOVA) followed by posthoc Tukey's test at $P < 0.05$. All statistical analysis was performed in R.

3. Results

3.1 Screening for nitrogen uptake-efficient lines

3.1.1 Nitrogen uptake capacity in lines of two winter wheat gene pools

To address the question whether plant breeding during the past decades improved nitrogen uptake efficiency in winter wheat, two panels of wheat lines were assembled in frame of the Genebank 2.0 project that consisted of either lines available before the "Green Revolution", abbreviated in the following as "unadapted lines", or elite lines that are mostly still on the market and represent adapted genetic material. 100 lines from each panel were precultured first for 10 d on full nutrient solution and then for 2 d on N-deficient nutrient solution to induce N uptake systems before nitrogen uptake capacity was determined. Among the elite lines, root N uptake capacity differed by almost factor 2, ranging approx. between 90 and 180 µmoles N g^{-1} root DW h^{-1} (Figure 3.1a). In the unadapted lines, root N uptake capacity differed slightly more, i.e. approx. between 70 and 180 µmoles N g^{-1} root DW h^{-1}.

In this hydroponic screening approach, ^{15}N-double labelled ammonium nitrate was supplied for 1 h to allow sufficient time for root-to-shoot translocation. In absolute terms, lines from the elite panel translocated between 10 and 44 µmoles N g^{-1} root DW h^{-1} to the shoots, which corresponds to approx. 10-40% of ^{15}N taken up by the roots (Figure 3.1b). In comparison, the unadapted lines translocated between 8 and 35 µmoles N g^{-1} root DW h^{-1} to the shoot, which is approx. 8-35% (Figure 3.1b). In both gene pools, there was a large genotypic variation in the N translocation rates with slightly larger variation in the elite lines. There was a trend in both panels that lines with higher uptake rates also translocated more N (Figure 3.1a b, insert), and indeed, there was a significant correlation between uptake and translocation rates in either wheat panel (r = 0.7-0.8; Figure 3.2a, b). This correlation indicates that translocation rates were strongly determined by the amount of root-absorbed N.

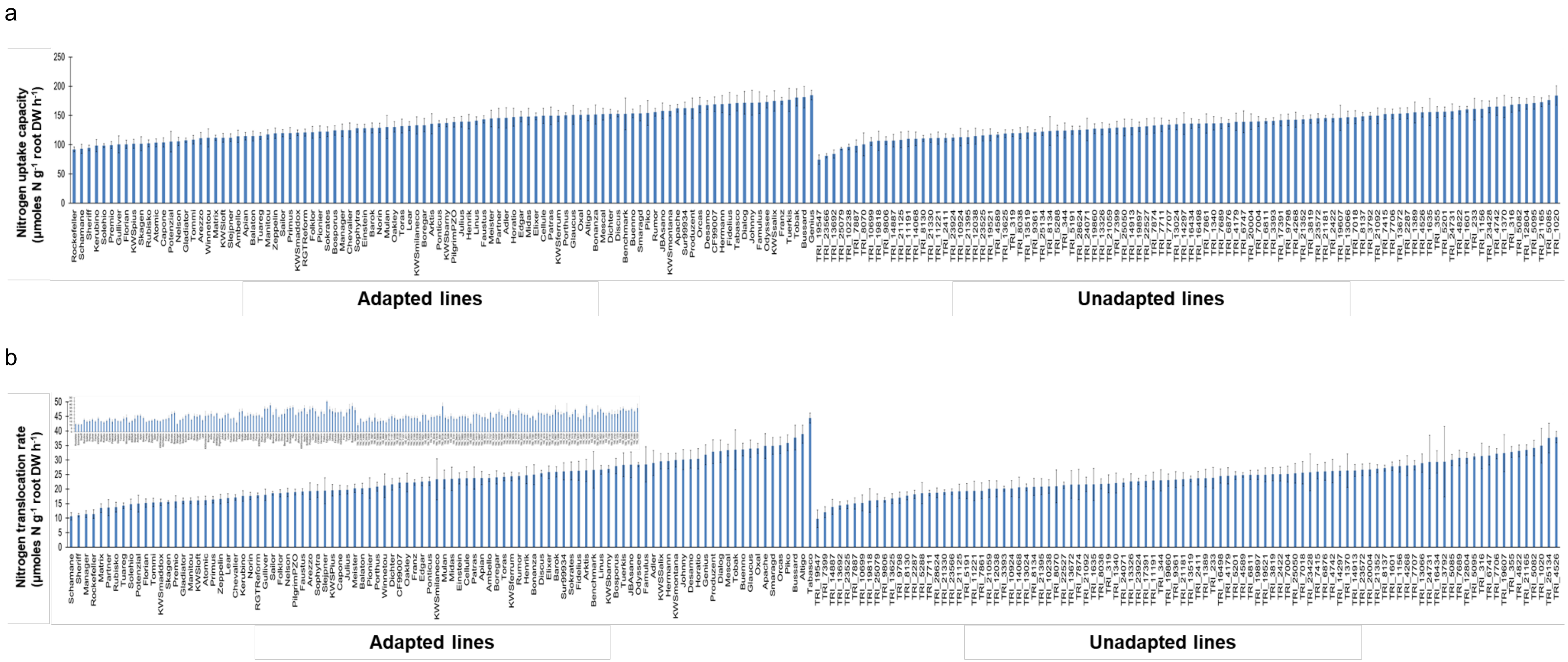

Figure 3.1. High-affinity nitrogen uptake capacity in roots of adapted lines and unadapted lines. (a) Nitrogen uptake capacity, (b) root-to-shoot translocation capacity of N. For comparison of both measures, the insert in (b) shows translocation rates of the same lines arranged in the same order as in (a). Plants were grown hydroponically on ammonium nitrate for 10 days and then in a nitrogen-free nutrient solution for 2 days. Roots were exposed to 200 µM double-labelled $^{15}NH_4{}^{15}NO_3$ for a period of 1 h in full nutrient solution. Bars represent means ± SE (n = 6 independent biological replicates). DW, dry weight.

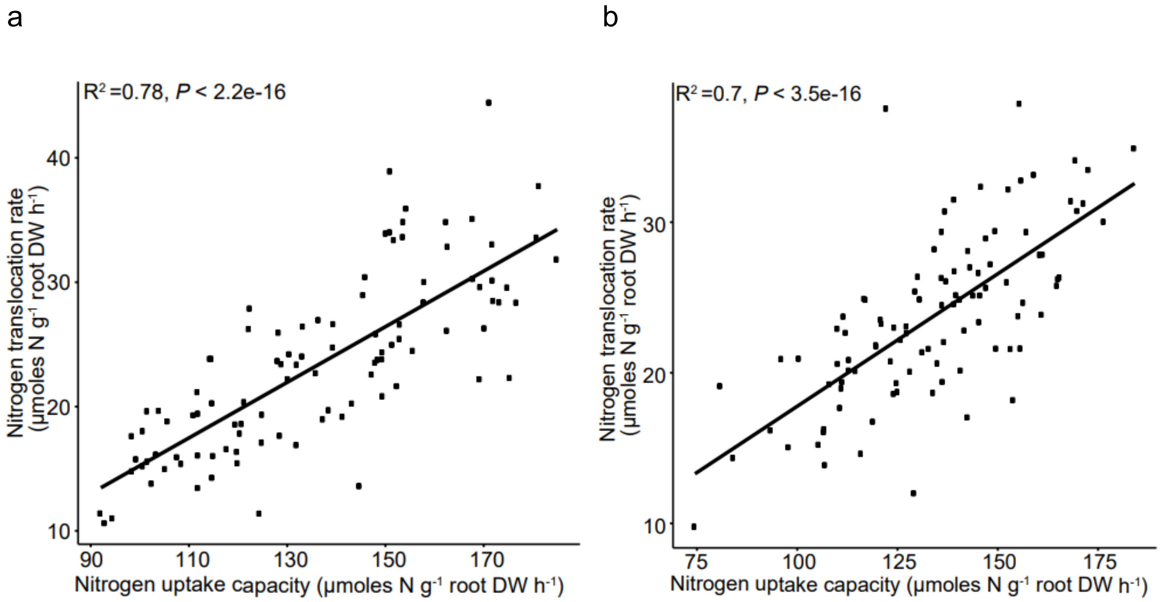

Figure 3.2. Correlation between uptake and root-to-shoot translocation capacity of nitrogen in the two wheat panels. (a) Nitrogen uptake capacity plotted against root-to-shoot translocation for adapted lines, (b) nitrogen uptake capacity plotted against root-to-shoot translocation for unadapted lines. R^2 represents the Pearson correlation value. DW, dry weight.

To rule out that variation between the two panels was due to biomass differences, population means were compared for root and shoot DW. However, both measures did not show significant differences between the two wheat panels (Figure 3.3a, b). Likewise, a direct comparison between the population means of root N uptake capacity and translocation rates confirmed a nearly similar and not significantly different growth performance of the elite and unadapted lines (Figure 3.3c, d).

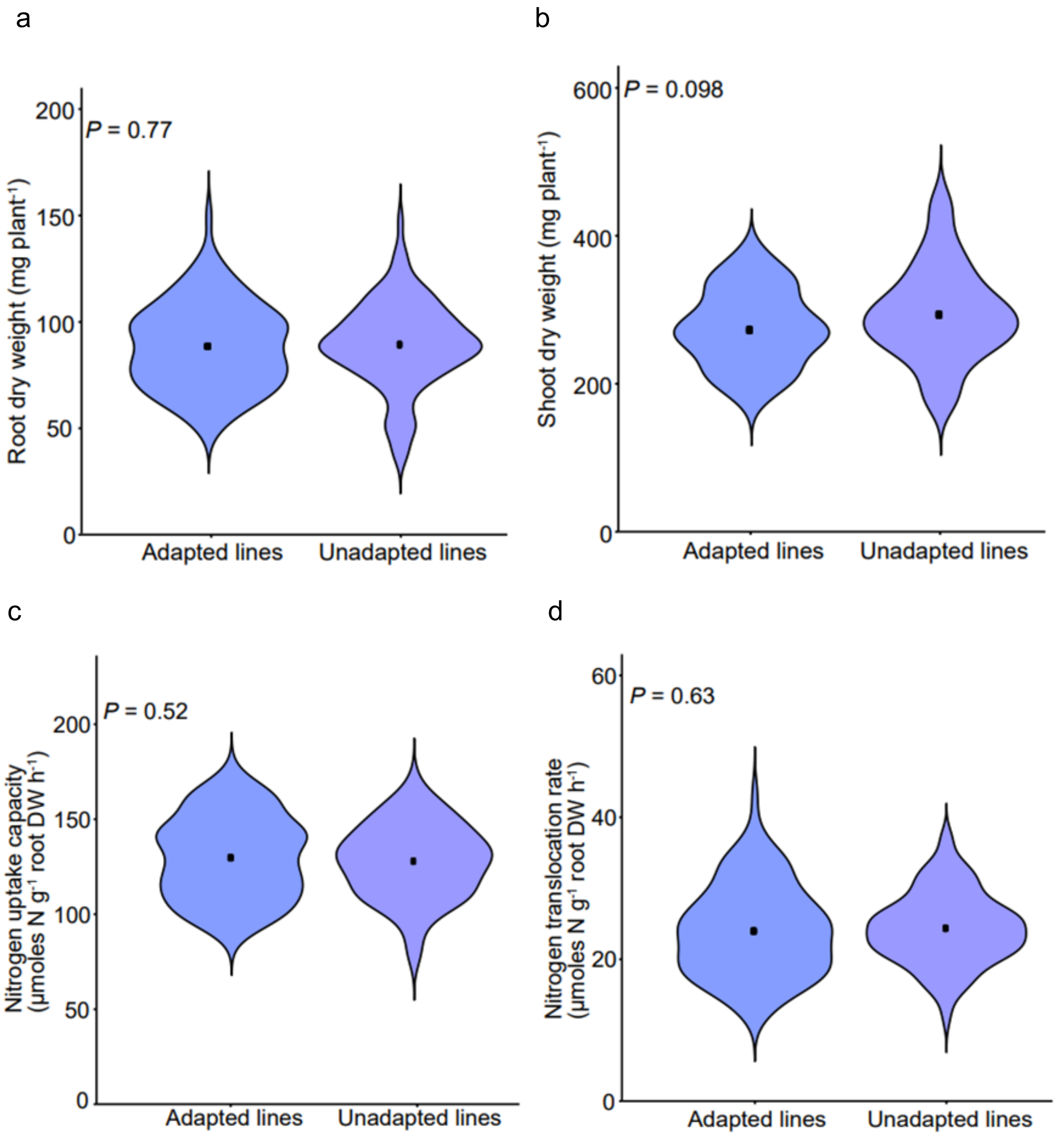

Figure 3.3. Comparison of the variation of phenotypic and physiological traits between elite and unadapted lines. Violin plots compare the distribution of (a) root dry weight (b) shoot dry weight (c) nitrogen uptake capacity and (d) root-to-shoot translocation rate among the 100 lines of each gene pool. Data are collected from plants grown hydroponically on ammonium nitrate for 10 days and then in a nitrogen-free nutrient solution for 2 days. Roots were exposed to 200 µM double-labelled $^{15}NH_4{}^{15}NO_3$ for a period of 1 h in prior to harvest. Black rectangles represent means for each gene pool, and p-values relate to differences between means according to ANOVA and Tukey's test. DW, dry weight.

3.1.2 Selection of contrasting lines from the screening approach

In the initial screening of N uptake rates, lines were identified in both gene pools, which significantly differed (Figure 3.1a). To further validate these differences and to obtain a more detailed picture of nitrogen uptake efficiency, contrasting lines were selected from either panel. From the elite gene pool, the lines Rockefeller, Sheriff, Solehio, Gulliver, Florian, Nelson were selected based on their low uptake capacity and Milaneco, Horatio, Famulus, Franz, Tobak, Genius based on their high uptake capacity. From the unadapted lines TRI_23566, TRI_10238 were selected due to their low uptake capacity, TRI_2411, TRI_4589, TRI_8038 and TRI_13625 for their intermediate uptake capacity and TRI_3792, TRI_24731, TRI_12804, TRI_21165 due to their high uptake capacity.

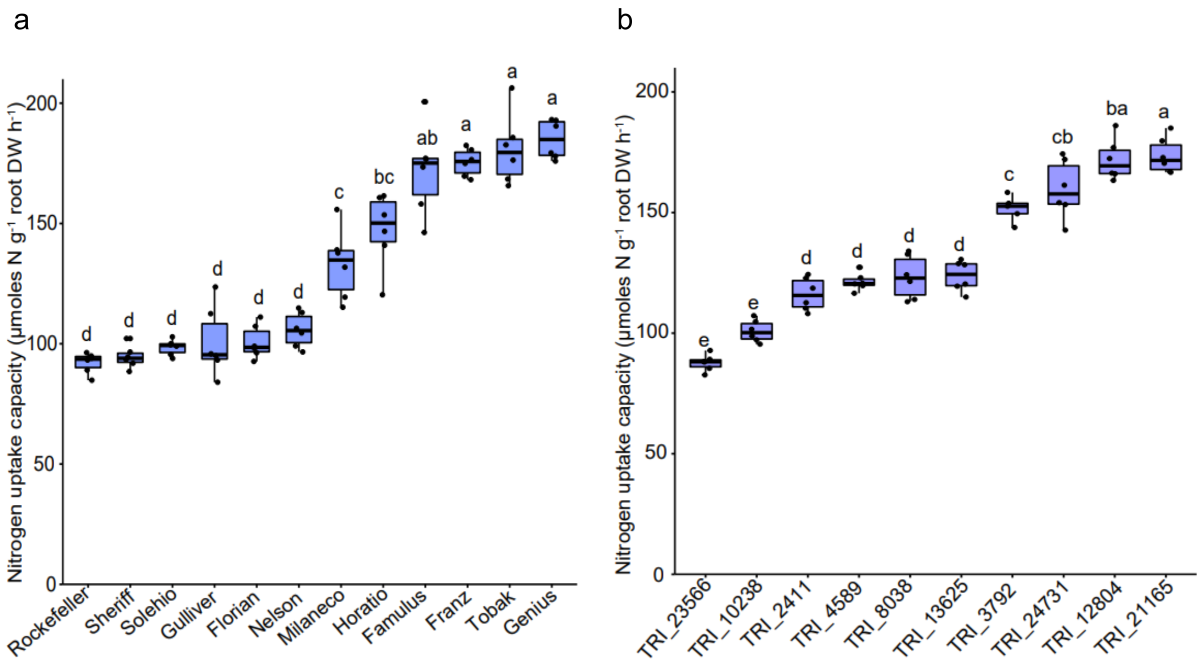

Figure 3.4. Variation in nitrogen uptake capacity of contrasting lines from two wheat panels. Nitrogen uptake capacity in (a) adapted lines and (b) unadapted lines. Plants were grown hydroponically on ammonium nitrate for 10 days and then in a nitrogen-free nutrient solution for 2 days. Roots were exposed to 200 µM double-labelled $^{15}NH_4{}^{15}NO_3$ for a period of 1 h in full nutrient solution. The boxes show the first quartile, median and third quartile; the whiskers indicate the minimum and maximum values (n = 6 independent biological replicates). Different letters represent significant differences among means according to ANOVA and Tukey's test at $P < 0.05$. DW, dry weight. Data refer to values presented in Figure 1.

Re-plotting the nitrogen uptake data from the screening approach (Figure 3.1a) showed that the selected lines formed groups that differed significantly in their nitrogen uptake rates, allowing to name them contrasting lines (Figure 3.4a, b). In the elite panel, Famulus, Franz, Tobak, Genius had almost 2-fold higher N uptake capacity than Rockefeller, Sheriff, Solehio, Gulliver, Florian, Nelson (Figure 3.4a). Within the unadapted plant material, N uptake in the four lines TRI_3792, TRI_12804, TRI_24731, TRI_3792 was significantly higher than in TRI_2411, TRI_4589, TRI_8038, TRI_13625 and, in turn, these were still higher than TRI_23566, and TRI_10238. These contrasting lines from each panel were assessed in further experiments.

3.2 Characterization of high- and low-affinity uptake capacities for ammonium and nitrate in selected contrasting lines

3.2.1 Comparison of high- and low-affinity uptake capacities of ammonium in plants from N-sufficient or N-deficient pre-culture

To address the question of whether differential N uptake capacities in contrasting lines were caused by differences in ammonium or nitrate uptake, selected contrasting lines from each panel (Figure 3.1a, Figure 3.4) were precultured in N-sufficient or N-deficient nutrient solution and subjected to uptake studies using single-labelled N forms.

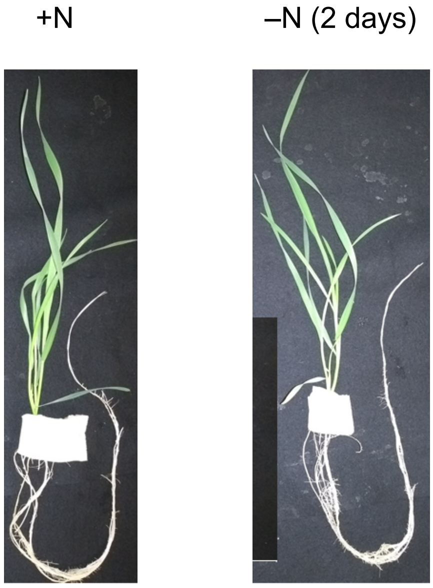

Figure 3.5. Visual appearance of adapted lines grown hydroponically on N-sufficient or N-deficient nutrient solution. Plants were grown hydroponically on ammonium nitrate for 10 days and then continued to grow on either 2 mM N or N-free nutrient solution for 2 days.

First, selected contrasting lines from each panel were assessed for their root and shoot biomass formed under N-sufficient or N-deficient conditions. For root and shoot growth no visible difference or symptoms were observed after 2 days of N deficiency (Figure 3.5).

In the contrasting lines from the adapted gene pool, there were no significant differences in root or shoot dry weight between plants grown for 2 days under N sufficiency or N deficiency (Figure 3.6a, b). Root dry weights only tended to be higher in N-deficient plants. By contrast, in the unadapted germplasm, the mean of root dry weights was significantly higher under N deficiency than under N sufficiency while shoot dry weights remained similar (Figure 3.6c, d). Thus, unadapted lines appeared to respond earlier or stronger than adapted lines with a root biomass increase under N deficiency, which is a typical root adaptive response (Giehl et al., 2014).

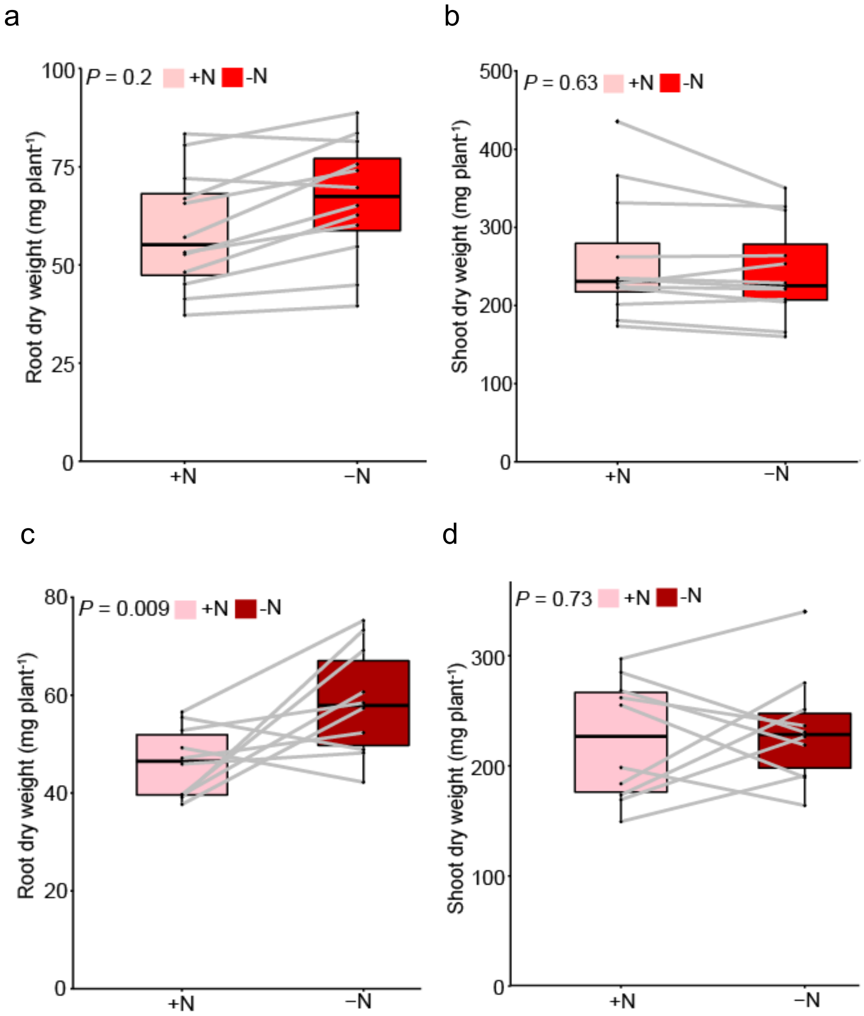

Figure 3.6. Comparison of root and shoot dry weights of contrasting lines under N-sufficient and N-deficient conditions. Paired box plots compare the distribution of root and shoot dry weights for contrasting adapted lines (a, b) and unadapted lines (c, d). Data are collected from plants grown hydroponically on 2 mM ammonium nitrate for 10 days and then on 2 mM (+N) or on N- free nutrient solution (-N) for 2 days. The boxes show the first quartile, median and third quartile; the whiskers indicate the minimum and maximum values. P-values indicate differences between means according to ANOVA and Tukey's test.

To figure out whether differences in nitrogen uptake were due to ammonium or nitrate, contrasting lines from each panel were precultured strictly under the same conditions as in the screening experiment, but this time 100 µM single-labelled $^{15}(NH_4)_2SO_4$ was used as N source for the N uptake study.

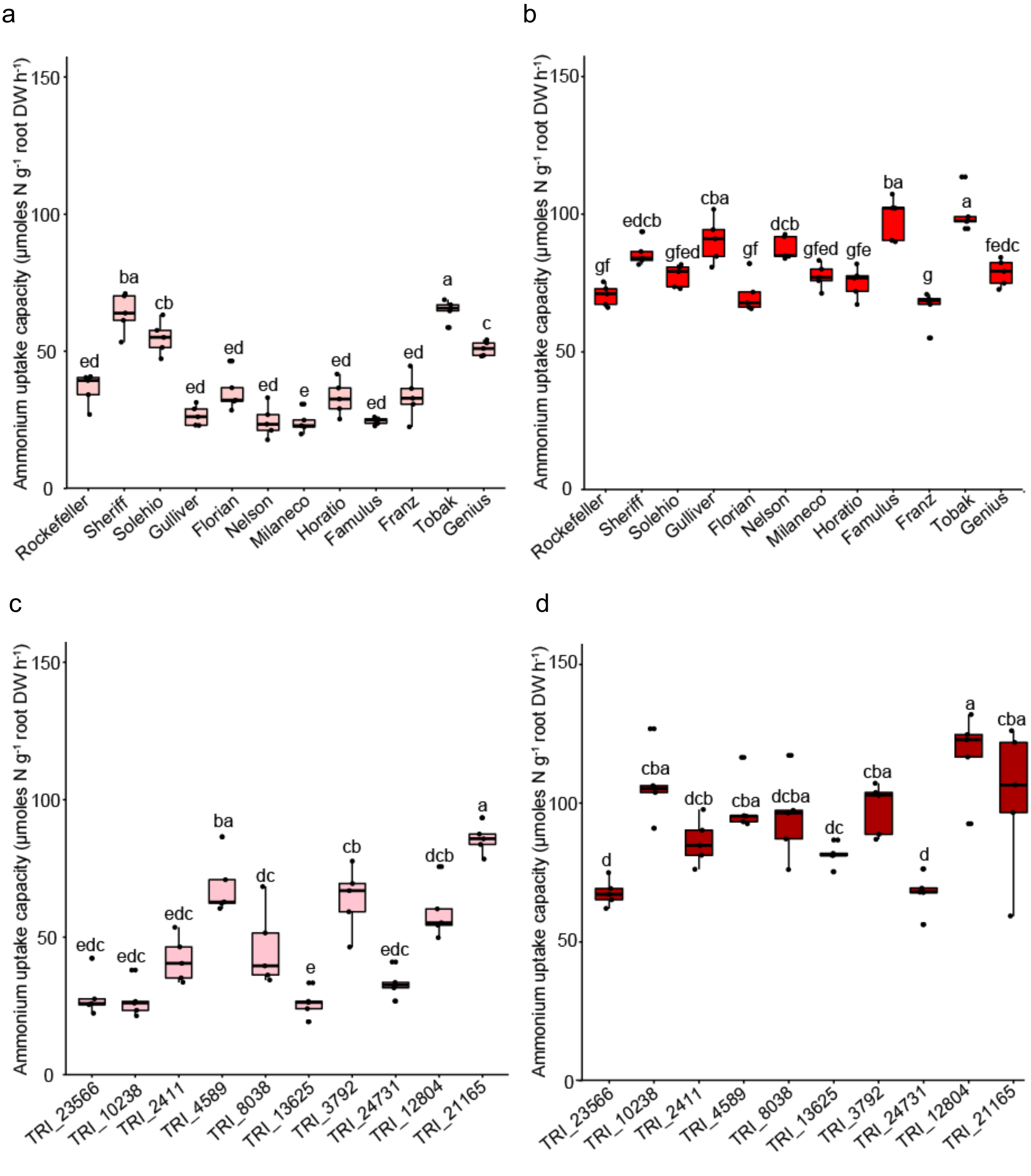

Figure 3.7. Phenotypic variation in high-affinity ammonium uptake capacity of contrasting lines grown under N-sufficient or N-deficient conditions. Ammonium uptake capacity for contrasting adapted lines (a, b) and unadapted lines (c, d). Plants were grown hydroponically on ammonium nitrate for 10 days and then on 2 mM N (+N) or on N-free nutrient solution (-N) for 2 days. Roots were exposed to 100 µM single-labelled $^{15}(NH_4)_2SO_4$ for a period of 1 h prior to harvest. The boxes show the first quartile, median and third quartile; the whiskers indicate the minimum and maximum values (n = 5 independent biological replicates). Different letters represent significant differences among means according to ANOVA and Tukey's test at P < 0.05. DW, dry weight.

In N-sufficient plants from the adapted panel, high-affinity ammonium uptake rates varied between approx. 24 and 72 µmoles NH_4^+ g^{-1} root DW h^{-1} (Figure 3.7a). The corresponding values increased from 60 to almost 120 µmoles NH_4^+ g^{-1} root DW h^{-1} when plants were N deficient (Figure 3.7b). While such an increase was to be expected due to the induction of high-affinity transport systems under low N (Gazzarrini et al., 1999), there was considerable genetic variation. In particular, the line Tobak showed consistently highest uptake rates under either N condition while Rockefeller, Franz and Florian were among those with the lowest uptake capacities.

Likewise, ammonium uptake capacities in the unadapted plant material also increased under N deficiency. However, the variation in uptake rates within the individual lines appeared to be greater than in the adapted lines (Figure 3.7c, d). Nonetheless, the line TRI_12804 achieved a significantly higher uptake rate than the best line from the adapated material.

The difference in high-affinity ammonium uptake capacity between the two N conditions provides information on its N responsiveness, i.e. the factor by which ammonium uptake is enhanced under low N. For that, the uptake rate achieved under high N (Figure 3.7a) was subtracted from that under low N (Figure 3.7b). When aligning values from the contrasting adapted lines, it turn out that some lines (e.g. Famulus; Nelson and Guliver) increased their ammonium uptake capacity under N-deficient condition more than others (Figure 3.8a), indicating stronger responsiveness to N deficiency. However, there was no evidence for a difference in this responsiveness between the contrasting lines, as both groups had weakly and strongly responding lines. In principle, the same observations were made in the unadapted panel. Here, the line TRI_10238 showed the highest increase in root ammonium uptake capacity under low N (Figure 3.8b).

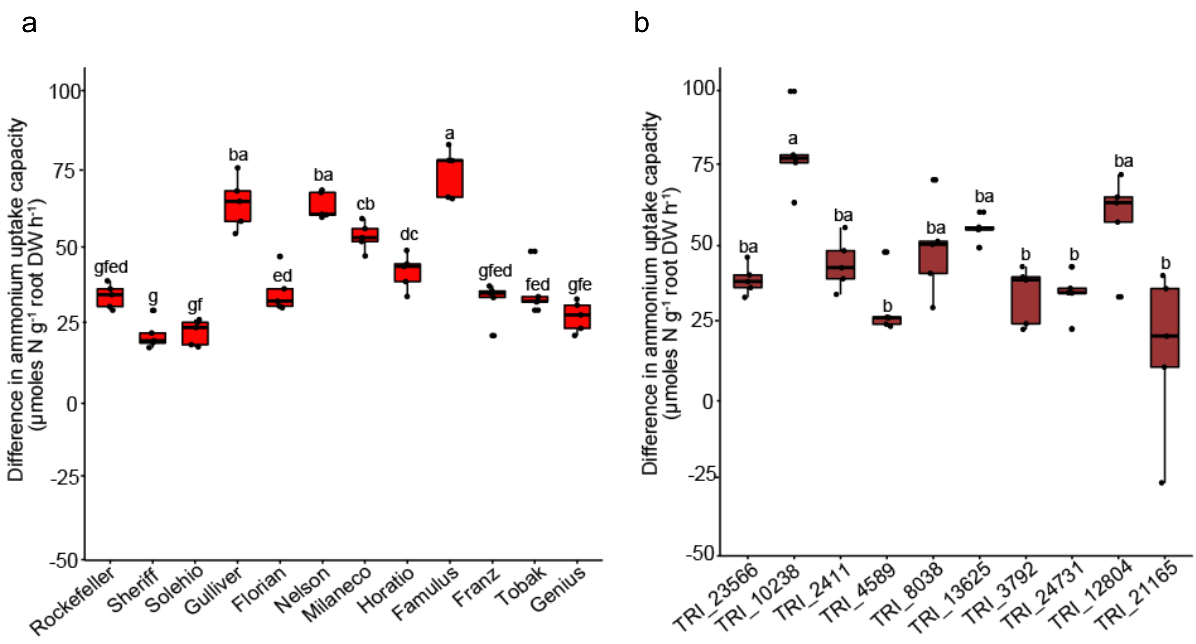

Figure 3.8. Genotypic differences in the N deficiency-induced increase of the high-affinity ammonium uptake capacity of contrasting lines from the (a) adapted and (b) unadapted panel. Values were obtained by subtracting the uptake rate of seedlings grown in N-sufficient condition (+N) from the uptake rate of seedlings grown in N-deficient conditions (-N). Plants were grown as described in Fig. 3.7. The boxes show the first quartile, median and third quartile; the whiskers indicate the minimum and maximum values; negative values indicate that uptake rate under +N were higher than under -N. Different letters indicate differences between means according to ANOVA and Tukey's test; n = 5. DW, dry weight.

The low-affinity transport capacity of the same contrasting lines from each panel was measured at 2 mM of external $^{15}NH_4^+$. Phenotypic variation within N-sufficient lines was around 50 µmoles NH_4^+ g^{-1} root DW h^{-1} and tended to become larger when plants were precultured under low N. In the adapted panel, the contrasting behaviour of Tobak and Rockefeller in ammonium uptake capacity in the high-affinity range was also observed in the low-affinity range (Figure 3.9a, b). While lines from the unadapted gene pool showed a similar range of low-affinity ammonium uptake capacities as lines of the adapted gene pool, uptake rates of one line, i.e. TRI_12804 achieved exceptionally high uptake rates under N-deficient conditions (Figure 3.9d).

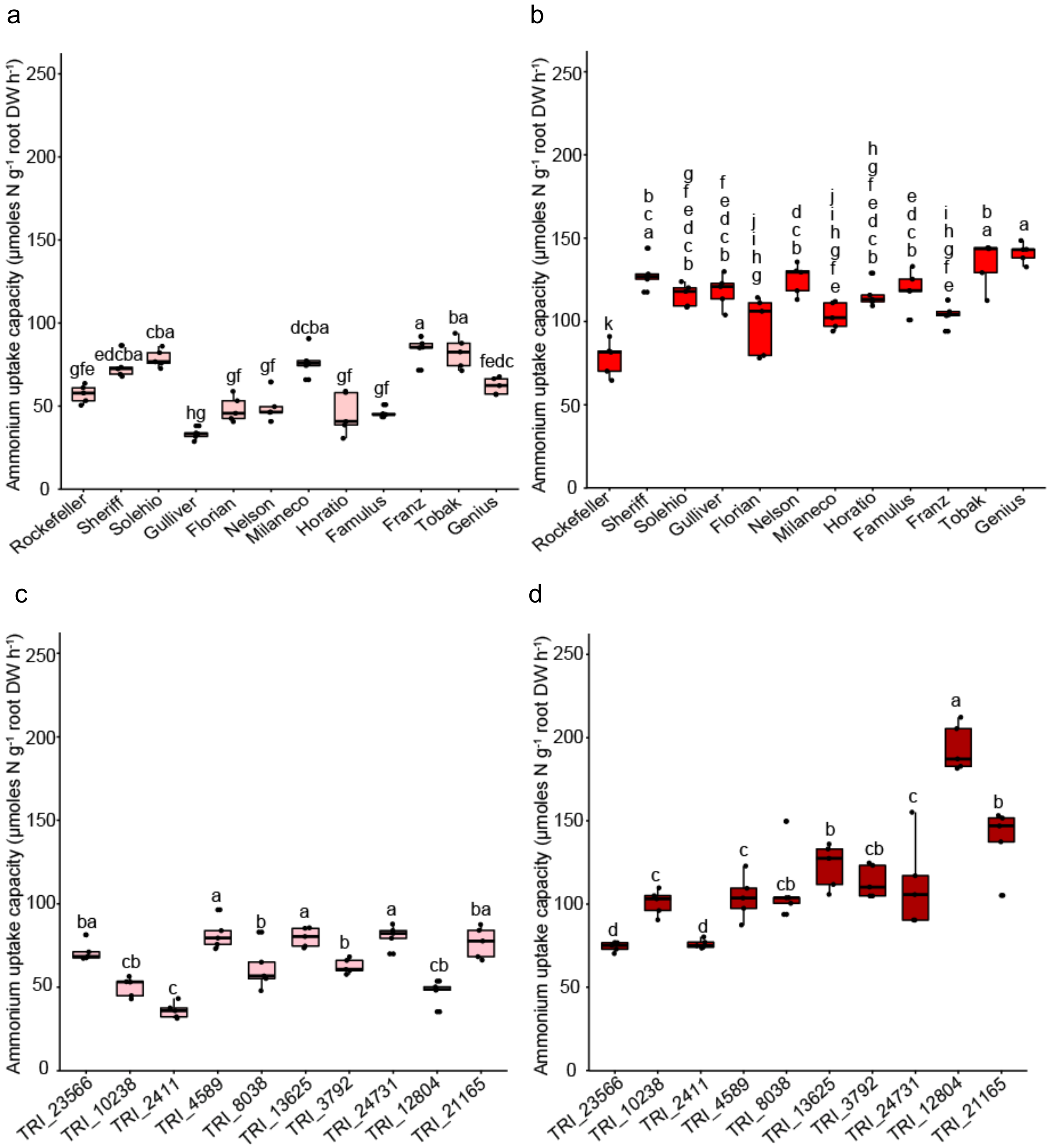

Figure 3.9. Phenotypic variation in low-affinity ammonium uptake capacity of contrasting lines grown under N-sufficient or N-deficient conditions. Ammonium uptake capacity for contrasting adapted lines (a, b) and unadapted lines (c, d). Plants were grown hydroponically on ammonium nitrate for 10 days and then on 2 mM N (+N) or on N-free nutrient solution (-N) for 2 days. Roots were exposed to 1 mM single-labelled $^{15}(NH_4)_2SO_4$ for a period of 1 h prior to harvest. The boxes show the first quartile, median and third quartile; the whiskers indicate the minimum and maximum values (n = 5 independent biological replicates). Different letters represent significant differences among means according to ANOVA and Tukey's test at P < 0.05. DW, dry weight.

In the high-affinity range, ammonium uptake capacity for adapted contrasting lines varied from 24 to 72 µmoles N g^{-1} root DW h^{-1} and 60 to 120 µmoles N g^{-1} root DW h^{-1} under N-sufficient and N-deficient conditions, respectively (Figure 3.7a, b). On the other hand, in the low-affinity range, the corresponding values increased from approx. 40 to 88 µmoles N g^{-1} root DW h^{-1} and from 85 to 135 µmoles N g^{-1} root DW h^{-1} under N-sufficient and N-deficient conditions, respectively (Figure 3.9a, b). This moderate increase suggested that the majority of the uptake capacity was conferred by the high-affinity transport system, in particular when plants were assessed under N-deficient conditions.

Hence it appears that with increasing external NH_4^+ concentrations root uptake capacity also increased in both conditions. The induction of the low-affinity ammonium uptake under low N was similar for the contrasting lines in both panels and also similar between adapted and unadapted lines (Figure 3.10). In the unadapted panel, again one line i.e TRI_12804 made an exception with the highest responsiveness among all lines (Figure 3.10b).

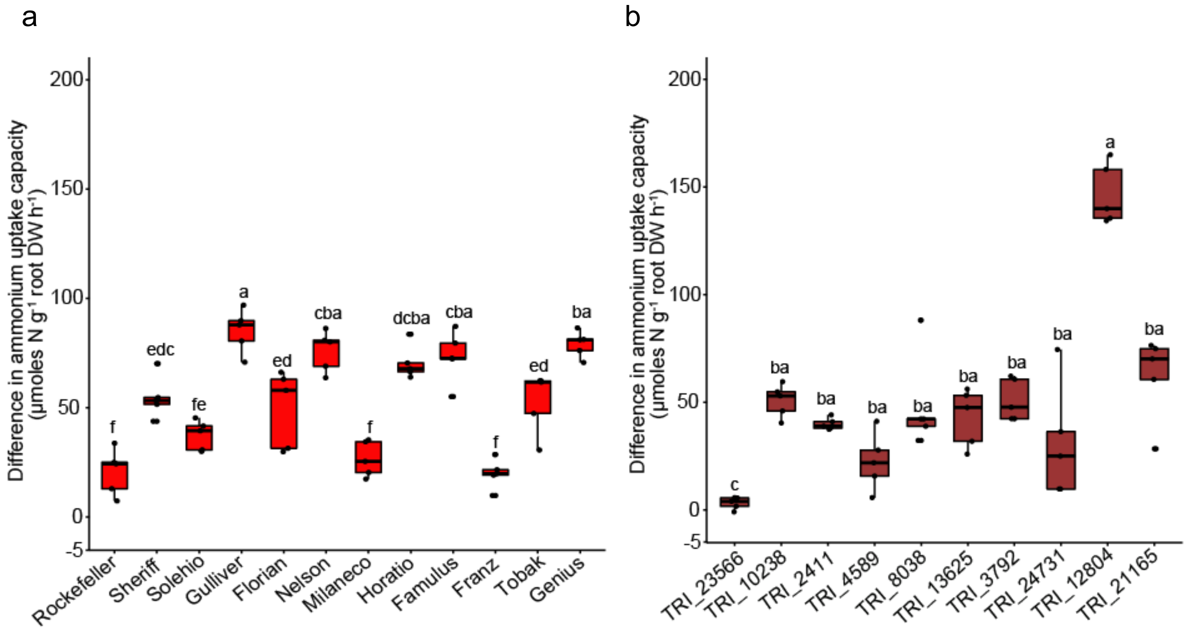

Figure 3.10. Genotypic differences in the N deficiency-induced increase of the low-affinity ammonium uptake capacity of contrasting lines from the (a) adapted and (b) unadapted panel. Values were obtained by subtracting the uptake rate of seedlings grown in N-sufficient condition (+N) from the uptake rate of seedlings grown in N-deficient conditions (-N). Plants were grown as described in Fig. 3.9. The boxes show the first quartile, median and third quartile; the whiskers indicate the minimum and maximum values; negative values indicate that uptake rate under +N were higher than under -N. Different letters indicate differences between means according to ANOVA and Tukey's test; n = 5. DW, dry weight.

3.2.2 Comparison of high- and low-affinity uptake capacities of nitrate in plants from N-sufficient or N-deficient pre-culture

After assessment of contrasting lines from both panels for high- and low-affinity ammonium uptake capacities under N-sufficient and N-deficient conditions, the phenotypic variation in nitrate uptake was examined. Thus, the same selected contrasting lines from each panel were precultured in the same way as in the previous experiments, before high-affinity nitrate uptake capacity was assessed at 200 µM single-labelled $K^{15}NO_3$ in N-sufficient and N-deficient plants.

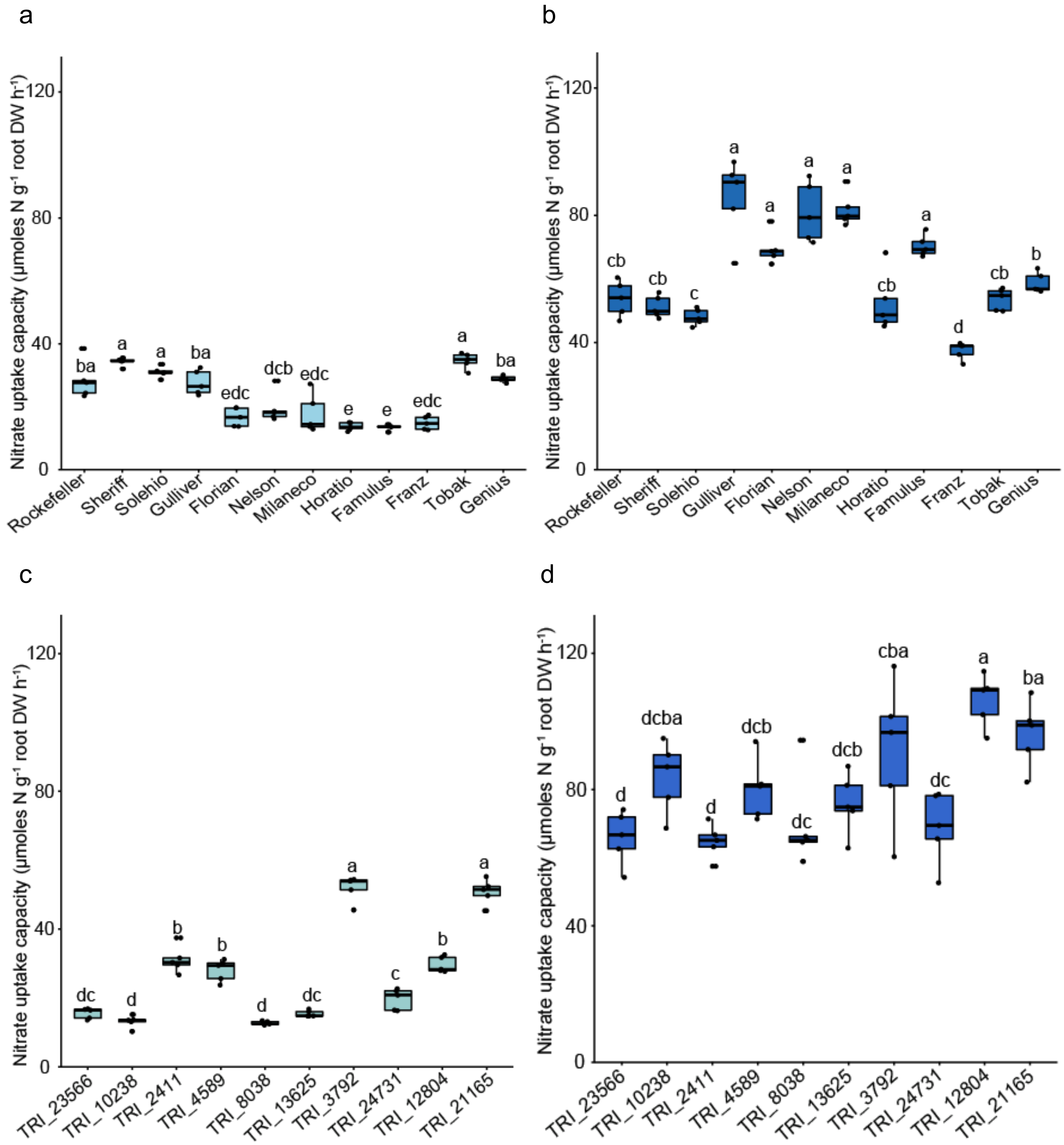

Figure 3.11. Phenotypic variation in high-affinity nitrate uptake capacity of contrasting lines grown under N-sufficient or N-deficient conditions. Nitrate uptake capacity for contrasting adapted lines (a, b) and unadapted lines (c, d). Plants were grown hydroponically on ammonium nitrate for 10 days and then on 2 mM N (+N) or on N-free nutrient solution (-N) for 2 days. Roots were exposed to 200 µM single-labelled $K(^{15}NO_3)$ for a period of 1 h prior to harvest. The boxes show the first quartile, median and third quartile; the whiskers indicate the minimum and maximum values (n = 5 independent biological replicates). Different letters represent significant differences among means according to ANOVA and Tukey's test at $P < 0.05$. DW, dry weight.

The mean values in high-affinity nitrate uptake capacity of contrasting lines from the adapted germplasm ranged approx. between 17 and 37 µmoles N g^{-1} root DW h^{-1} in N-sufficient plants, whilst in N-deficient plants, it ranged between approx. 35 and 90 µmoles N g^{-1} root DW h^{-1} (Figure 3.11a, b). While Tobak tended to show higher uptake rates than Rockefeller under N sufficiency, uptake rates under N deficiency were almost the same. In the unadapted gene pool, nitrate uptake in contrasting lines ranged between, approx. between 17 and 55 µmoles N g^{-1} root DW h^{-1} and between approx. 60 and 115 µmoles N g^{-1} root DW h^{-1} for N-sufficient and N-deficient plants, respectively (Figure 3.11c, d).

Although uptake rates increased in all lines with nitrogen starvation, contrasting lines from the unadapted gene pool achieved higher nitrate uptake capacities than lines from the adapted gene pool, irrespective of whether plants were precultured under N-sufficient or N-deficient conditions. Interestingly, the notably elevated high-affinity uptake capacity for ammonium in the unadapted lines TRI_12804 and TRI_23566 observed under N-sufficient and N-deficient conditions (Figure 3.7c, d) was also observed for nitrate (Figure 3.11c, d). In particular, under N deficiency TRI_12804 showed the highest nitrate uptake capacity among all lines (Figure 3.11d).

After observing N responsiveness on the high- and low-affinity ammonium uptake capacity for contrasting adapted and unadapted lines between the two conditions, the N deficiency-induced responsiveness in nitrate uptake was examined. The adapted and unadapted lines, which showed high N responsiveness in high-affinity ammonium uptake capacity (Figure 3.8a, b) were not the same as for high-affinity nitrate uptake (Figure 3.12a, b). Moreover, there were no apparent differences in N deficiency-induced responsiveness among the contrasting lines nor between the adapated and unadapted lines (Figure 3.12a, b).

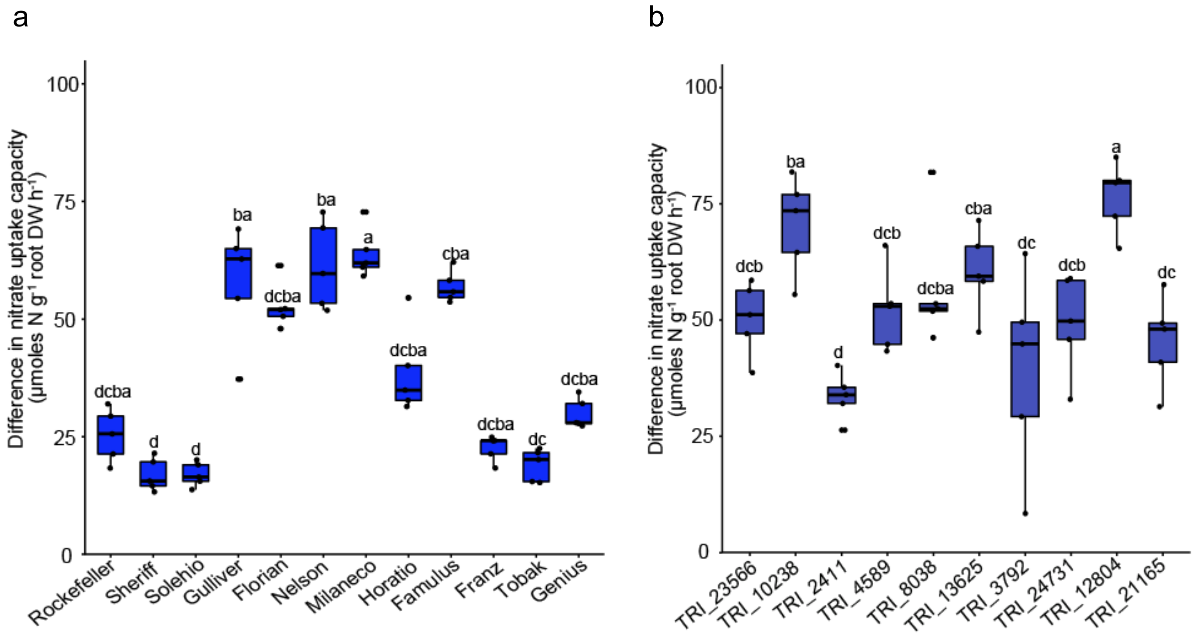

Figure 3.12. Genotypic differences in the N deficiency-induced increase of the high-affinity nitrate uptake capacity of contrasting lines from the (a) adapted and (b) unadapted panel. Values were obtained by subtracting the uptake rate of seedlings grown in N-sufficient condition (+N) from the uptake rate of seedlings grown in N-deficient conditions (-N). Plants were grown as described in Fig. 3.11. The boxes show the first quartile, median and third quartile; the whiskers indicate the minimum and maximum values; negative values indicate that uptake rate under +N were higher than under -N. Different letters indicate differences between means according to ANOVA and Tukey's test; n = 5. DW, dry weight.

When the low-affinity transport capacity of ^{15}N-labeled nitrate was measured in roots of contrasting lines from the adapted gene pool, values increased only slightly from N sufficiency to N deficiency (Figure 3.13a, b). Accordingly, the order of lines did not change considerably. Notably, Tobak was again showing the highest uptake capacity irrespective of N preculture. In contrast, Rockefeller, which was among the weakest in ammonium uptake, took in a middle position in the ranking of the lines.

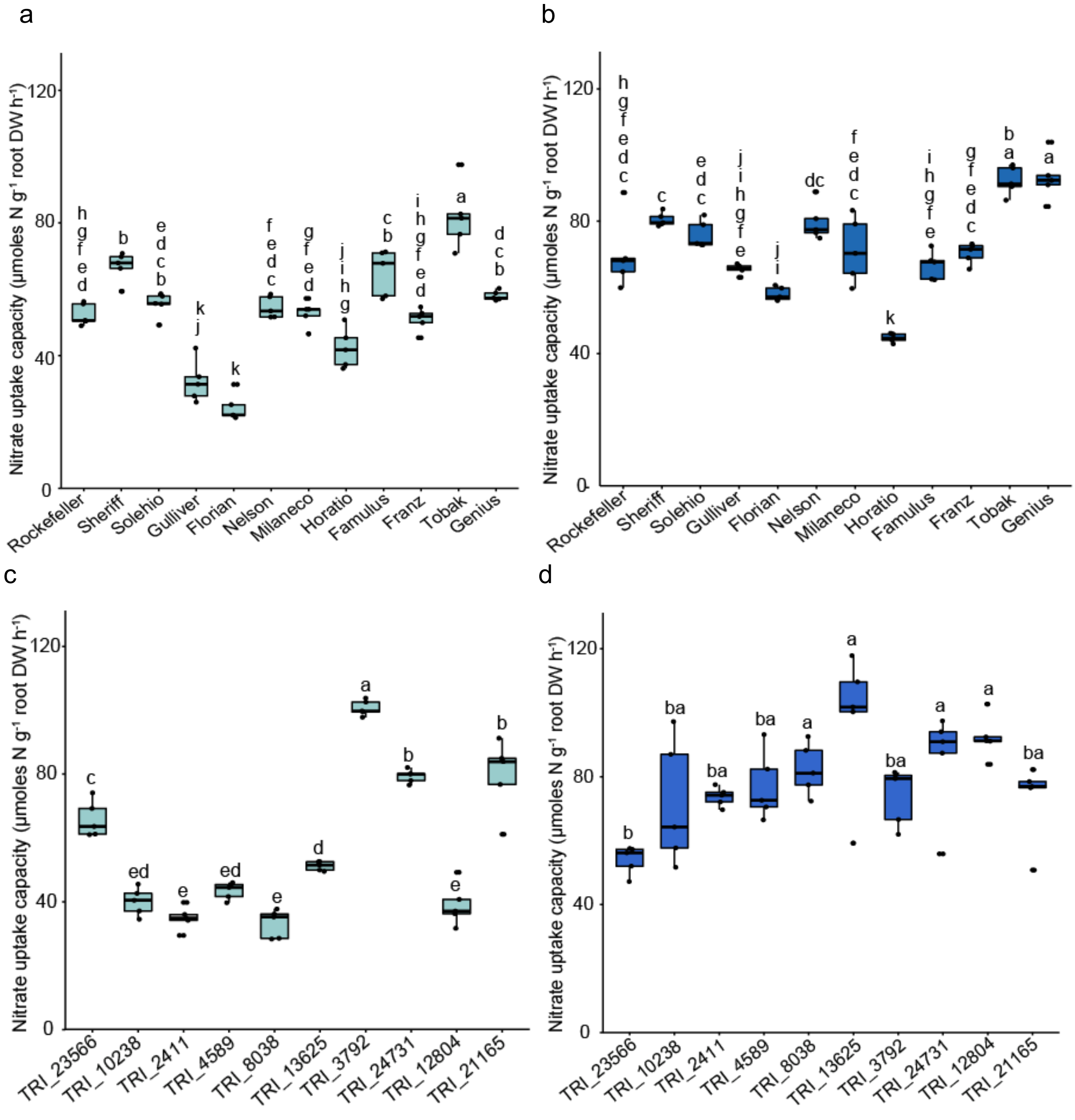

Figure 3.13. Phenotypic variation in low-affinity nitrate uptake capacity of contrasting lines grown under N-sufficient or N-deficient conditions. Nitrate uptake capacity for contrasting adapted lines (a, b) and unadapted lines (c, d). Plants were grown hydroponically on ammonium nitrate for 10 days and then on 2 mM N (+N) or on N-free nutrient solution (-N) for 2 days. Roots were exposed to 2 mM single-labelled $K(^{15}NO_3)$ for a period of 1 h prior to harvest. The boxes show the first quartile, median and third quartile; the whiskers indicate the minimum and maximum values (n = 5 independent biological replicates). Different letters represent significant differences among means according to ANOVA and Tukey's test at $P < 0.05$. DW, dry weight.

In general, a similarly weak increase in nitrate uptake capacity from N-sufficient to N-deficient plants was also observed in the unadapted contrasting lines. Referring to high-affinity nitrate uptake, the best performing line TRI_12804 also performed very well and TRI_23566 performed poor in low-affinity uptake after N-deficient preculture (Figure 3.13d). In contrast, the other line TRI_10238 showed large variation among its replicas, not allowing to assess its position in the ranking of low-affinity nitrate uptake capacity under N deficiency (Figure 3.13d).

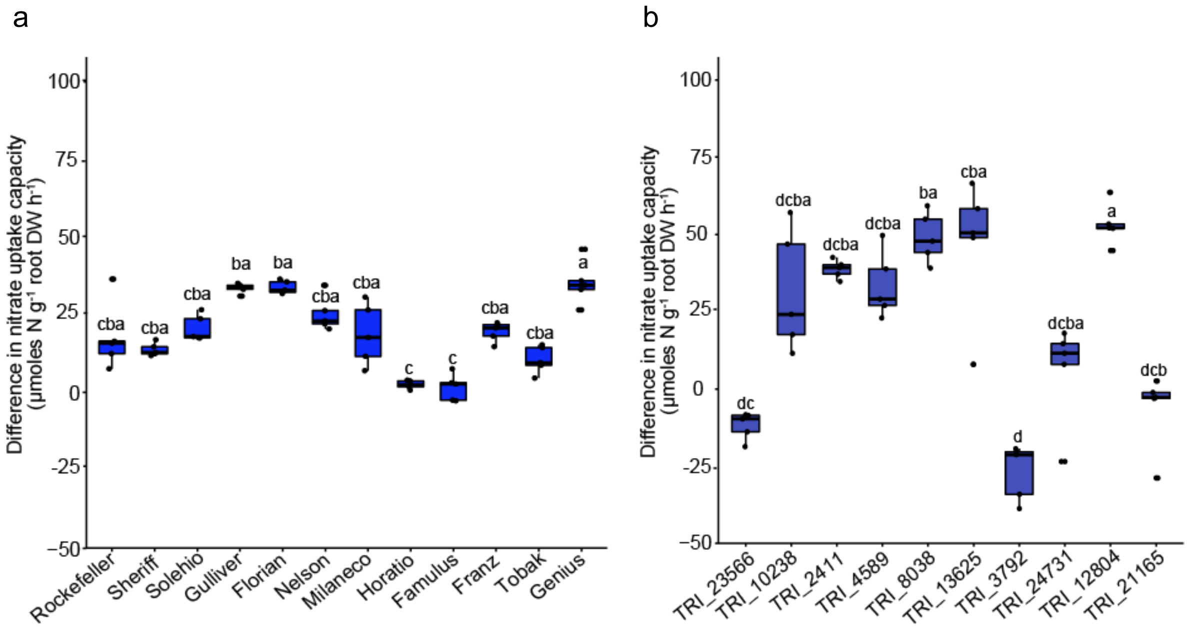

Figure 3.14. Genotypic differences in the N deficiency-induced increase of the low-affinity nitrate uptake capacity of contrasting lines from the (a) adapted and (b) unadapted panel. Values were obtained by subtracting the uptake rate of seedlings grown in N-sufficient condition (+N) from the uptake rate of seedlings grown in N-deficient conditions (-N). Plants were grown as described in Fig. 3.13. The boxes show the first quartile, median and third quartile; the whiskers indicate the minimum and maximum values; negative values indicate that uptake rate under +N were higher than under -N. Different letters indicate differences between means according to ANOVA and Tukey's test; n = 5. DW, dry weight.

For the low-affinity nitrate uptake capacity (Figure 3.14a, b), N responsiveness of adapted and unadapted lines was much lower than for high-affinity nitrate uptake (Figure 3.12a, b). Some of the lines in the unadapted panel had a negative mean value, meaning that these lines didn’t increase but actually decreased its nitrate uptake capacity under low N relative to high N conditions.

To examine if the ammonium uptake capacity relates to the nitrate uptake capacity of the same line, a correlation was made across all lines from one panel. In this case, high-affinity uptake capacities for ammonium and nitrate were plotted against each other, for values obtained for N-sufficient or N-deficient plants separately and compared between the two wheat panels.

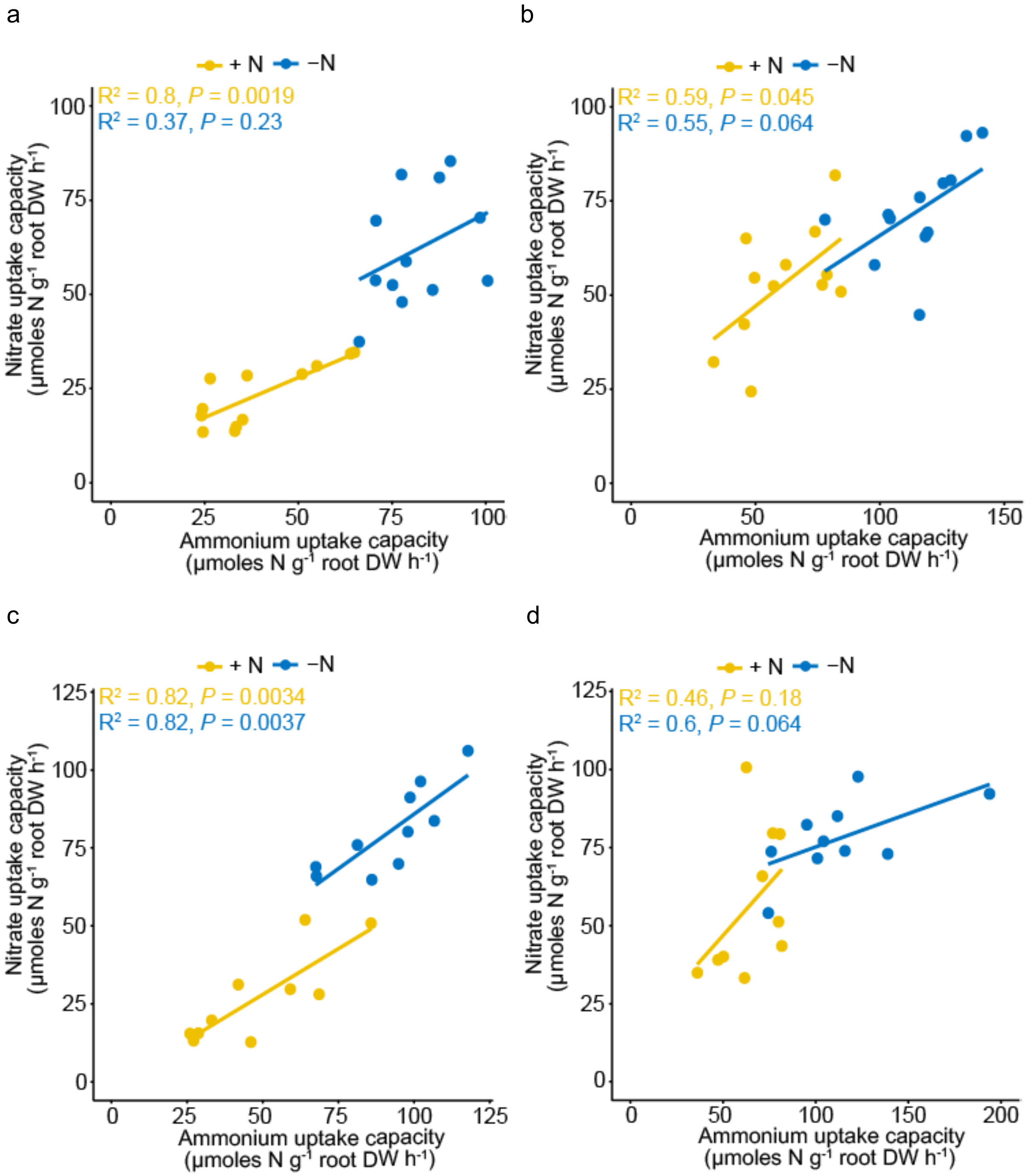

Figure 3.15. Correlation between ammonium and nitrate uptake capacity in contrasting lines of two wheat panels. (a) High-affinity ammonium uptake capacity plotted against high-affinity nitrate uptake capacity for adapted lines, (b) Low-affinity ammonium uptake capacity plotted against low-affinity nitrate uptake capacity for adapted lines, (c) High-affinity ammonium uptake capacity plotted against high-affinity nitrate uptake capacity for unadapted lines, (d) Low-affinity ammonium uptake capacity plotted against low-affinity nitrate uptake capacity for unadapted lines. +N represents nitrogen sufficient and -N represents nitrogen deficient condition for 2 days, R^2 represents the Pearson correlation value. DW, dry weight.

Regarding the adapted lines, high-affinity ammonium uptake capacity correlated significantly with high-affinity nitrate uptake capacity when plants were N sufficient (Figure 3.15a). However, in N-deficient plants correlation got lost, suggesting that ammonium and nitrate uptake capacities are differentially upregulated in the individual lines. In the low-affinity range, where uptake rates were less different between N-sufficient and N-deficient plants, the correlation was weak (Figure 3.15b).

In the unadapted lines, there was a highly convincing correlation between high-affinity ammonium and nitrate uptake capacities irrespective of N preculture (Figure 3.15c). By contrast, this correlation got lost in the low-affinity range (Figure 3.15d). The latter confirms the lower importance of the plant N status for low-affinity uptake systems, while the former may point to common regulatory mechanisms enhancing high-affinity ammonium and nitrate capacities in common in unadapted germplasm.

3.3 Root system architecture of contrasting lines in the elite gene pool

Variation in root N uptake capacity may also be caused by differences in root system architecture (Giehl et al., 2014). To verify differences in root morphological traits, 6 contrasting wheat lines from the elite panel were pre-cultured for 10 days under high and low N before individual seminal roots were combed, scanned and analysed for quantitative root traits.

Representative images of single seminal roots from two contrasting lines showed as most obvious difference that lateral roots elongated when grown under low N (LN) (Figure 3.16a). The total number of seminal roots did not change when plants were pre-cultured under HN or LN (Figure 3.16b). Actually, no significant difference among lines in this trait was expected because the number of seminal roots developed before the LN treatment set in. However, average seminal root length was significantly higher when plants were grown under HN than under LN, especially Sheriff and Solehio showed a drastic response to N (Figure 3.16c). Thus, genotypic variation for seminal root length was high under HN but not under LN. Regarding lateral root development, lateral number per seminal root, as well as the average seminal root length, were both higher in N-deficient plants. However, the three lines with high N uptake capacity (Franz, Tobak, Genius) were not superior to the other three lines in these root traits, especially not under low N culture. Thus, the high N uptake capacity of Franz, Tobak and Genius was most likely not caused by higher root length.

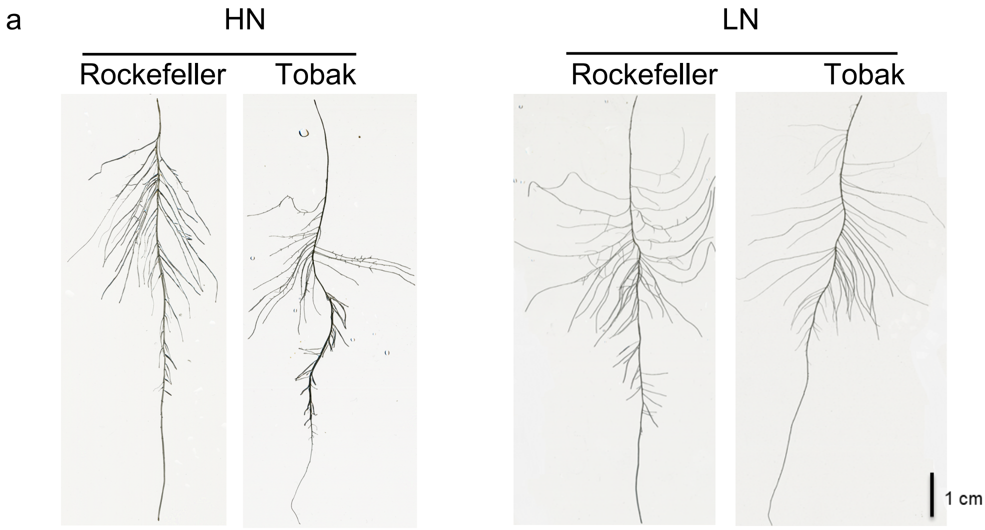

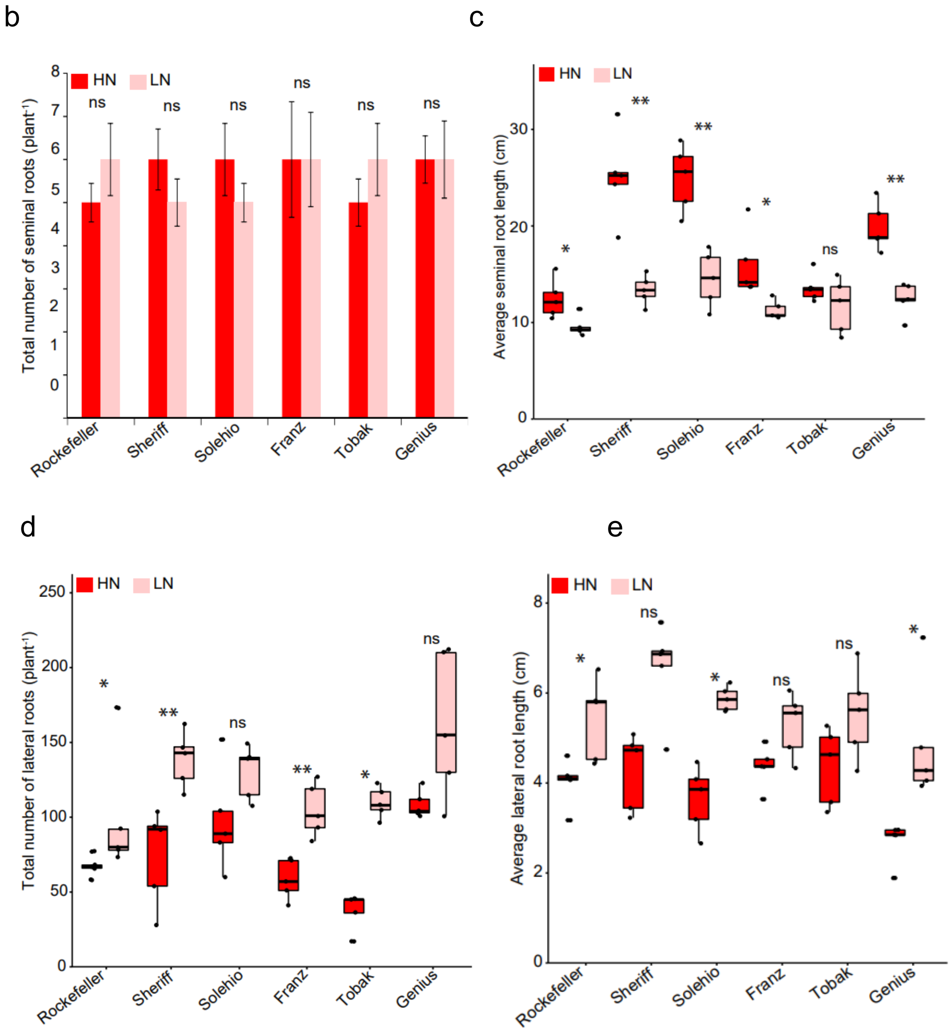

Figure 3.16. Analysis of root system architecture of adapted lines with contrasting N uptake capacity. (a) Representative images of a single seminal root and lateral roots of the line Rockefeller (low N uptake capacity) and Tobak (high N uptake capacity). (b) Total number of seminal roots, (c) average seminal root length, (d) total number of lateral roots, and (e) average lateral root length. Plants were grown hydroponically for 10 days on 1 mM (HN) or 100 μM (LN) ammonium nitrate. The boxes show the first quartile, median and third quartile; the whiskers indicate the minimum and maximum values (n = 5 independent biological replicates). Significant differences between HN and LN in a single line are indicated with * at $P < 0.05$ or with ** at $P < 0.01$ according to Tukey's test. ns, not significant. HN = high nitrogen, LN = low nitrogen. Scale bars, 1 cm.

3.4 Detailed physiological analysis of 2 contrasting adapted lines

3.4.1 Short- and long-term ammonium and nitrate uptake on 2 contrasting lines in the high- and low-affinity substrate concentration range

In the previous uptake experiments (Figure 3.1a, Figure 3.7, Figure 3.9, Figure 3.11, Figure 3.13) ammonium or nitrate uptake were determined over a period of 1 h. Such a longer-term period allows sufficient enrichment of the tracer and in roots and shoots and decreases the error rate among replicas when many lines are examined at the same time.

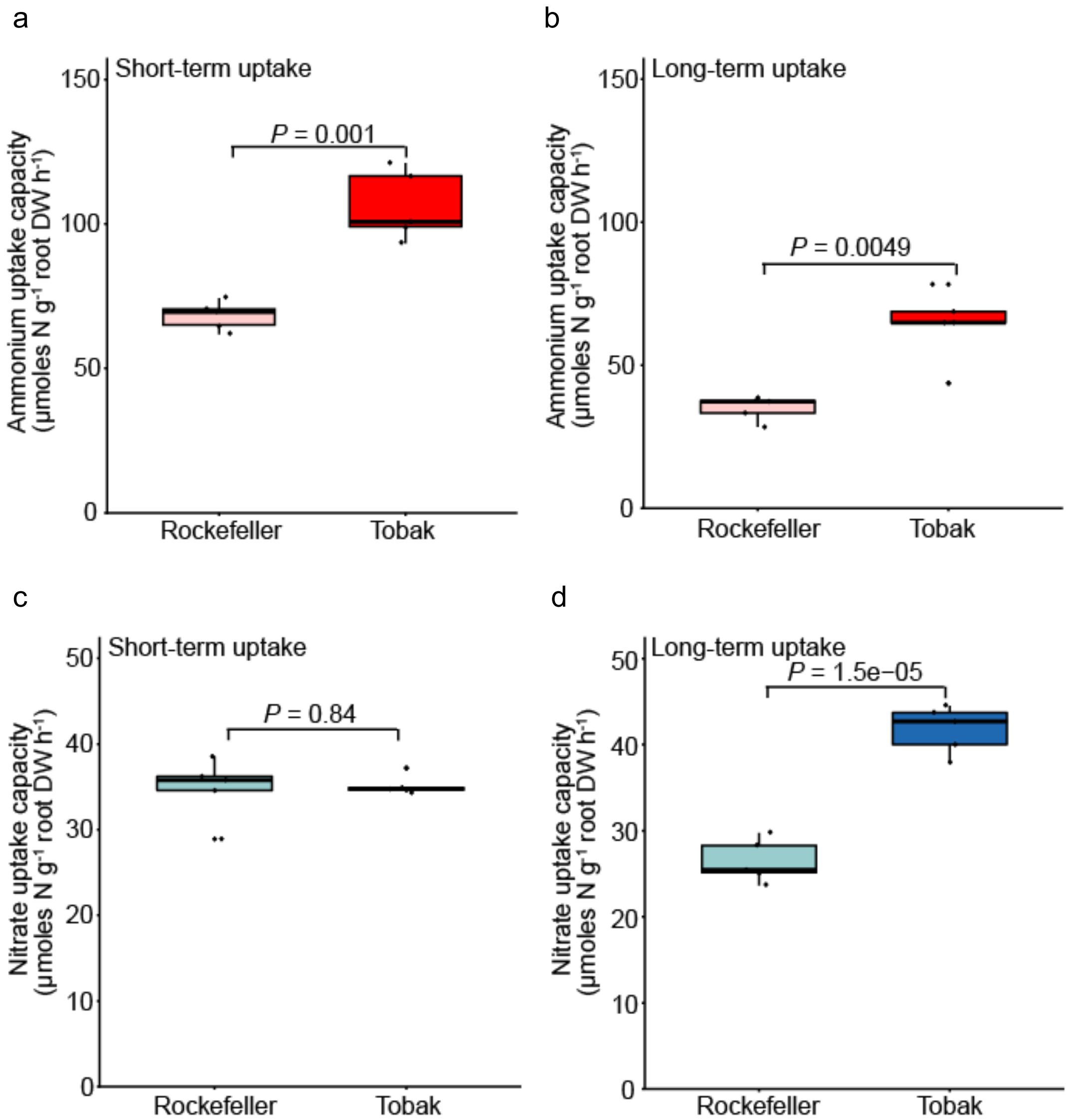

Figure 3.17. High-affinity ammonium and nitrate uptake capacity as determined over short or long-term in two contrasting adapted lines. (a, b) High-affinity ammonium uptake capacity for Rockefeller and Tobak as determined within 6 min (short term; a) or 1 h (long term; b) and (c, d) high-affinity nitrate uptake capacity for Rockefeller and Tobak as determined within 6 min (short term; c) or 1 h (long term; d). Plants were grown hydroponically on ammonium nitrate for 10 days and then on N-free nutrient solution (-N) for 2 days. Roots were exposed to 100 µM single-labelled $^{15}(NH_4)_2SO_4$ or 200 µM $K(^{15}NO_3)$ for a period of 6 min or 1 h prior to harvest. The boxes show the first quartile, median and third quartile; the whiskers indicate the minimum and maximum values (n = 5 independent biological replicates). P-values indicate differences between means according to ANOVA and Tukey's test. DW, dry weight.

On the other hand, ammonium and nitrate uptake rates will not remain constant but become repressed over time due to systemic N saturation signals repressing transport capacities (Glass, 2002). To verify whether the genotypic differences in N uptake over the long term observed between Tobak with high and Rockefeller with low nitrogen uptake capacity are also reflected over the short term, ammonium and nitrate influx was compared in both lines.

Short-term influx analysis measured after 2 days of N deficiency showed that the $^{15}NH_4^+$ uptake capacity is 2-fold higher in Tobak than in Rockefeller, whereas there was no difference in $^{15}NO_3^-$ uptake (Figure 3.17a, c). In comparison, over the long-term ammonium uptake rates decreased due to systemic repression taken place within the uptake period of 1 h, while the superior uptake capacity of Tobak over Rockefeller remained (Figure 3.17c). Unexpectedly, nitrate uptake rates by Tobak were approx. 1.5-fold higher than in Rockefeller (Figure 3.17d).

When referring to the absolute values, the capacity for high-affinity $^{15}NH_4^+$ uptake was in each case higher than for $^{15}NO_3$ (Figure 3.17), suggesting a relative preference of N-deficient roots for uptake of NH_4^+ over NO_3^-.

The capacity for low-affinity uptake was examined at 2 mM of external $^{15}NH_4$ and $^{15}NO_3$ again over a period of 6 min or 1 hr. Here, plants were precultured under high N in order to maintain expression low-affinity transport systems at a high level. Tobak showed approx. 25% higher $^{15}NH_4$ uptake capacity than Rockefeller irrespective of whether uptake rates were determined within 6 min or 1 hr (Figure 3.18a, c). In principle, the same observation was made for nitrate. However, the apparently higher nitrate influx determined within 6 min was not significantly different between the two lines due to a large variation of uptake rates in the biological replicates of Rockefeller (Figure 3.18b, d).

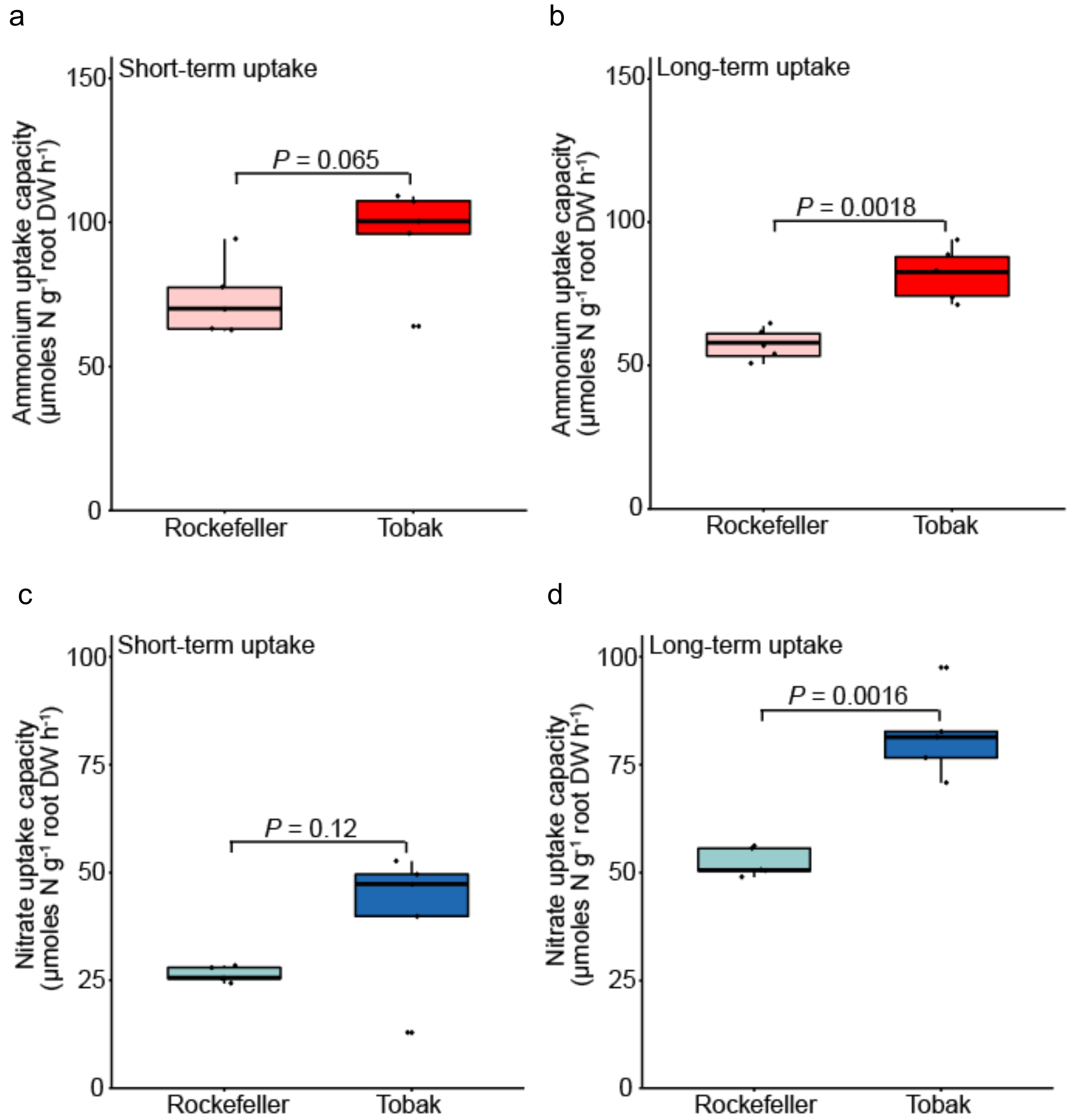

Figure 3.18. Low-affinity ammonium and nitrate uptake capacity as determined over short or long-term in two contrasting adapted lines. (a, b) Low-affinity ammonium uptake capacity for Rockefeller and Tobak as determined within 6 min (short term; a) or 1 h (long term; b) and (c, d) low-affinity nitrate uptake capacity for Rockefeller and Tobak as determined within 6 min (short term; c) or 1 h (long term; d). Plants were grown hydroponically on ammonium nitrate for 10 days and then on N-free nutrient solution (-N) for 2 days. Roots were exposed to 1 mM single-labelled $^{15}(NH_4)_2SO_4$ or 2 mM $K(^{15}NO_3)$ for a period of 6 min and 1 h prior to harvest. The boxes show the first quartile, median and third quartile; the whiskers indicate the minimum and maximum values (n = 5 independent biological replicates). P-values indicate differences between means according to ANOVA and Tukey's test. DW, dry weight.

3.4.2 Impact of the N nutritional status on N uptake capacity in the contrasting wheat lines Rockefeller and Tobak

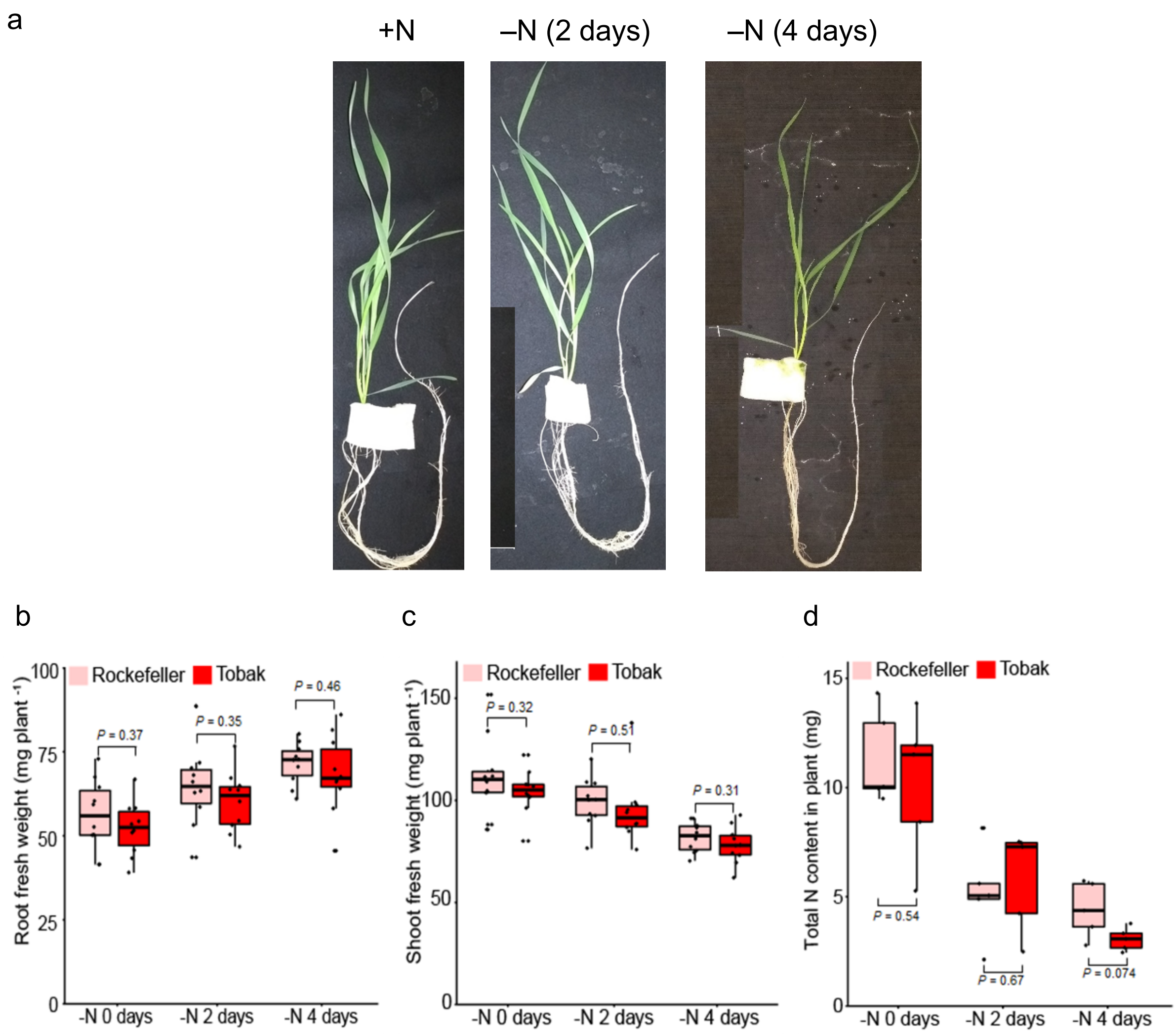

Figure 3.19. Impact of a nitrogen starvation treatment on growth and N content of two contrasting adapted wheat lines. (a) Visual appearance of adapted lines grown hydroponically under 0, 2 or 4 days of N starvation, (b) root fresh weight, (c) shoot fresh weight, (d) total nitrogen (N) content. Hydroponically grown Rockefeller and Tobak plants were precultured on ammonium nitrate and then either continued to grow on 2 mM N (-N 0 d) or transferred to N-free nutrient solution (-N) for 2 or 4 days. At harvest, all plants were 12 d old. The boxes show the first quartile, median and third quartile; the whiskers indicate the minimum and maximum values (n = 10 independent biological replicates). P-values indicate differences between means according to ANOVA and Tukey's test.

Short- and long-term ammonium and nitrate uptake capacity results showed that Tobak has mostly a higher uptake capacity than Rockefeller for either N form (Figure 3.17, Figure 3.18). To investigate whether the superior uptake capacity of Tobak is maintained under prolonged N starvation, i.e. when high-affinity uptake systems become more induced, both lines were grown hydroponically as in the previous experiments but this time plants were subjected to nitrogen starvation for a period of 0, 2 or 4 days.

Under prolonged N starvation, plants became lighter green and on day 4 slightly chlorotic (Figure 3.19a). As expected, root fresh weight slightly increased over the starvation period while shoot fresh weights decreased, but there was no significant difference observed between Rockefeller and Tobak (Figure 3.19b, c). There was also an approx. 2-fold drop into the plant N content which tended to be stronger in Tobak than in Rockefeller (Figure 3.19d). Taken together, the N starvation treatment induced the expected growth response in both lines, allowing direct comparison of subsequently measured N uptake rates.

Before harvesting the plants, long term nitrogen uptake capacity was determined in both, the high- and low-affinity concentration range. Like in the initial screening experiment, also here ^{15}N-double labelled ammonium nitrate was supplied for 1 h. In both the high- and low-affinity range Tobak had an up to 25% higher nitrogen uptake capacity than Rockefeller (Figure 3.20a, b). While in the high-affinity range, N uptake increased with increasing time of N starvation to the same extent in both lines (Figure 3.20a), Rockefeller increased its low-affinity uptake capacity for N to a lower extent than Tobak (Figure 3.20b).

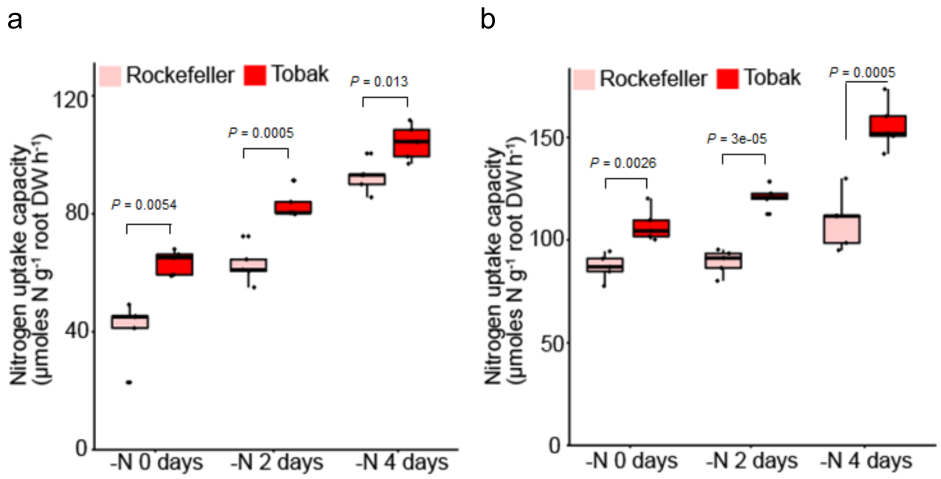

Figure 3.20. Impact of a nitrogen starvation treatment on high and low-affinity nitrogen uptake in two contrasting adapted wheat lines. (a, b) Nitrogen uptake capacity of Rockefeller and Tobak in the (a) high-affinity or (b) low-affinity concentration range. Hydroponically grown Rockefeller and Tobak plants were precultured on ammonium nitrate and then either continued to grow on 2 mM N (-N 0 d) or transferred to N-free nutrient solution (-N) for 2 or 4 days. At harvest, all plants were 12 d old. Roots were exposed to 200 µM (a) or 1 mM (b) double-labelled $^{15}NH_4{}^{15}NO_3$ for a period of 1 h in full nutrient solution. The boxes show the first quartile, median and third quartile; the whiskers indicate the minimum and maximum values (n = 5 independent biological replicates). P-values indicate differences between means according to ANOVA and Tukey's test. DW, dry weight.

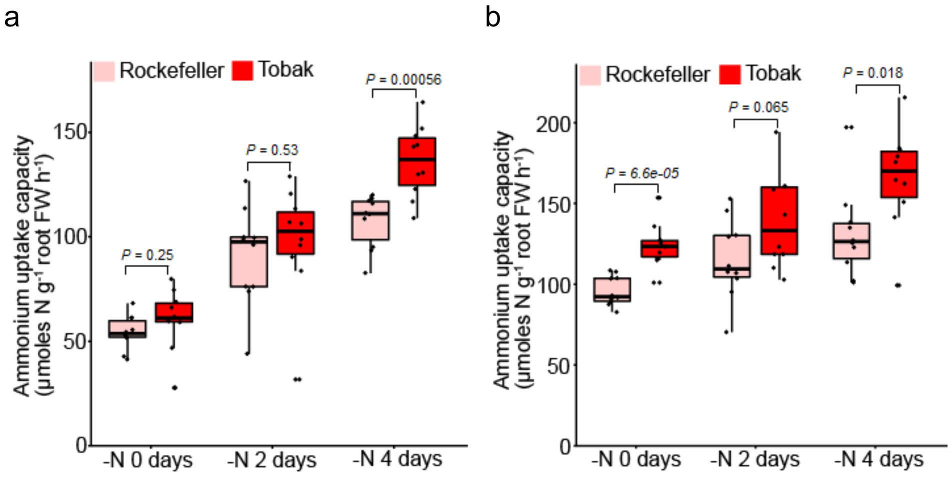

Figure 3.21. Impact of a nitrogen starvation treatment on high- and low-affinity ammonium uptake capacity in two contrasting adapted wheat lines. Ammonium uptake capacity of Rockefeller and Tobak in the (a) high-affinity or (b) low-affinity concentration range. Hydroponically grown Rockefeller and Tobak plants were precultured on ammonium nitrate and then either continued to grow on 2 mM N (-N 0 d) or transferred to N-free nutrient solution (-N) for 2 or 4 days. At harvest, all plants were 12 d old. Roots were exposed to 100 µM (a) or 1 mM (b) $^{15}(NH_4)_2SO_4$ for a period of 6 min in full nutrient solution. The boxes show the first quartile, median and third quartile; the whiskers indicate the minimum and maximum values (n = 10 independent biological replicates). P-values indicate differences between means according to ANOVA and Tukey's test. FW, fresh weight.

To verify whether the same N status-dependent increase is also reflected at the level of the high-affinity ammonium uptake capacity, short-term $^{15}NH_4^+$ uptake capacity was measured at 200 µM or 2 mM ammonium. In the high-affinity range, ammonium influx increased with the period of preculture under N starvation in both lines. However, the increase in uptake capacity was stronger for Tobak, resulting in a significantly higher uptake capacity after 4 d of N starvation (Figure 3.21a). In the low-affinity range, the N starvation-induced increase in ammonium uptake capacity was weaker and significantly higher in Tobak only at day 0 but no longer after 2 or 4 d of N starvation (Figure 3.21b). These results indicated that at least a large part of the superior N uptake in Tobak was also reflected in higher ammonium uptake capacity, which was more evident in the high-affinity range.

3.4.3 Transcript abundance of *AMT* genes in the lines Rockefeller and Tobak in response to N starvation

When precultured under N deficiency for two days, the lines Rockefeller and Tobak from the adapted wheat panel showed significant differences with a higher ammonium uptake capacity of Tobak in the high- and low-affinity concentration range (Figure 3.21a, b). To investigate whether these differences are due to differential expression of *AMT* genes, a new hydroponic experiment was performed in which both lines were grown again under same conditions as before to collect root material for RNA extraction and gene expression analysis. In the qPCR analysis, transcript abundance of *AMT2* could not be detected due to technical difficulties in the qPCR amplification of *AMT2*. After 2 days of N deficiency, *AMT1.1* and *AMT1.2* mRNA levels were about half of N-adequate plants while after 4 days of N deficiency there was no more difference to control treatments (Figure 3.22a, b). Transcript levels of both genes, *AMT1.1* and *AMT1.2,* did not show considerable differences between Rockefeller and Tobak, except for a small difference in *AMT1.1* after 4 days of N deficiency (Figure 3.22a, b).

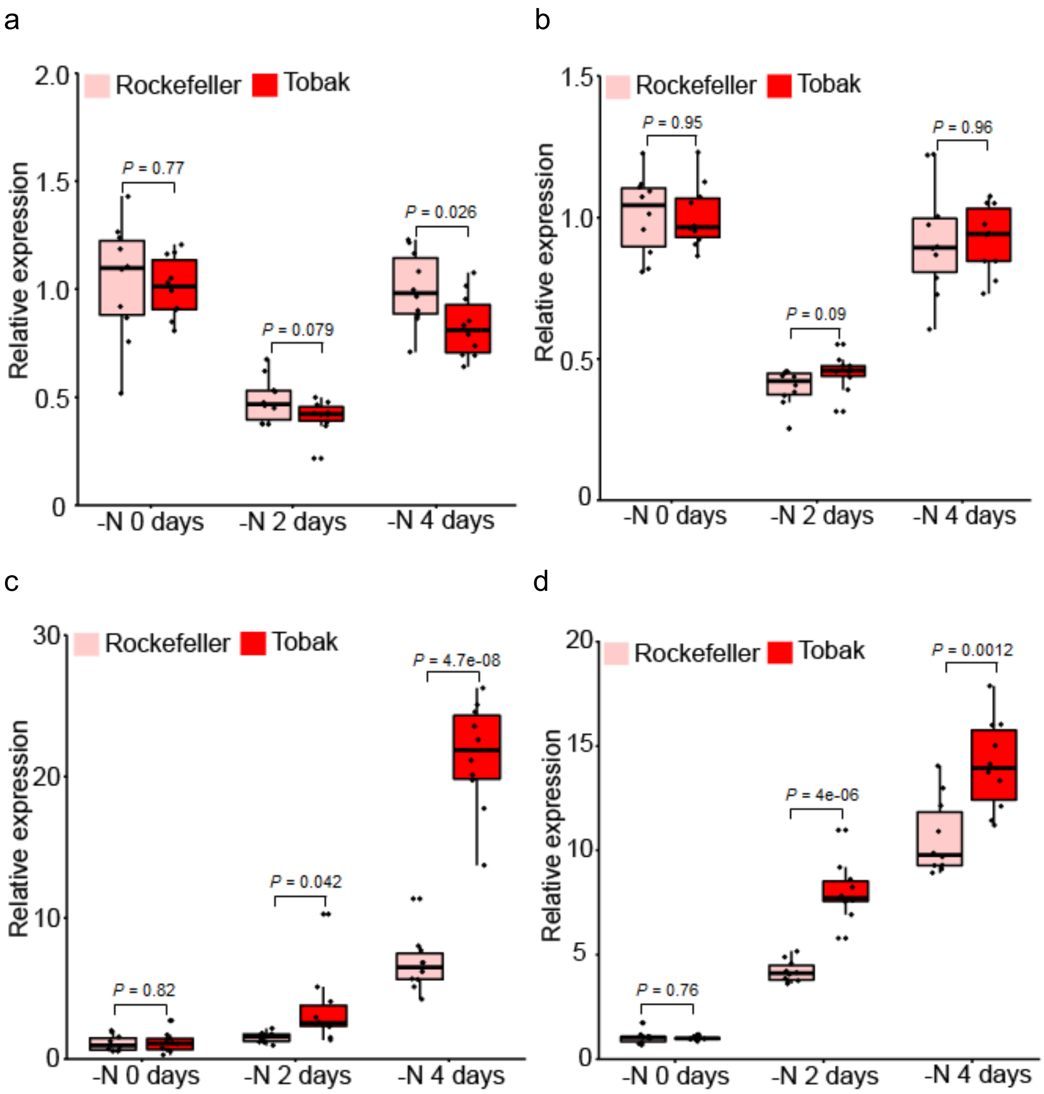

Figure 3.22. Transcript abundance of *AMT* genes in the lines Rockefeller and Tobak in response to N deficiency. Relative expression levels of (a) *AMT1.1* (b) *AMT1.2* (c) *AMT3.1* (d) *AMT3.2*. Plants were grown hydroponically for 12 days on 2 mN NH_4NO_3 continuously (-N 0 days) or on N-free nutrient solution for 2 or 4 days (-N 2 or 4 days, resp.). On 12 d, roots were exposed to 100 µM single-labelled $^{15}(NH_4)_2SO_4$ for a period of 6 min in full nutrient solution. The boxes show the first quartile, median and third quartile; the whiskers indicate the minimum and maximum values (n = 10 independent biological replicates). P-values indicate differences between means according to ANOVA and Tukey's test; n = 10.

In contrast, *AMT3.1* and *AMT3.2* transcript levels continuously increased under N deficiency in both lines. Interestingly, in Tobak starved for 4 days under N deficiency, this increase resulted in up to 15-20 times higher transcript levels than under N-adequate conditions, while the corresponding increase was just 5-10 times in Rockefeller (Figure 3.22c, d). Thus, the upregulation of *AMT3.1* gene expression was approx. 3 times higher in Tobak than in Rockefeller, and for *AMT3.2* still 1.5- to 2-fold.

To identify the *AMT* genes contributing most to the NH_4^+ influx that had been determined in the previous experiment (Figure 3.21), high-affinity NH_4^+ influx was correlated with *AMT* transcript levels. In both lines, transcript levels of *AMT1.1* and *AMT1.2* did not correlate with NH_4^+ influx (Figure 3.23a, b). On the other hand, *AMT3.1* and *AMT3.2* transcript levels of both Rockefeller and Tobak correlated significantly with NH_4^+ influx (Figure 3.23c, d). Notably, the steeper slope of Tobak in the correlation with *AMT3.1* mRNA levels indicated a more intense upregulation of *AMT3.1* than in Rockefeller. For *AMT3.2* transcripts, the correlation to NH_4^+ influx was highly similar in both lines. These findings suggest that in particular the stronger responsiveness of *AMT3.1* to N deficiency was responsible for the superior NH_4^+ uptake capacity in Tobak.

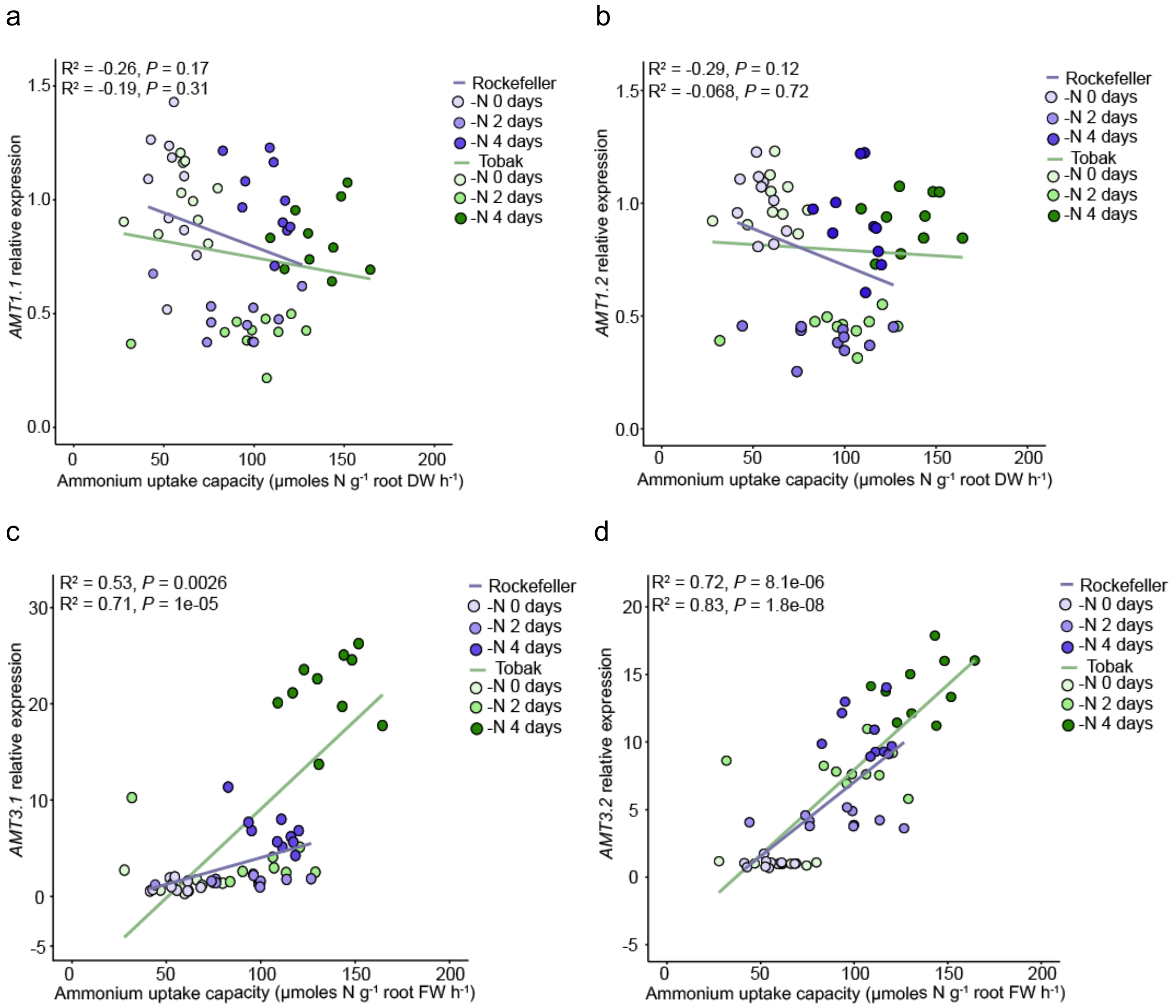

Figure 3.23. Correlation between *AMT* transcript levels and high-affinity ammonium uptake capacity in the lines of Rockefeller and Tobak. High-affinity ammonium influx was plotted against relative transcript abundance of (a) *AMT1.1* (b) *AMT1.2* (c) *AMT3.1,* or (d) *AMT3.2*. Plants were grown hydroponically for 12 days on 2 mN NH_4NO_3 continuously (-N 0 days) or on N-free nutrient solution for 2 or 4 days (-N 2 or 4 days, resp.). R^2 represents the Pearson correlation coefficient. FW, fresh weight.

By re-sequencing qPCR amplicons of *AMT3.1* and *AMT3.2*, it was found that there was only little variation in the coding region at the level of the amino acid sequence between Rockefeller and Tobak, with 1 or 3 amino acid substitutions in *AMT3.1* and *AMT3.2*, respectively (Supplementary figure 4, Supplementary figure 5).

3.5 Identification and phylogenetic analysis of ammonium transporter (*AMT*) genes in wheat

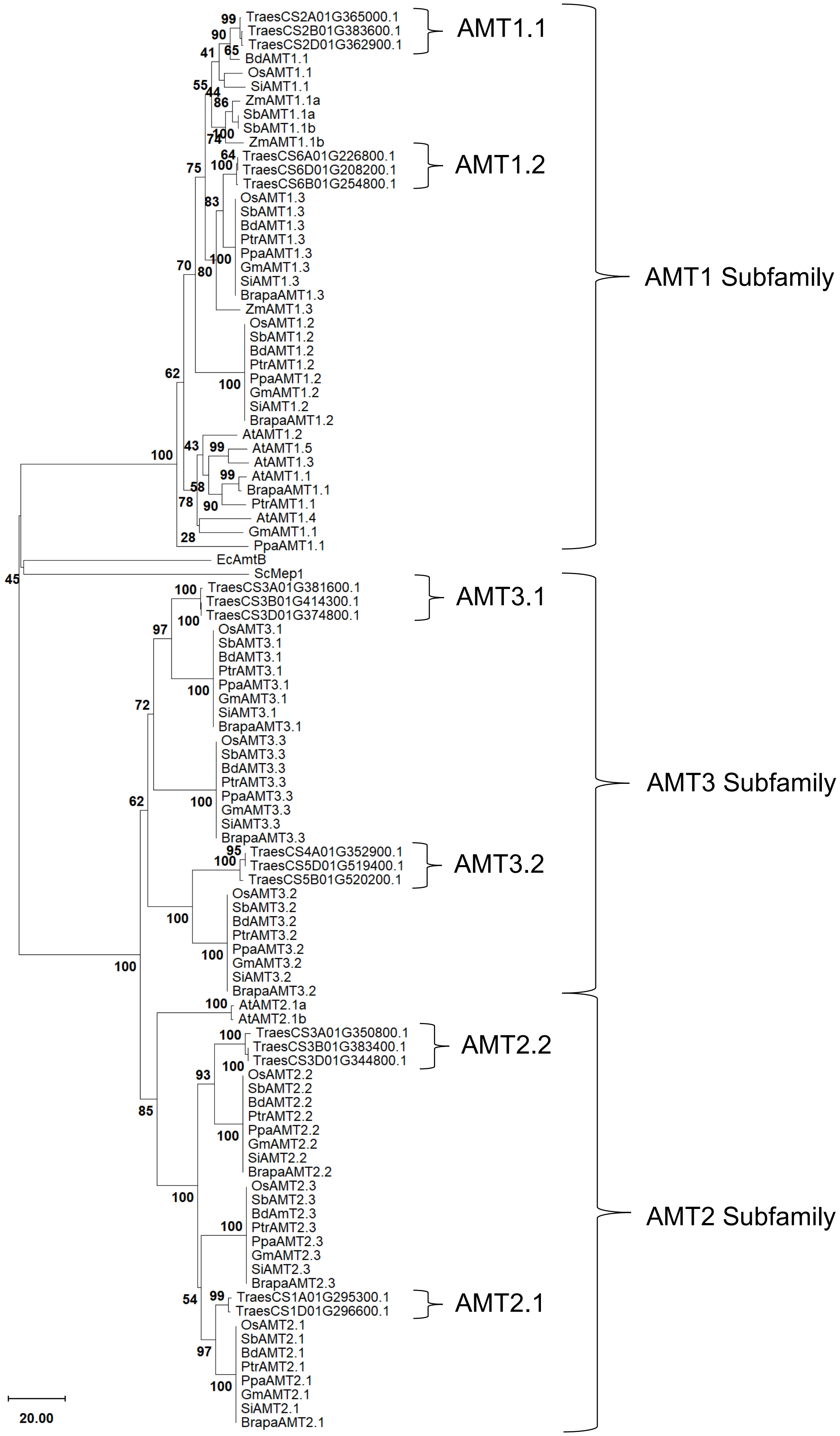

Figure 3.24. Phylogenetic analysis of wheat *AMT* genes. Neighbour-joining tree of the ammonium transporter (AMT) gene family was made by MEGA software using bootstrap values from 1000 replications. Sequence names consist of species code (first letter of genus and first letter of species name) and the AMT number. Species codes: *Ec, Escherichia coli; Sc, Sacchromyces cerevisiae; At, Arabidopsis thaliana; Os, Oryza sativa; Gm, Glycine max; Zm, Zea mays; Bd, Brachypodium distachyon; Sb, Sorghum bicolor; Si, Setaria italica; Brapa, Brassica rapa; Ptr, Populus trichocarpa; Ppa, Physcomitrella patens; Traes, Triticum aestivum.*

High-affinity ammonium transport in plant roots is mediated through membrane proteins of the ammonium transporter (AMT) family. To obtain *AMT* sequences of the the Chinese spring wheat genome (IWGSC), published rice, Arabidopsis and maize AMT sequences were used to extract AMT protein sequences from wheat. Protein blast search revealed highly similar sequences of AMTs in wheat. Phylogenetic analysis based on protein sequence alignment indicated that in wheat six sequences are clustered together with members of the three AMT subfamilies from other species (Figure 3.24). In each subfamily, three almost identical sequences represent the gene copies derived from the A, B and D genome. Only for one of the AMT2 proteins, the corresponding sequence from the B genome was not found. Thus, each AMT subfamily consisted of two paralogs, which were named AMT1.1 and 1.2, AMT2.1 and 2.2. as well as AMT3.1 and 3.2.

3.6 Allele mining and haplotype analysis

High or low ammonium uptake capacity in contrasting lines can result from amino acid variations in the protein sequences. To identify allelic variants in AMT protein sequences, genomic sequences of *AMT1.1* and *AMT1.2* were isolated from the A, B and D genome sequence of Chinese Spring (CS).

Table 4. Chromosomal positions of *AMT1.1* coding sequences in the cultivar Chinese Spring.

Triticum aestivum Chinese Spring Genome	2A01G365000	chr2A: 608871057 - 608872541
	2B01G383600	chr2B: 547057072 - 547058556
	2D01G362900	chr2D: 468856174 - 468857658

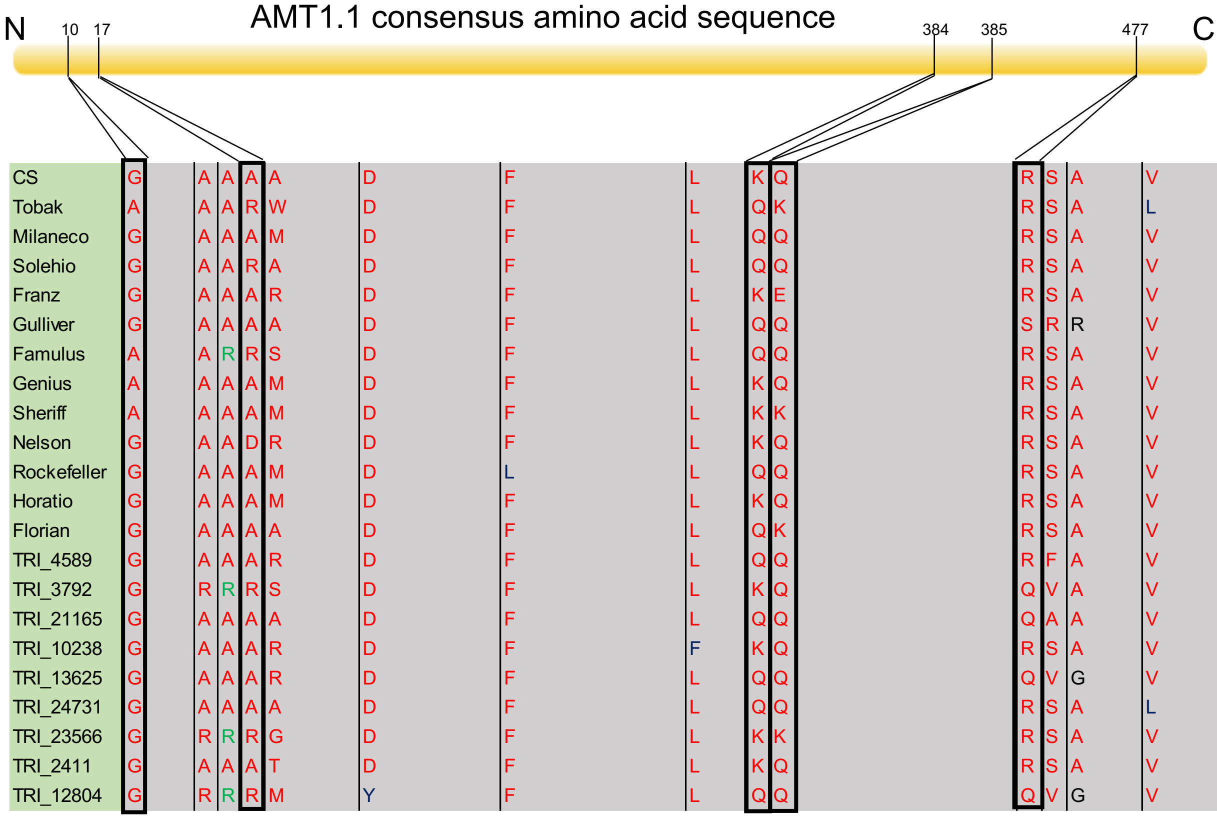

Figure 3.25. Allelic variation in AMT1.1 protein sequences of wheat lines from two panels. Allelic variation in the coding region of AMT1.1 was determined by Sanger sequencing and alignment using the cultivar Chinese Spring (CS) as reference. Adapted lines are represented by full names while unadapated lines are encoded by a TRI identifier. Black boxes indicate amino acid substitutions in several lines. Numbers indicate amino acid positions in the CS sequence.

From a consensus sequence of the three AMT1.1 copies in Chinese Spring, primers were designed that were used to amplify the genomic sequences of *AMT1.1* from a total of 22 contrasting wheat lines from the adapted and unadapted gene pool. Re-sequencing of the coding regions and translation to the protein sequence allowed to identify single amino acid polymorphisms through the alignment of protein sequences from all 22 contrasting lines (Figure 3.25; Supplementary figure 1). Based on the identified allelic variants, haplotype groups of at least 3 cultivars were formed. Then, the ammonium uptake capacity as determined previously (Figure 3.7) was related to the amino acid variation in these haplotype groups. A total of five haplotypes groups were identified in the contrasting wheat lines from the adapted and unadapted gene pool and used in this analysis (Figure 3.25).

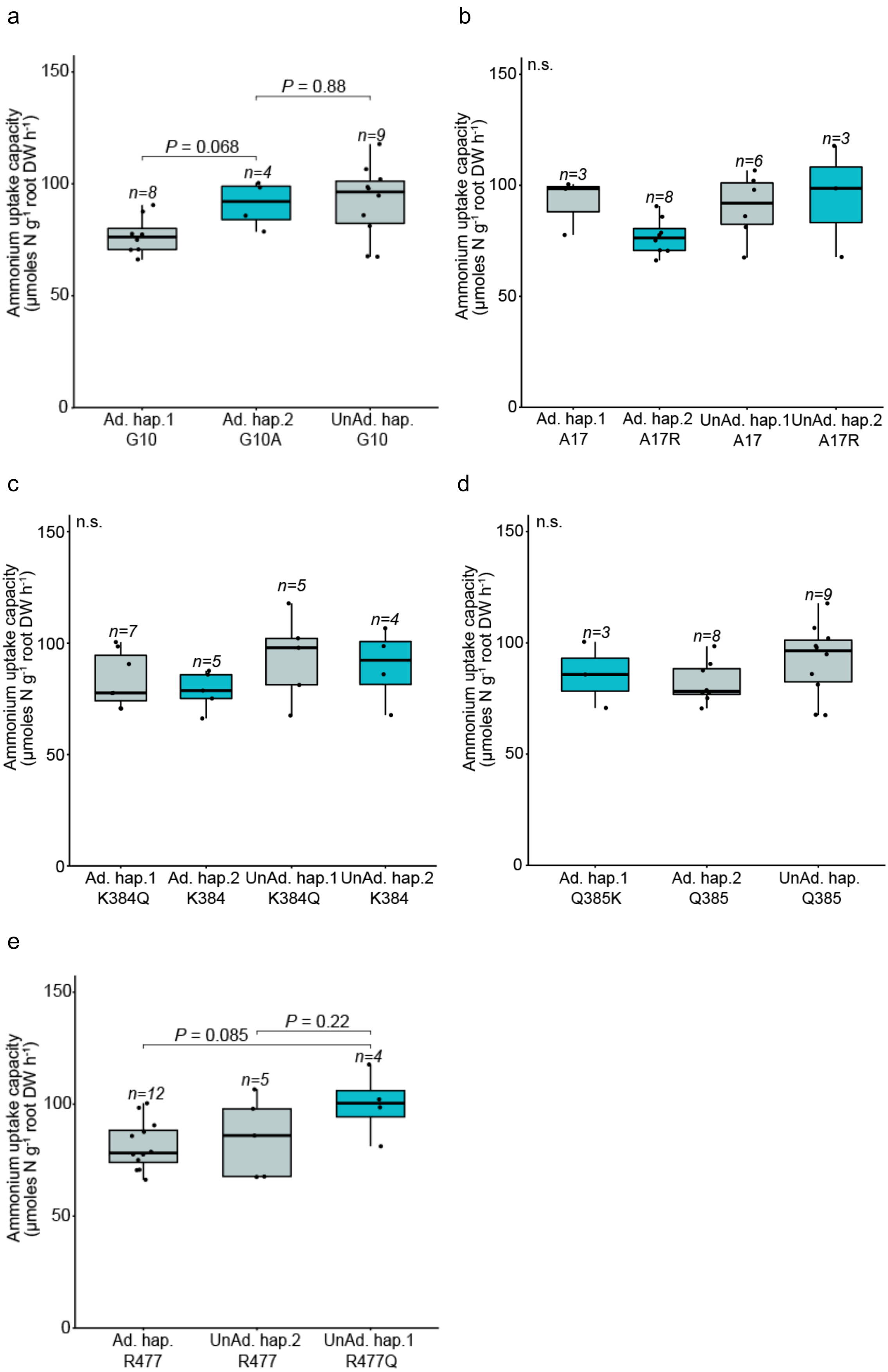

Figure 3.26. High-affinity uptake capacities for NH_4^+ of lines from different AMT1.1 haplotype groups. Haplotype groups were formed based on single amino acid substitutions identified in at least 3 out of at least 20 lines at the following positions: (a) G10 (b) A17 (c) K384 (d) Q385 (e) R477. Ammonium uptake rates were taken from (Figure 3.7b, d). n = no. of lines in a haplotype group from the adapted (Ad.) or unadapted (UnAd.) wheat panel. The boxes show the first quartile, median and third quartile; the whiskers indicate the minimum and maximum values. P-values indicate differences between means according to ANOVA and Tukey's test; n.s., no significant differences. DW, dry weight.

The first haplotype group, in which the G10A substitution was located near to the N terminus in AMT1.1, tended to coincide with higher uptake rates compared the reference sequence of 8 adapted lines (G10) but this difference was not significant. The uptake capacity of the prevalent haplotype at this position in the unadapted lines (G10) did not differ significantly from that in the adapted lines, irrespective of whether they carried G10 or G10A (Figure 3.26a). Further haplotype groups in A17, K384 or Q385 did not correlated with ammonium uptake capacity (Figure 3.26b, c, d). Also in the last haplotype group (Figure 3.26e), 4 unadapted lines carrying allele R447Q, which is located close to the C terminus in AMT1.1, showed no significantly difference in the NH_4^+ uptake capacity when compared to 12 adapted lines (R477) or to 5 remaining unadapted lines (R477). Overall, these data did not provide evidence for allelic variation in AMT1.1 that may be associated with an increased ammonium uptake capacity.

Subsequently, AMT1.2 sequences were compared to Chinese Spring and among contrasting adapted and unadapted lines. At four different positions, single amino acid substitutions were identified and used to assemble haplotype groups (Figure 3.27).

Table 5. Chromosomal positions of *AMT1.2* coding sequences in the cultivar Chinese Spring.

Triticum aestivum Chinese Spring Genome	6A01G226800	Chr6A: 426965977 - 426967488
	6B01G254800	Chr6B: 458486142 - 458487653
	6D01G208200	Chr6D: 293801964 - 293803475

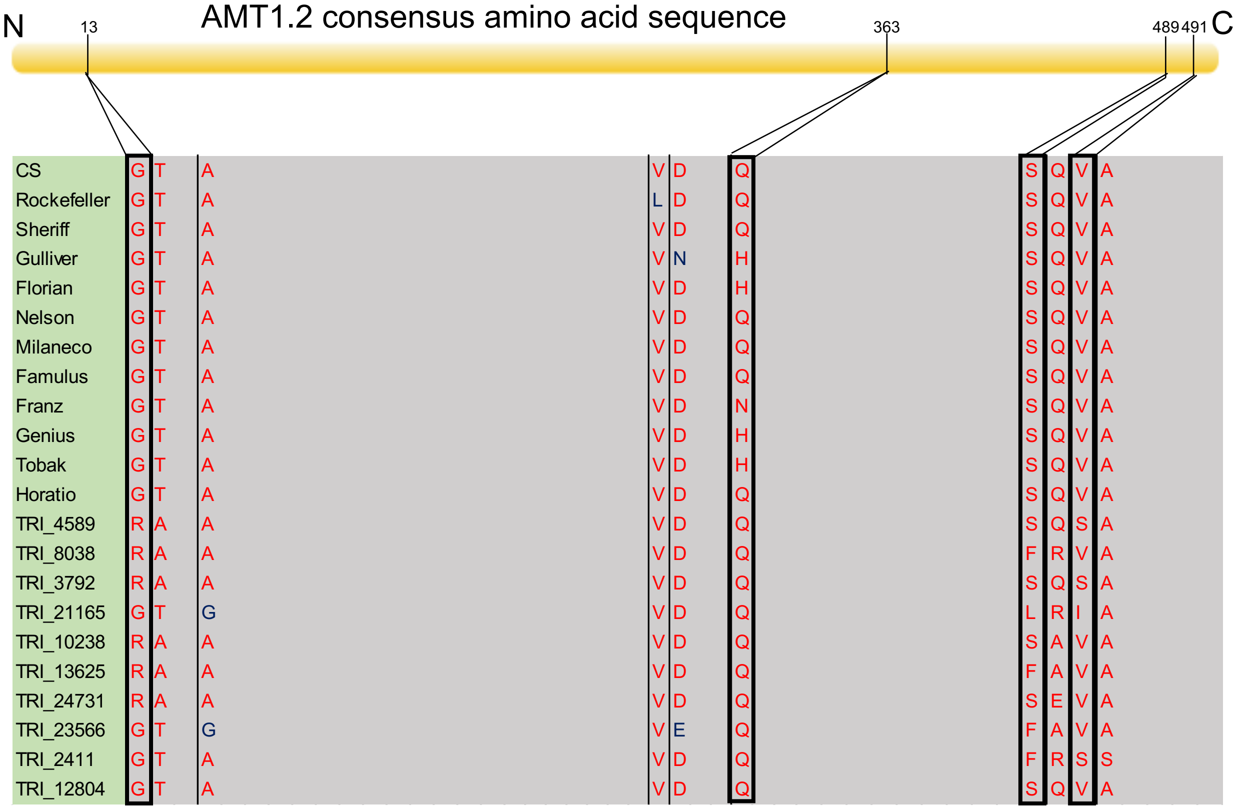

Figure 3.27. Allelic variation in AMT1.2 protein sequences of wheat lines from two panels. Allelic variation in the coding region of AMT1.2 was determined by Sanger sequencing and alignment using the cultivar Chinese Spring (CS) as reference. Adapted lines are represented by full names while unadapated lines are encoded by a TRI identifier. Black boxes indicate amino acid substitutions in several lines. Numbers indicate amino acid positions in the CS sequence.

From identified sequence variation four haplotypes groups were formed, but none of these four haplotype groups differed significantly in the ammonium uptake capacity (Figure 3.28a-d). Thus, the resequencing of *AMT1.2* genes from adapted and unadapted lines revealed no allelic variation that may be related to an altered ammonium uptake capacity.

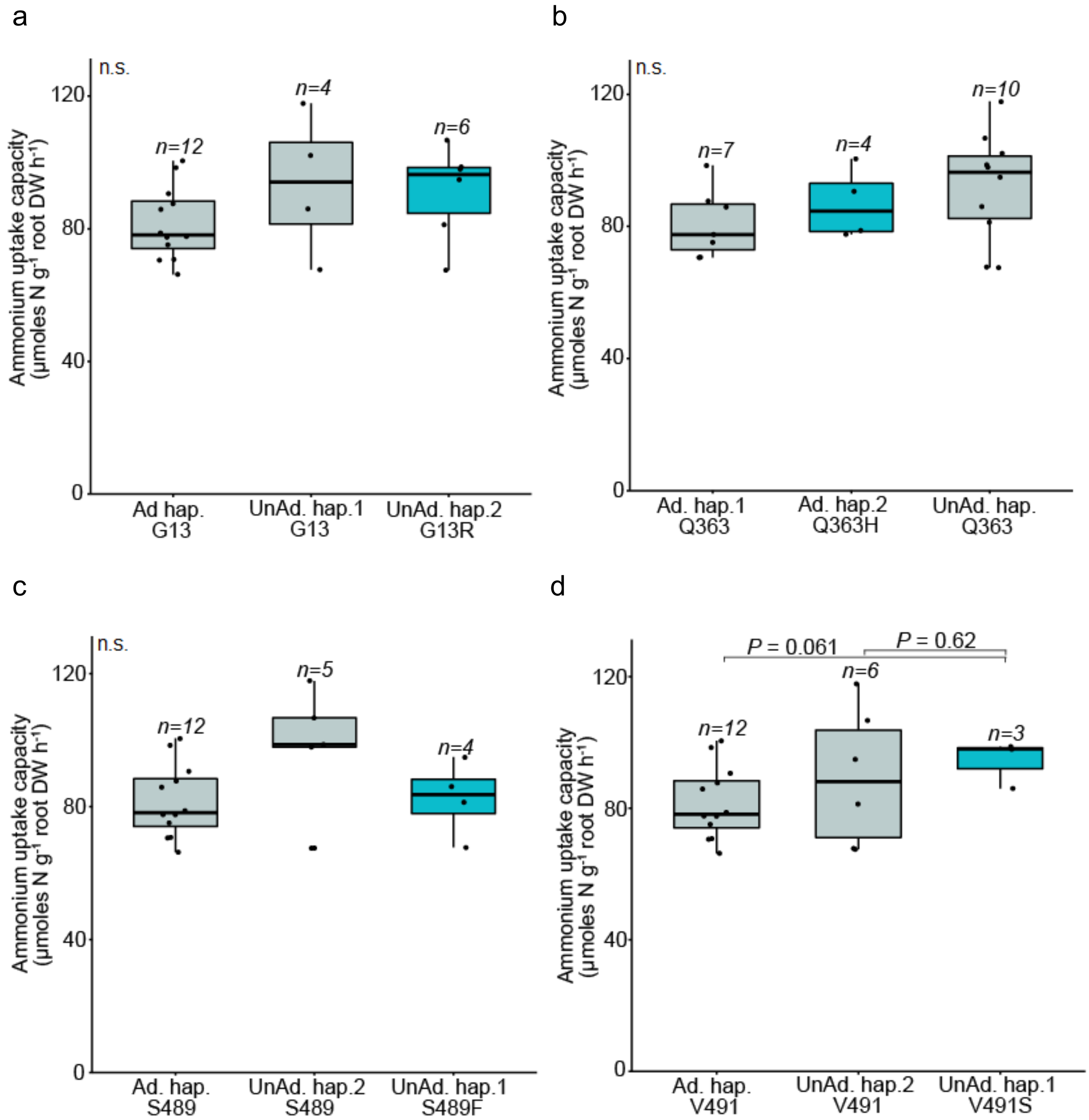

Figure 3.28. High-affinity uptake capacities for NH_4^+ of lines from different AMT1.2 haplotype groups. Haplotype groups were formed based on single amino acid substitutions identified in at least 3 out of at least 20 lines at the following positions: (a) G13 (b) Q363 (c) S489 (d) V491. Ammonium uptake rates were taken from (Figure 3.7b, d). n = no. of lines in a haplotype group from the adapted (Ad.) or unadapted (UnAd.) wheat panel. The boxes show the first quartile, median and third quartile; the whiskers indicate the minimum and maximum values. P-values indicate differences between means according to ANOVA and Tukey's test; n.s., no significant differences. DW, dry weight.

Identified allelic variants in the protein sequence of AMT1.1 or AMT1.2 could make significant changes in protein structure and folding and thus their biochemical properties. To address this point, homology modelling was performed by predicting the *ab-initio* protein structure from the translated AMT1.1 amino acid sequences obtained through re-sequencing. To build the reference structure for an AMT1.1 model the *Saccharomyces cerevisiae* AMT B protein was used (5aex1.B) (van den Berg et al., 2016).

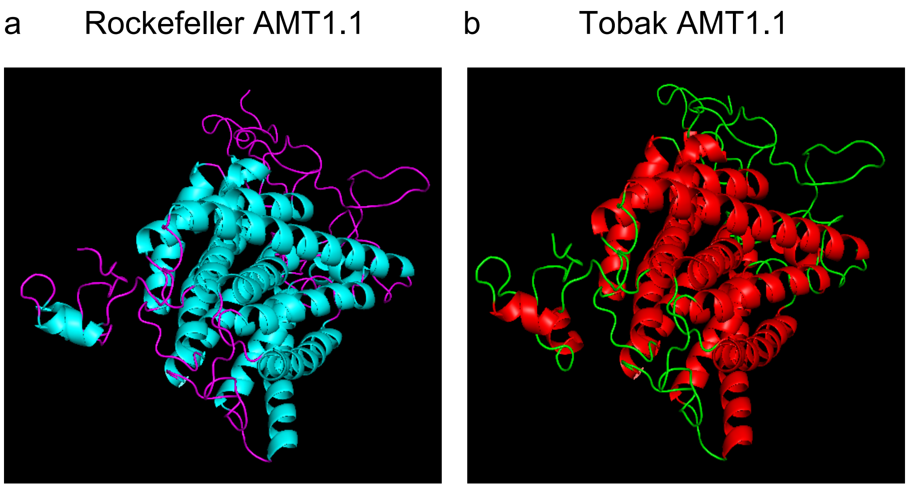

Figure 3.29. Homology modelling (ab-initio protein structure prediction) of the AMT1.1 protein on contrasting adapted wheat lines Rockefeller and Tobak in reference to Saccharomyces cerevisiae *AMT B* protein *(5Aex1.B).*

Comparing the AMT1.1 protein structures from all adapted lines did not show any apparent changes in protein folding or structure (data not shown). For instance, AMT1.1 structures of Rockefeller and Tobak, which showed consistently highly contrasting ammonium uptake rates among the adapted lines, exhibited no apparent difference (Figure 3.29), although there were 7 amino acid positions in which Rockefeller differed from Tobak (Figure 3.25). Following the same approach, AMT1.2 protein structures were predicted for all adapted lines including Rockefeller and Tobak. Interestingly, the protein structure of AMT1.2 in Tobak possessed a beta-sheet structure, which was absent in Rockefeller (Figure 3.30). Actually, also other adapted contrasting lines differed in the formation of this beta-sheet structure. Adapted lines like Sheriff, Genius, Nelson, Famulus, Tobak, Solehio were predicted to form a beta-sheet, whereas lines like Rockefeller, Horatio, Milaneco, Franz, Florian and Gulliver didn't have a beta-sheet (Figure 3.30).

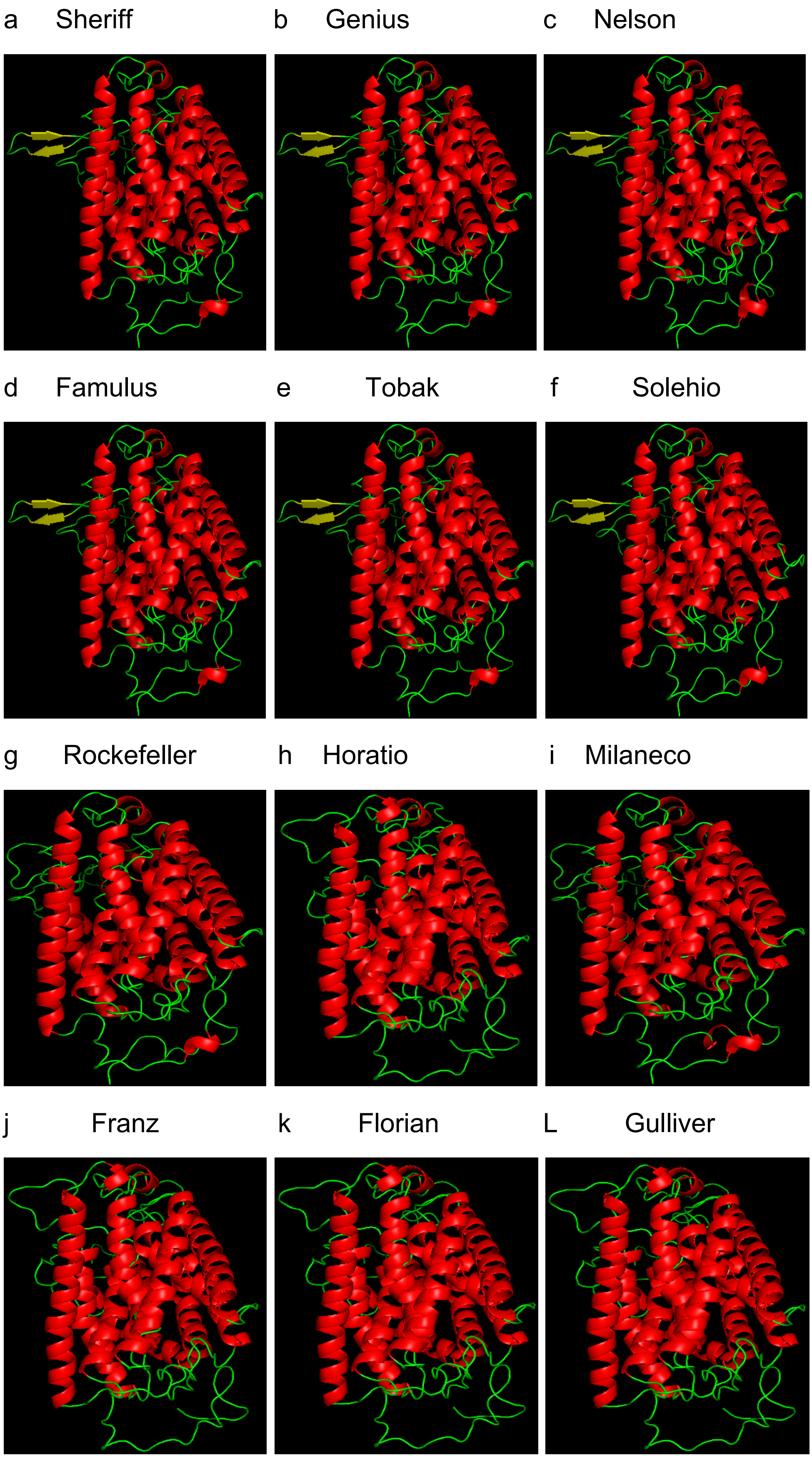

Figure 3.30. Homology modelling (ab-initio protein structure prediction) of the AMT1.2 protein on contrasting adapted wheat lines in reference to the Saccharomyces cerevisiae AMT B protein *(5Aex1.B).*

Hence, the beta-sheet structure of AMT1.2 was taken as a structural trait to form haplotype groups, which were interrogated for their ammonium uptake capacity. It appears that lines forming a beta-sheet in AMT1.2 have a significantly higher ammonium uptake capacity than those without a beta-sheet (Figure 3.31).

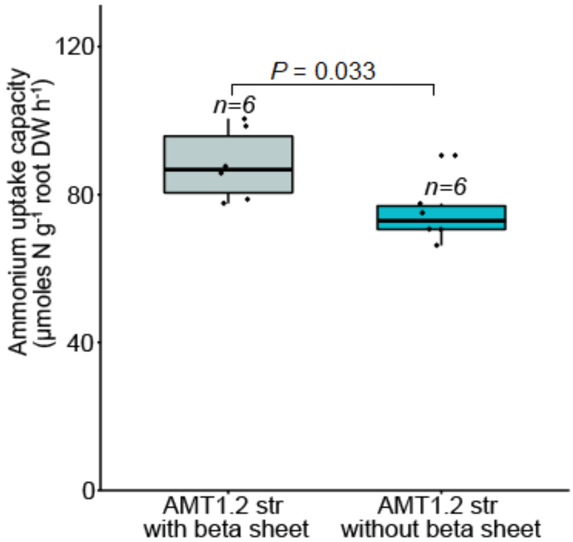

Figure 3.31. High-affinity NH_4^+ uptake capacities for two haplotype groups differing in AMT1.2 protein structure. Variation in protein structure was related exclusively to a predicted beta-sheet structure and haplotype groups were formed according to the modelling approach in (Figure 3.30). High-affinity ammonium uptake rates were taken from (Figure 3.7b, d). n = lines observed on contrasting adapted pool. The boxes show the first quartile, median and third quartile; the whiskers indicate the minimum and maximum values. The P-value indicates a significant difference between means according to ANOVA and Tukey's test. DW, dry weight.

The genomic sequence of LOC_Os10g40600, encoding a nitrate transporter referred to as *NRT1.1B* in rice, was used as a reference sequence to identify the corresponding genomic sequence in the Chinese Spring wheat A, B and D genome. In rice, *NRT1.1B* has a nitrate transport activity under both low and high nitrate conditions (Hu et al., 2015).

Table 6. Chromosomal positions of *NRT1.1b* coding sequences in the cultivar Chinese Spring.

Triticum aestivum Chinese Spring Genome	1A01G211000	Chr1A: 373770969 - 373774760
	1B01G224900	Chr1B: 403541257 - 403543754
	1D01G214200	Chr1D: 299576089 - 299578360

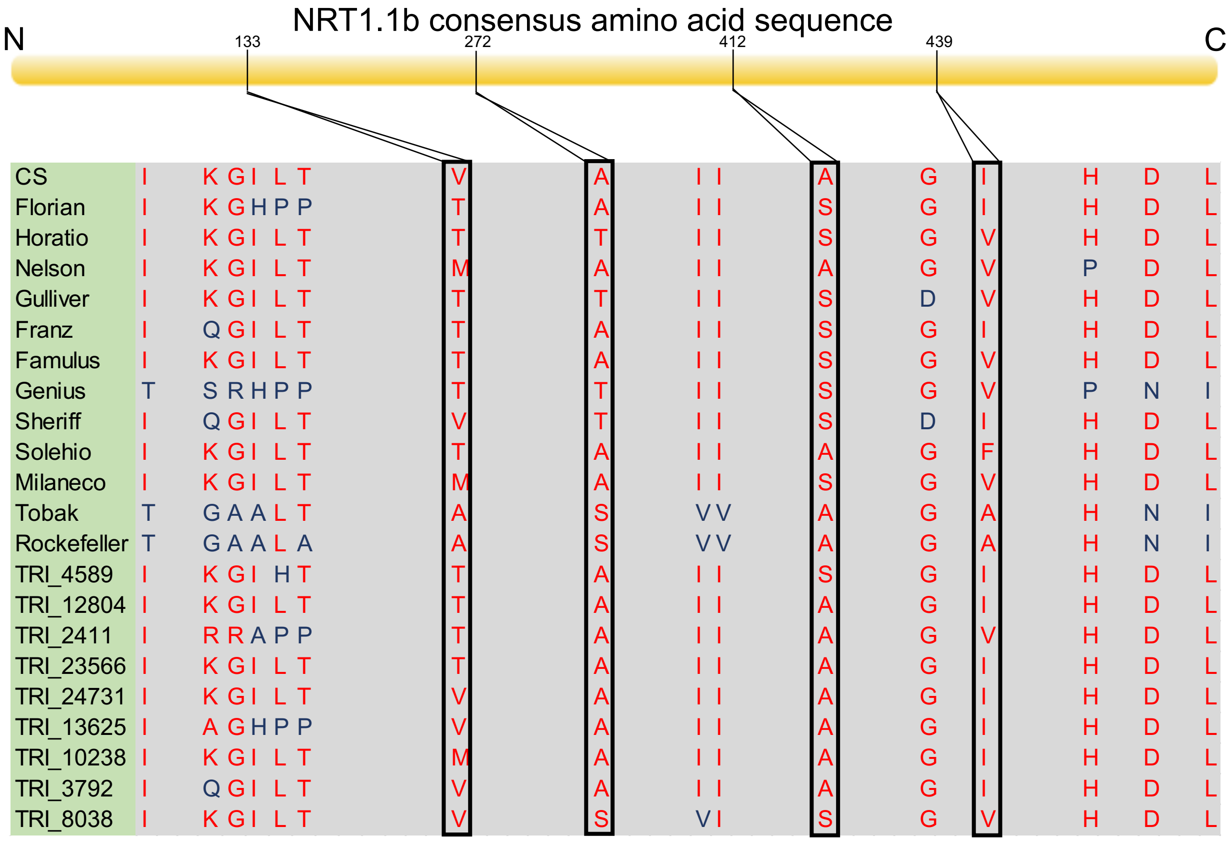

Figure 3.32. Allelic variation in NRT1.1b protein sequences of wheat lines from two panels. Allelic variation in the coding region of NRT1.1b was determined by Sanger sequencing and alignment using the cultivar Chinese Spring (CS) as reference. Adapted lines are represented by full names while unadapated lines are encoded by a TRI identifier. Black boxes indicate amino acid substitutions in several lines. Numbers indicate amino acid positions in the CS sequence.

The *NRT1.1B* coding sequence was re-sequenced from contrasting adapted and unadapted lines. Sequence analysis revealed variation at several positions within the protein sequence of NRT1.1B, although there was no amino acid signature found that was overrepresented in the adapted or unadapted lines (Figure 3.32). Out of all identified allelic variations, only a few allelic variants were suitable to form haplotype groups, which allows to investigate if they correlate with variation in high- or low-affinity nitrate uptake capacity. With regard to high-affinity nitrate uptake, there were only tendencies of different uptake capacities between haplotype groups with substitutions at V133 or A412 (Figure 3.33a-c). However, at V432 unadapted lines showed a significantly higher high-affinity nitrate uptake capacity than adapted lines carrying the V439I substitution, but this difference disappeared when referring to the other control group i.e. adapted lines with the V432 haplotype (Figure 3.33d).

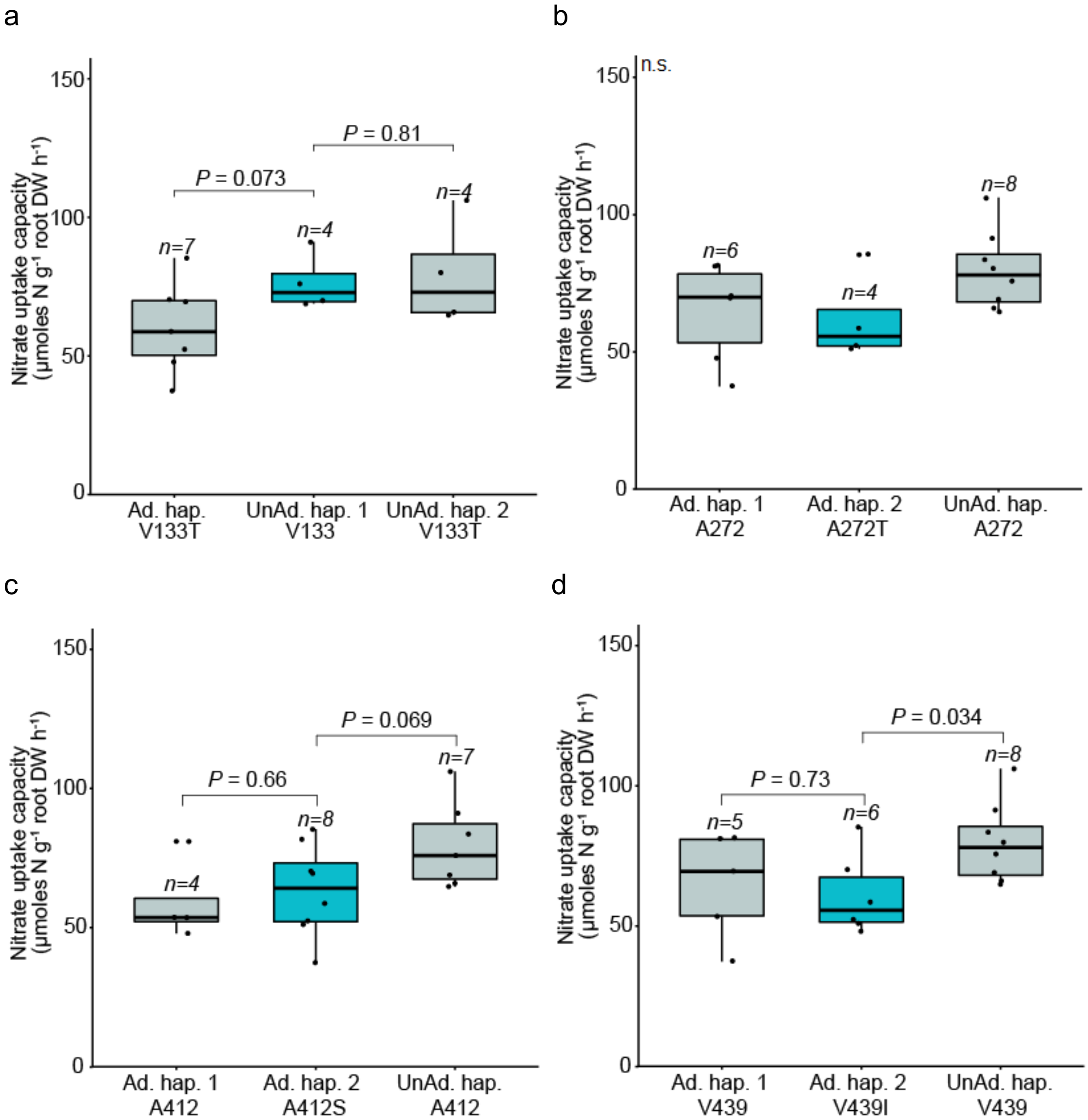

Figure 3.33. High-affinity uptake capacities for NO_3^- of lines from different NRT1.1b haplotype groups. Haplotype groups were formed based on single amino acid substitutions identified in at least 3 out of at least 20 lines at the following positions: (a) V133 (b) A272 (c) A412 (d) V439. Nitrate uptake rates were taken from (Figure 3.11b, d). n = no. of lines in a haplotype group from the adapted (Ad.) or unadapted (UnAd.) wheat panel. The boxes show the first quartile, median and third quartile; the whiskers indicate the minimum and maximum values. P-values indicate differences between means according to ANOVA and Tukey's test; n.s., no significant differences. DW, dry weight.

Since NRT1.1 also contributes to low-affinity nitrate uptake, the same haplotype groups were investigated for differences in the low-affinity uptake capacity. However, no significant difference was found between the haplotype groups differing at V133, A272, A412 or V439 (Figure 3.34a-d). Taken together, allelic variations in the coding region of *NRT1.1B* did not reveal evidence for variation in high- or low-affinity nitrate uptake capacity.

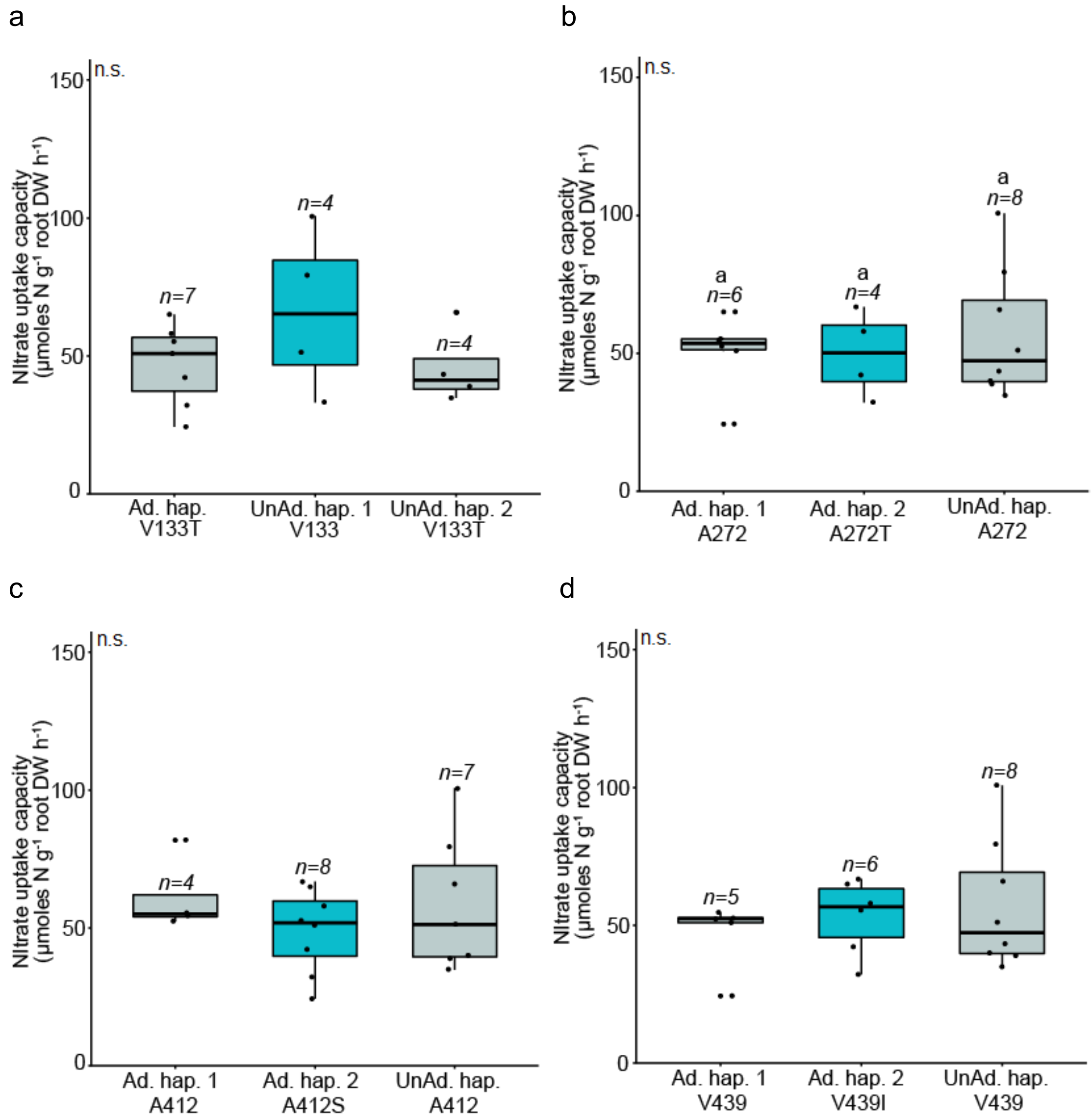

Figure 3.34. Low-affinity uptake capacities for NO_3^- of lines from different NRT1.1b haplotype groups. Haplotype groups were formed based on single amino acid substitutions identified in at least 3 out of at least 20 lines at the following positions: (a) V133 (b) A272 (c) A412 (d) V439. Nitrate uptake rates were taken from (Figure 3.13a, c). n = no. of lines in a haplotype group from the adapted (Ad.) or unadapted (UnAd.) wheat panel. The boxes show the first quartile, median and third quartile; the whiskers indicate the minimum and maximum values. P-values indicate differences between means according to ANOVA and Tukey's test; n.s., no significant differences. DW, dry weight.

3.7 Variation in *AMT1* and *NRT1.1* transcript levels in selected contrasting lines from both panels in dependence of N supply conditions

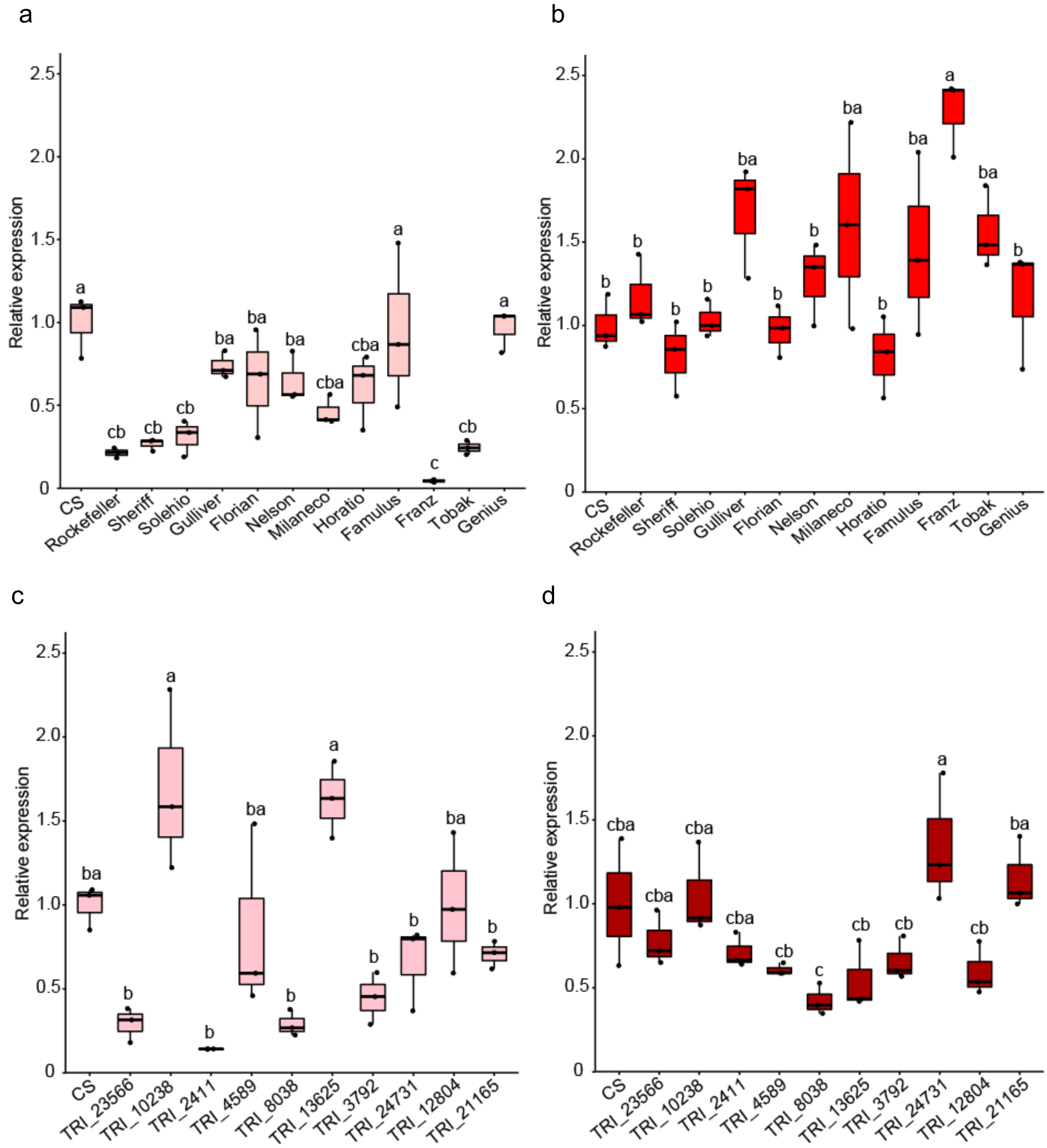

Figure 3.35. Genotypic variation in the *AMT1.1* transcript abundance of contrasting lines grown under N-sufficient or N-deficient conditions. *AMT1.1* transcript levels were determined in contrasting adapted lines (a, b) and unadapted lines (c, d). Plants were grown hydroponically on ammonium nitrate for 10 days and then on 2 mM N (+N) (a, c) or on N-free nutrient solution (-N) for 2 days (b, d). The boxes show the first quartile, median and third quartile; the whiskers indicate the minimum and maximum values (n = 3 independent biological replicates). Different letters represent significant differences among means according to ANOVA and Tukey's test at $P < 0.05$.

To address the question whether different ammonium uptake rates are determined by the gene expression level of an individual AMT gene, qPCR was performed on contrasting adapted and unadapted lines, which were precultured hydroponically on adequate N supply for 10 days before plants were transferred for 2 days on N-sufficient or N-deficient nutrient solution and root RNA was extracted. In N-adequate plants, *AMT1.1* transcript levels varied among the contrasting lines from the adapted and unadapted panel by approx. 10- and 15-fold, respectively (Figure 3.35a, c). Under N deficiency, this variation decreased to 2- to 3-fold, as transcript abundance was at a considerably higher level in most of the lines. Notably, Rockefeller and Tobak did not differ in their transcript abundance under N-sufficient conditions, whereas in N-deficient conditions Tobak tended to have higher relative expression levels of *AMT1.1* but this difference was not statistically significant. Interestingly, unadapted lines showed a lower increase in *AMT1.1* transcript levels under N deficiency than the adapted lines (Figure 3.35d), suggesting that these plants either experienced less N deficiency or had a lower responsiveness to N deficiency.

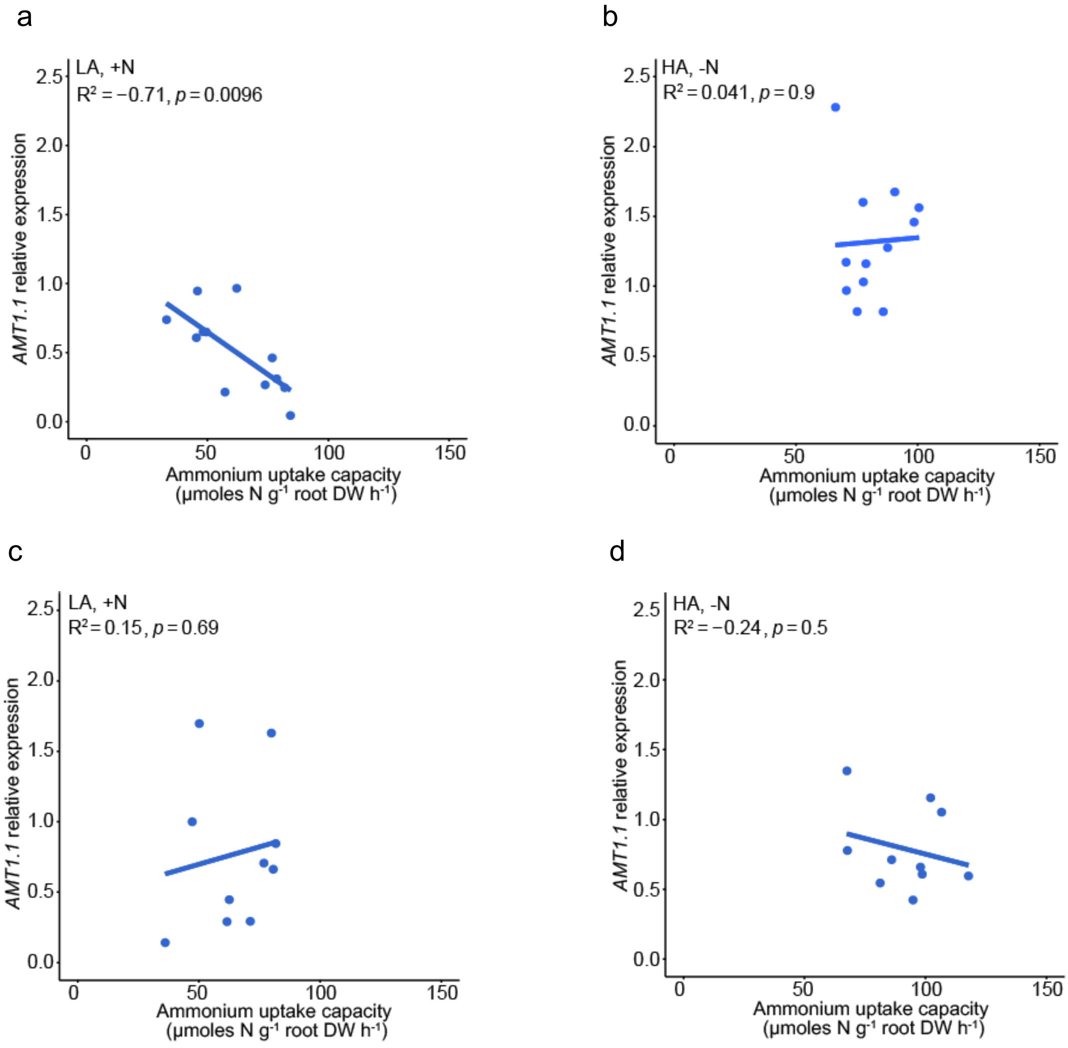

Figure 3.36. Correlation between high- and low-affinity uptake rates of ammonium and relative transcript abundance of *AMT1.1*. Correlations were determined for plants from the (a, b) adapted or unadapted panel grown under (a, c) N-sufficient conditions or (b, d) N-deficient conditions. Ammonium uptake rates were taken from (Figure 3.9a, c) or (Figure 3.7b, d). R^2 represents the Pearson correlation coefficient. P-values indicate differences between means according to ANOVA and Tukey's test. LA, Low-affinity, HA, High-affhinity, DW, dry weight.

To investigate whether genotypic differences in low-affinity ammonium uptake rates determined in N-sufficient plants (Figure 3.9a, c) or high-affinity uptake rates determined in N-deficient plants (Figure 3.7b, d) are associated with *AMT1.1* transcript levels determined here (Figure 3.35), correlation analyses were conducted. However, when *AMT1.1* transcript levels were related to high- and low-affinity uptake rates, there were no correlations found, except for one significant negative correlation between *AMT1.1* transcript levels and low-affinity ammonium uptake under N-sufficient conditions (Figure 3.36). This would indicate that low-affinity ammonium uptake is higher when *AMT1.1* becomes repressed. However, this observation was not confirmed in lines from the unadapted panel.

From the same root material also *AMT1.2* transcript levels were determined for lines from the adapted and unadapted panel. Under N-sufficient conditions *AMT1.2* transcript abundance varied by approx. 20-fold in adapted and in unadapted lines, except for the line Genius, which exhibited much higher transcript levels (Figure 3.37a, c).

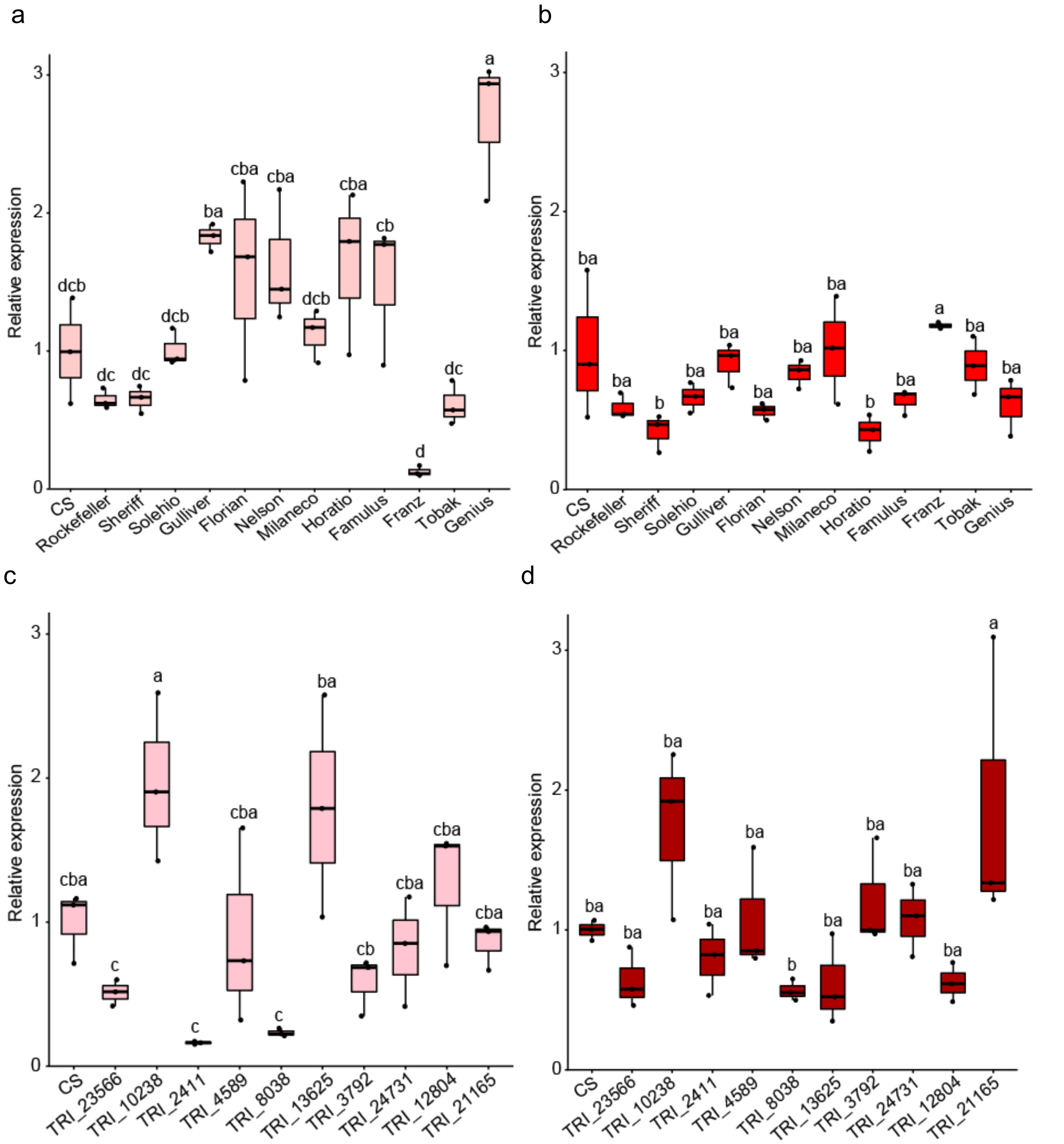

Figure 3.37. Genotypic variation in the *AMT1.2* transcript abundance of contrasting lines grown under N-sufficient or N-deficient conditions. *AMT1.2* transcript levels were determined in contrasting adapted lines (a, b) and unadapted lines (c, d). Plants were grown hydroponically on ammonium nitrate for 10 days and then on 2 mM N (+N) (a, c) or on N-free nutrient solution (-N) for 2 days (b, d). The boxes show the first quartile, median and third quartile; the whiskers indicate the minimum and maximum values (n = 3 independent biological replicates). Different letters represent significant differences among means according to ANOVA and Tukey's test at $P < 0.05$.

Unexpectedly, after 2 days of N deficiency transcript abundance of *AMT1.2* was not increased or even less than in N-adequate plants, irrespective of whether lines derived from the adapted or unadapted panel (Figure 3.37b, d). This observation indicated that *AMT1.2* gene expression levels respond poorly to N deficiency in wheat. There was no trend for different expression levels between the contrasting lines within one panel; this also held true for the contrasting lines Rockefeller and Tobak.

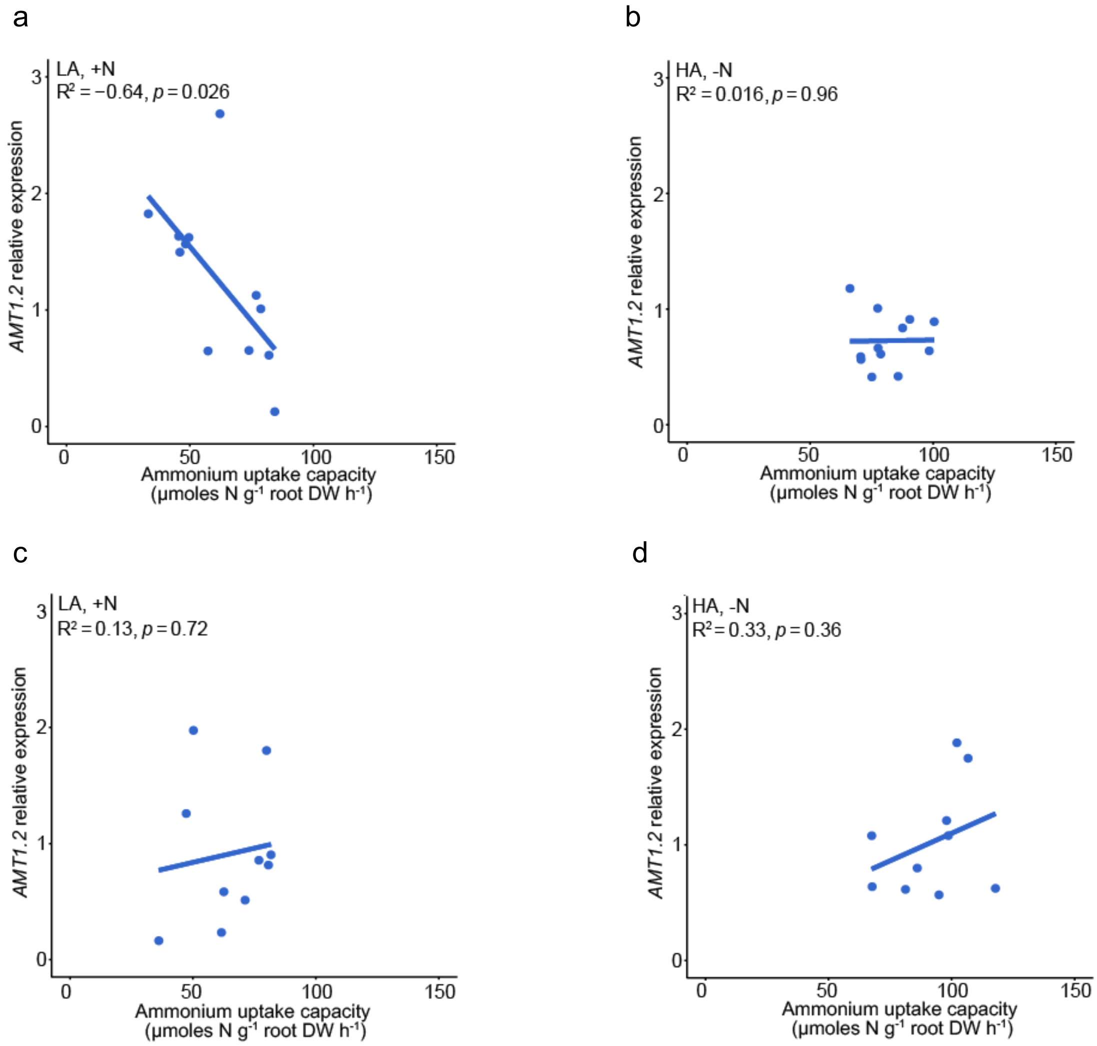

Figure 3.38. Correlation between high- and low-affinity uptake rates of ammonium and relative transcript abundance of *AMT1.2*. Correlations were determined for plants from the (a, b) adapted or (c, d) unadapted panel grown under (a, c) N-sufficient conditions or (b, d) N-deficient conditions. Ammonium uptake rates were taken from (Figure 3.9a, c) or (Figure 3.7b, d). R^2 represents the Pearson correlation coefficient. P-values indicate differences between means according to ANOVA and Tukey's test. LA, Low-affinity, HA, High-affhinity, DW, dry weight.

When *AMT1.2* transcript levels were related to high- and low-affinity uptake rates, there was only one significant correlation found for *AMT1.2* transcript levels correlating negatively with low-affinity ammonium uptake under N-sufficient conditions (Figure 3.38). As for *AMT1.1*, this observation was not made in lines from the unadapted gene pool.

The same approach was also conducted for the nitrate-responsive gene *NRT1.1*, which is upregulated in most plant species under adequate N supply but repressed under N deficiency (Wang et al., 1998).

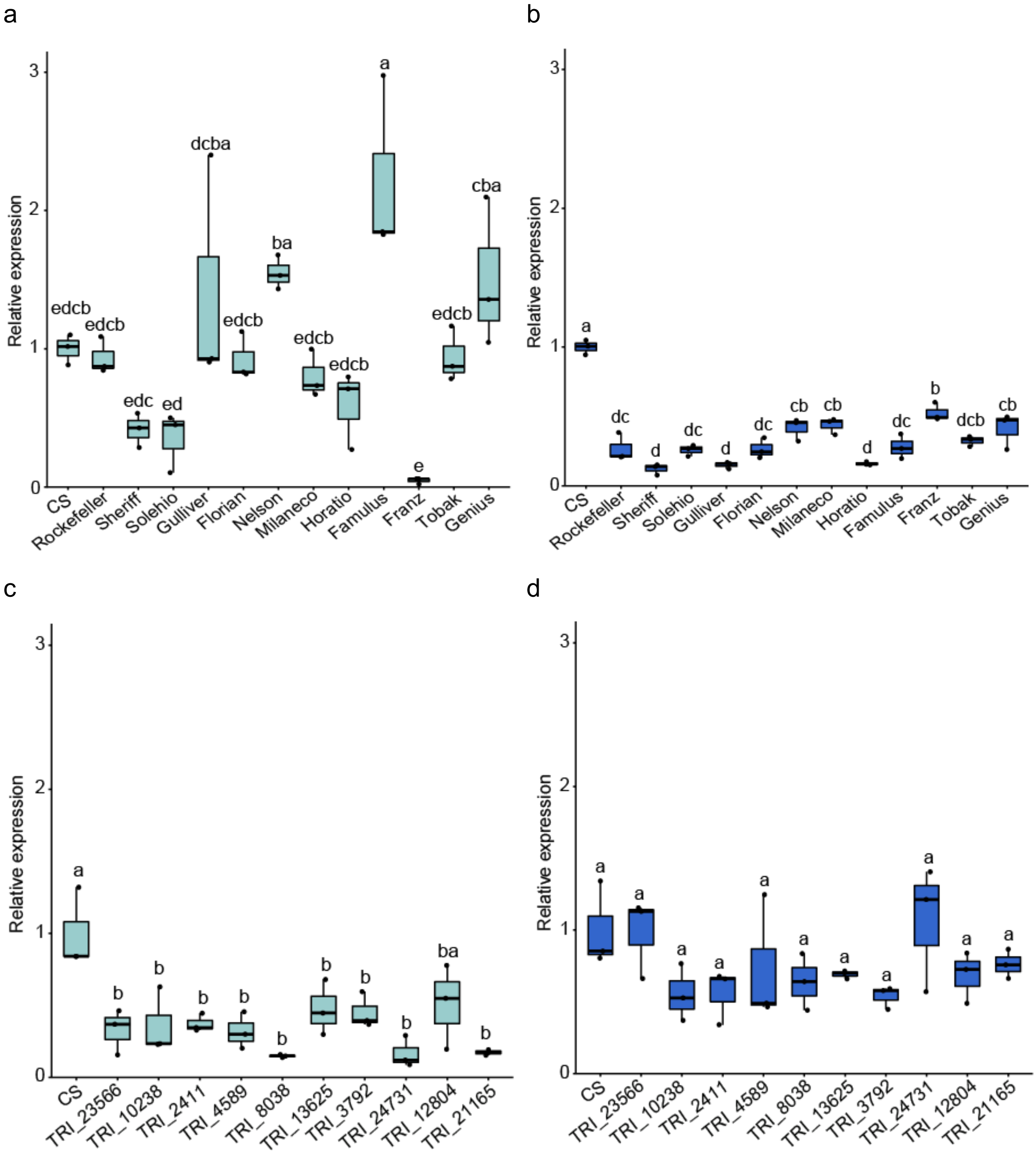

Figure 3.39. Genotypic variation in *NRT1.1b* transcript abundance of contrasting lines grown under N-sufficient or N-deficient conditions. *NRT1.1b* transcript levels were determined in contrasting adapted lines (a, b) and unadapted lines (c, d). Plants were grown hydroponically on ammonium nitrate for 10 days and then on 2 mM N (+N) (a, c) or on N-free nutrient solution (-N) for 2 days (b, d). The boxes show the first quartile, median and third quartile; the whiskers indicate the minimum and maximum values (n = 3 independent biological replicates). Different letters represent significant differences among means according to ANOVA and Tukey's test at $P < 0.05$.

Under N-sufficient conditions, there was a large variation in *NRT1.1* transcript abundance among the adapted lines with a slight tendency of higher transcript abundance in the lines selected for higher N uptake capacity (Figure 3.39a). Under N deficiency, transcript levels dropped and any difference between the two contrasting groups disappeared; this also held true for Rockefeller and Tobak (Figure 3.39b). In the unadapted panel, average *NRT1.1* transcript abundance was quite low under N sufficiency but increased under N deficiency (Figure 3.39c, d). This was in opposite trend to the lines from the adapted panel. Irrespective of the N supply conditions, unadapted lines showed no apparent difference among the contrasting lines. When *NRT1.1b* transcript levels were related to high- and low-affinity uptake rates of nitrate, no correlations were found (Figure 3.40).

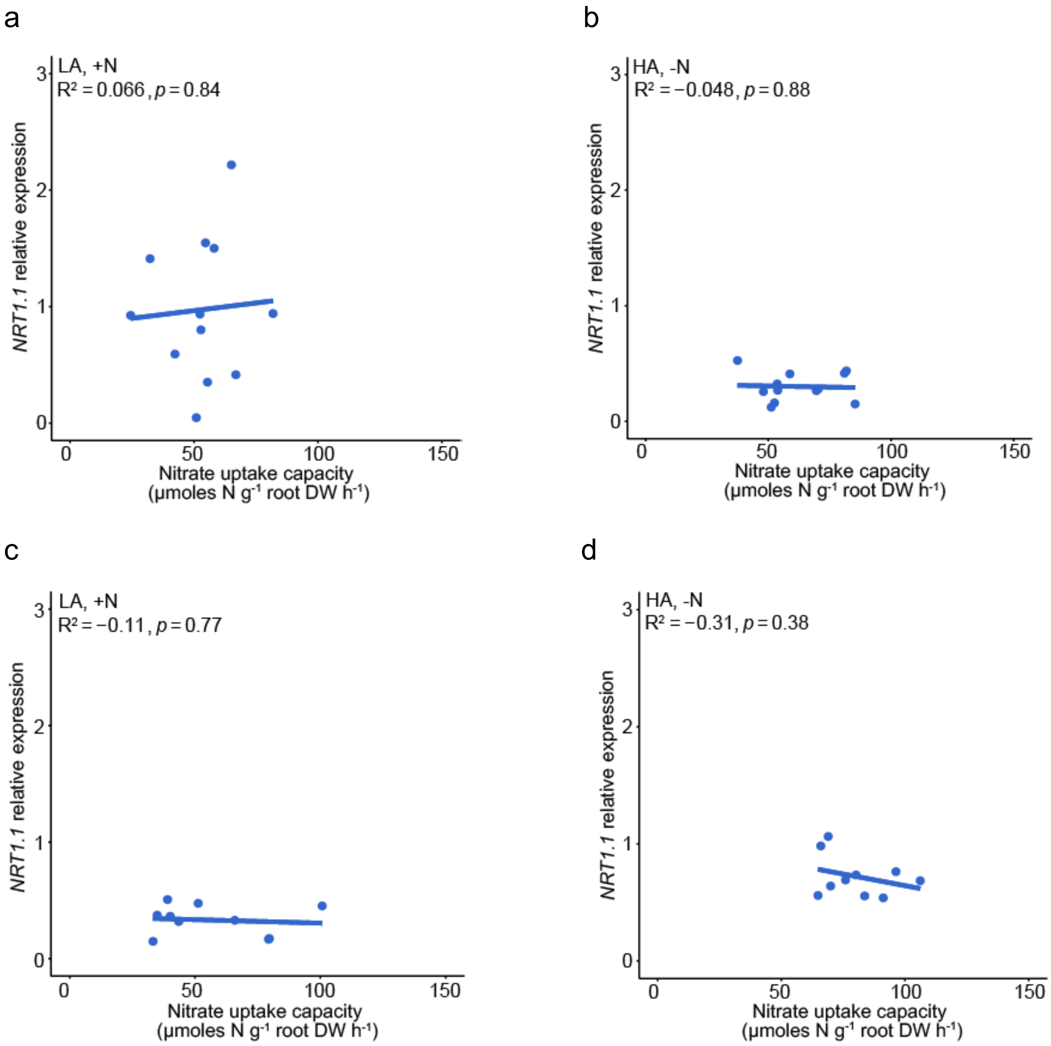

Figure 3.40. Correlation between high- and low-affinity uptake rates of nitrate and relative transcript abundance of *NRT1.1b*. Correlations were determined for plants from the (a, b) adapted or (c, d) unadapted panel grown under (a, c) N-sufficient conditions or (b, d) N-deficient conditions. Nitrate uptake rates were taken from (Figure 3.13a, c) or (Figure 3.11b, d). R^2 represents the Pearson correlation coefficient. P-values indicate differences between means according to ANOVA and Tukey's test. LA, Low-affinity, HA, High-affhinity, DW, dry weight.

4. Discussion

Nitrogen (N) is an essential mineral element required for the biosynthesis of nucleic acids, proteins, and essential pigments such as chlorophyll. Since N fertilizer supply in agricultural plant production is usually large and a decisive factor for economic crop production worldwide, efficient N uptake is of great importance for food security (Hu et al., 2015). Economizing N fertilization to crop residues after harvest or the starter dressing in autumn will increase the risk of N immobilization and low N availability to winter cereals, especially during the early vegetative development. Therefore, it is important to identify whether there are genotypic differences in the capacity for N uptake during the juvenile development of cereal crops, which may be used later to improve the breeding of N uptake-efficient cultivars. Since such genotypic differences may be related to morphological as well as to physiological plant traits that both differ and show high plasticity in response to the N nutritional status, it is important to investigate genotypic differences at multiple levels.

The present study focused on the first-level variation in physiological traits that directly relate to plant N uptake by assessing lines from two different winter wheat panels. The first panel represented a gene pool with lines released before the green revolution while the second panel harboured lines released after the green revolution, i.e. current elite lines. In an attempt to select lines along their N uptake capacity, a large screening was conducted that represented the basis for the subsequent selection of contrasting lines, i.e. lines with particular high or low uptake capacity for deeper investigation of the morphological or physiological traits causing different N uptake. In parallel, a re-sequencing approach was conducted that focused primarily on major transporter genes for ammonium (AMT1.1 and AMT1.2) and for nitrate (NRT1.1). Aiming at identifying allelic differences in the genome sequence that cause non-synonymous amino acid substitutions, it was attempted to relate these differences to N uptake capacities. While such allelic variations in the coding sequences could only be identified in case of AMT1.2, the current thesis uncovered that the expression levels of genes from a so-far poorly recognized subfamily of AMT3-type ammonium transporters showed a remarkable response to N deficiency that coincides with higher ammonium uptake capacities in contrasting lines.

4.1 Physiological and phenotypic traits responsible for the variation in nitrogen uptake capacity in lines from two winter wheat gene pools

The need for improving N uptake efficiency (NUpE) traits requires research on physiological and phenotypic aspects contributing to N uptake by the roots from the soil and its translocation to above-ground tissues. Previous studies found differences in N uptake capacity among genotypes and their correlation with biomass (Haefele et al., 2008; Katsura et al., 2010). (Li et al. 2017) mentioned that uptake-efficient lines had higher root dry weight, which helps increasing the N uptake capacity. (Górny et al. 2011) confirmed from their research work on winter wheat that both, ancient and current wheat lines showed fair contribution of different uptake- or utilization-related efficiency factors as a basis to pyramid the responsible genes by crossing. Other studies revealed that most breeding effects on NUE were associated with changes in

N uptake efficiency (le Gouis et al., 2000; Muurinen et al., 2006). Thus, traits such as N uptake capacity and root biomass are both suitable factors when searching for NUpE traits.

During the early vegetative growth phase, kinetic parameters of nitrate uptake are promising to distinguish differences in NUpE (Pang et al., 2015). When N uptake capacity in roots was determined in lines released before the green revolution (unadapted lines) or after the green revolution (adapted lines), uptake rates were determined in the high-affinity range, i.e. at 200 µM double-labelled $^{15}NH_4{}^{15}NO_3$, during a period of 1 h, which corresponds - in physiological terms - to a relatively long time period, because during exposure to the ^{15}N-labeled N source feed-back regulation on the transcriptional and posttranslational regulation of AMTs and NRTs may have set in (Lanquar et al., 2009; Jacquot et al., 2020). Nonetheless, the comparison of N uptake capacities in different lines from either gene pool revealed that efficient lines had approx. twofold higher uptake rates (Figure 3.4). A comparison between the population means of the uptake or translocation rates did not identify differences between the two gene pools (Figure 3.3c, d). At the same time, there were also no significant differences in the population means for root or shoot biomass (Figure 3.3a, b), although unadapted lines are mostly affected in plant height und thus in shoot biomass, which is a trait controlled by dwarfing genes (Gooding et al., 2012).

With regard to the tight and highly similar correlation between N uptake rate and the N translocation rate (Figure 3.2), it became evident that the uptake rate as the precedent step had a stronger impact on genotypic differences than the translocation rate. This observation justified the approach to investigate in more depth the N uptake-related parameters causing differential uptake capacities in both gene pools.

4.2 Genotypic differences in N-dependent regulation of high- and low-affinity N transport capacities

In this study, wheat lines contrasting in N uptake capacity were selected from each of the panels according to their low- and high-affinity uptake rates determined under N-sufficient and N-deficient pre-culture. As previously shown, N starvation for a few days increases the ammonium and nitrate uptake capacity in roots by induction or de-repression of the corresponding high-affinity AMT1 and NRT2 transporters (Gazzarrini et al., 1999; Gansel et al., 2001). Since de-repression of *NRT2* genes depends on the nitrate sensor NRT1.1 (Ho et al., 2009) and since allelic variation in the coding region of NRT1.1b in rice was shown to be responsible for superior nitrate uptake efficiency (Hu et al., 2015), NRT1.1 was considered of more relevance here. However, under field conditions wheat plants may not be continuously in a suboptimal N nutritional status. With regard to varying temperature and precipitation particularly in late autumn after winter wheat has been sown, it may be expected that the plant N status changes, becoming deficient when shoot growth is accelerated, e.g. under warm air temperatures, or becoming saturated when shoot growth rates and N demand decline, e.g. when temperature drops but soil N mineralisation is still high. Such scenarios require consideration of the N responsiveness of N uptake systems, which has been claimed as highly promising target when breeding for N-efficient crops (Swarbreck et al., 2019).

N responsiveness is based on a comparison of N uptake between N-sufficient and N-deficient plants. When contrasting lines from the initial screening (Figure 3.1) were cultivated under adequate or deficient N supply before examining the high-affinity uptake capacity for NH_4^+, it turned out that the differences between some of the contrasting lines got lost, irrespective of whether contrasting lines derived from the elite or unadapted gene pool (Figure 3.7). Since the initial screening was based on uptake rates of double-labeled $^{15}NH_4{}^{15}NO_3$, one likely explanation for this discrepancy is that here only uptake rates of ammonium were assessed while a part of the genotypic differences was due to differential nitrate uptake rates. However, the parallel assessment of high-affinity uptake rates for nitrate did not yield a complementary result, i.e. that those N uptake-efficient lines with lower ammonium uptake rates showed higher uptake rates of nitrate (Figure 3.11). Thus, it was concluded that separately determined high-affinity uptake rates of ammonium and nitrate do not simply add up to yield those determined under concomitant supply of NH_4NO_3. This is likely due to the fact that either N form has a regulatory influence of the uptake systems of the other. For instance, in ammonium-supplied Arabidopsis plants the nitrate transceptor NRT1.1 can downregulate gene expression of *AMT1* transporters and the corresponding high-affinity uptake capacity, while NRT1.1 itself is differentially regulated by ammonium (Hachiya & Sakakibara, 2016; Jian et al., 2018).

Recently, N responsiveness has been defined by the capacity of plants to induce morphological and physiological changes according to the external availability of N to induce N uptake and assimilation (Swarbreck et al., 2019). Following this scheme, N responsiveness was calculated here by the difference in uptake rates between N-deficient and N-sufficient plants, because N-deficient plants induce high-affinity transporters for ammonium and nitrate (Wang et al., 1998; Gazzarrini et al., 1999; Gansel et al., 2001). Indeed, across all contrasting lines in the adapted gene pool, average high-affinity uptake rates for ammonium were approx. twofold higher and those for nitrate approx. threefold higher (Figure 3.7). While individual lines with high ammonium uptake capacity, like Famulus, also showed a high responsiveness, others, like Tobak, did not (Figure 3.8). Moreover, the consistent contrast in high-affinity ammonium uptake observed between Tobak and Rockefeller, was not reflected in different N responsiveness. This would imply that Famulus may gain superior ammonium uptake efficiency by strongly upregulating AMT1-type transporters as soon as N deficiency sets in, whereas the genotypic difference between Tobak and Rockefeller may rather rely on differences in the ground level at which *AMT1* genes are expressed or on biochemical properties resulting from differences in the coding sequence.

With respect to high-affinity nitrate uptake, N-deficient preculture in contrasting lines led even to threefold higher uptake rates (Figure 3.11). In the unadapted gene pool, this difference was in tendency even larger. Interestingly, in the adapted gene pool N responsiveness reflected closely the nitrate uptake rates achieved after N-deficient preculture (Figure 3.12). For instance, Gulliver, Milaneco, Nelson and Famulus were the lines with highest uptake rates under N deficiency and at the same time also those with highest values in N responsiveness. Such a relation was not observed for unadapted lines, suggesting that N responsiveness may indeed represent a promising breeding target to enhance nitrate uptake efficiency in elite cultivars but less in unadapted germplasm.

When the same approach was applied to assess genotypic differences in low-affinity uptake efficiency, observations were somewhat different. As expected, average low-affinity ammonium uptake rates across all lines were approx. 50% higher than high-affinity uptake rates in both, N-deficient and N-sufficient plants (Figure 3.9). Low-affinity ammonium transporters are not yet clearly identified at the molecular level but most likely include non-selective cation channels, including AKT1 and maybe HAK-type K channels (Hoopen et al., 2010; Straub et al., 2017). However, some of the AMT1-type transporters do also contribute to low-affinity transport. In Arabidopsis, in particular AMT1.2 with the lowest in-vivo Km value is supposed to take over a considerable share of the overall low-affinity transport capacity (Duan et al., 2018) and *AMT1.2* is also induced under N deficiency (Yuan et al., 2007). Genotypic differences among elite lines remained similar as observed for high-affinity ammonium uptake, in particular the sharp contrast between Tobak and Rockefeller (Figure 3.9). In contrast, this and other genotypic differences among elite lines also expressed in different N responsiveness, suggesting that the upregulation of the low-affinity uptake capacity under N deficiency may be under heavier transcriptional control than the high-affinity capacity. However, it must be kept in mind that in this approach the uptake period of 1 h may involve further regulatory processes displaying at the posttranscriptional level (Lanquar et al., 2009). Remarkably, one line from the unadapted gene pool, namely TRI_12804, showed low- and high-affinity ammonium uptake rates that were far above average, and in both cases this corresponded also to an enhanced N responsiveness (Figure 3.7, Figure 3.10). To a somewhat lesser extent this also held true for high- and low-affinity nitrate uptake (Figure 3.11, Figure 3.14). This line may merit attention in future investigations on N uptake efficiency in wheat.

In contrast to low-affinity ammonium uptake, low-affinity nitrate uptake rates were 2-3-fold higher than high-affinity ones under adequate N supply, but their further increase under N deficiency was much less pronounced, in particular in adapted lines (Figure 3.13). This is in agreement with the notion that low-affinity nitrate transport systems are hardly substrate-inducible and that NRT1-type low-affinity nitrate transporters are not upregulated but mostly downregulated under N deficiency (Wang et al., 1998). Hence, their N responsiveness was low and highly variable, emphasizing that in this scenario N responsiveness is not a valuable measure when selecting N uptake-efficient lines.

4.3 Evaluation of the role of morphological root traits for genotypic differences in ammonium uptake capacity in adapted wheat lines

Root system architecture is critically important for understanding root morphological alterations that allow increasing resource capture, especially of water and nutrients to support growth and development. Modulations in root system architecture are an important factor in steering N acquisition. Plants depend on morphological changes to adapt to the plant-available amounts and forms of individual nutrients, which was reflected here by growing the plants under low or high N conditions. Due to the time-consuming process when determining root traits from hydroponically-grown plants, roots traits were taken here only from contrasting lines of the adapted gene pool to verify whether there is a relation between morphological root traits and ammonium uptake capacity.

Results of the present experiments focused on seminal roots and their first-order lateral roots, although at later time points, here after 12 days, all wheat plants also proliferated nodal roots. These nodal roots, however, remained in average below a length of 0.5 cm (data not shown). Nodal roots represent shoot-borne roots developing immediately after tillering has set in to provide anchorage of the plant in the soil and to support resource uptake especially during the reproductive growth phase of the plant (Shorinola et al., 2019). The length and density of second-order lateral roots were also not assessed here, because second-order lateral roots could not be imaged due to technical reasons. Thus, some relevant information may have gone lost, since this root type is also responsive to nutrient conditions (Giehl et al., 2014).

In general, seminal root length decreased while lateral root length increased under N deficiency (Figure 3.16c, e). In most cultivars, also the number of lateral roots increased significantly (Figure 3.16d). In agreement with previous work (Jia et al., 2019; Ma et al., 2014) the present study also found that under low N conditions there is an increase in lateral root number and lateral root length, which accounts for a large part of the total root length (Figure 3.16). In Arabidopsis, an increase in lateral root number or density was only reported for second-order but not for first-order lateral roots (Gruber et al., 2013). This discrepancy may be due to the plant species, growth conditions, and the depth, by which root traits were analyzed. Interestingly, here it appeared that those wheat lines that strongly increased lateral root number, in turn, formed shorter lateral roots (Figure 3.16d, e). At first glance, this compensatory mechanism may be due to a limiting availability of assimilates. However, a recent investigation in Arabidopsis has shown that these traits are under tight hormonal regulation, with brassinosteroids promoting root elongation and de-novo synthesis of auxin promoting lateral root emergence under low N (Jia et al., 2019; Jia et al., 2021). A previous study in Arabidopsis has reported that under low N the tryptophan aminotransferase gene *TAR2* is up-regulated and responsible for the de-novo synthesis of the auxin (Ma et al., 2014). The overexpression of *TAR2* in Arabidopsis increased the auxin concentration in the primary root tip, lateral root tip, and lateral root primordium, thereby increasing lateral root number in response to low N conditions (Shao et al., 2017). Assuming that genotypes forming more seminal roots lose their ability to elongate seminal and lateral roots under N deficiency, plant breeding would have to consider a lower seminal root number as advantageous. Since seminal root number is under strict genetic control, such a trade-off would have to be addressed in advanced selection and breeding approaches.

4.4 The putative role of structural differences in AMT1 and NRT1.1 proteins in differential ammonium and nitrate uptake capacities

Exploring the genomic diversity among re-sequenced wheat lines from global breeding programs revealed large haplotypic diversity in wheat genome assemblies (Walkowiak et al., 2020). As haplotypic diversity causing phenotypic variation is a major factor in breeding progress (Brinton et al., 2020), it was hypothesized here that the phenotyopic variation found in ammonium uptake among the different wheat lines may be due to allelic variation in the genome sequence. Mining the genome sequence of Chinese Spring and subsequent phylogenetic analysis with AMT sequences from a number of species allowed clustering the wheat AMT genes into three subfamilies, AMT1, AMT2 and AMT3. For each of the three subfamilies two homologs were identified, each consisting of the three paralogs on the A, B and D genome, except for AMT2.1 for which the paralog on the B genome remained uncovered (Figure 3.24). Since in previous studies homologs of the AMT1 subfamily were shown or considered being of major importance for ammonium uptake (Konishi & Ma, 2021), members of the AMT2 family may take over preferential functions in long-distance transport from roots to shoots (Giehl et al., 2017), while members of the AMT3 subfamily were shown to become expressed after mycorrhizal infection (Koegel et al., 2017). Therefore, emphasis in finding correlations between ammonium uptake rates and AMT genes were placed primarily on the AMT1 subfamily.

19 and 21 completely resequenced *AMT1.1* and *AMT1.2* genes, respectively, from contrasting adapted and unadapted wheat lines provided an insight into the coding sequence variation in two major high-affinity ammonium transporter genes. Referring to the genome sequence of Chinese Spring, 14 different amino acid positions in the peptide sequence of AMT1.1 were found to be substituted (Figure 3.25), confirming a rather high degree of sequence conservation. Haplotype groups consisting of at least three lines carrying an amino acid substitution in one of the substituted positions were then compared in their ammonium uptake capacity. However, ammonium uptake capacities in none of these haplotype groups differed significantly from each other (Figure 3.26). For AMT1.2, 10 amino acid positions were found to be substituted (Figure 3.27), but also here none of these substitutions coincided with either lower or higher ammonium uptake capacities. Thus, the resequencing approach of these two AMT genes did not allow identifying allelic variation that may relate to altered ammonium uptake capacities. This result was considered 'unfortunate' regarding the fact that single amino acid substitutions have been identified to confer a profound impact on ammonium transport properties of AMT proteins. For instance, a single Q57H substitution in Arabidopsis AMT1.1 leads to a 10-fold increase in transport capacity together with a 100-fold decrease in substrate affinity relative to the wild-type form (Loqué et al., 2009). More recently, a twin-histidine motif in the core structure of AMT1- and AMT2-type transporters has been proven responsible for altering transport capacity as well as mediating NH_4^+ deprotonation and the related substrate selectivity, i.e. by conferring discrimination between NH_4^+ and K^+ (Ganz et al., 2020).

The weakness of the above-described approach lies in the fact that it considers the impact only of a single amino acid substitution on ammonium transport capacities. To account for structural changes in AMT1 proteins conferred by more than one amino acid substitution, a protein modelling approach was taken. Since the structure of plant AMT proteins has not yet been successfully elucidated, AMT sequences from wheat were compared to the characterized structures of EcAmtB and ScMep2 from E. coli and yeast, respectively (Khademi et al., 2004; van den Berg et al., 2016). When the AMT1.1 protein structure, obtained by *ab initio* homology-based modelling, was predicted for the two adapted lines Rockefeller and Tobak, which differed in 6 out of 14 variable amino acid positions in AMT.1.1 (Figure 3.25) and consistently in ammonium uptake rates (Figure 3.19, Figure 3.18), no obvious structural difference was found (Figure 3.29). For AMT1.2, protein structures from all 12 re-sequenced lines of the adapted gene pool were compared (Figure 3.30). Here, two obvious structural differences were identified, i.e. a beta-sheet present in 6 out of the 12 proteins and a small alpha-helix present in 8 out of the 12 proteins. Comparing ammonium uptake rates in relation to the presence or absence of the beta-sheet revealed a significant difference in a way that AMT1.2 proteins with a beta-sheet showed significantly higher uptake rates than those without (Figure 3.31). Confirming this observation by structure-function relations of AMT1.2 in the unadapted lines would be an important step in future studies.

Hu et al. (2015) reported that the difference in nitrate uptake capacity between *indica*- and *japonica*-type subspecies in rice is due to a single amino acid substitution in NRT1.1b. NRT1.1b is a closely related homolog to NRT1.1/NPF6.3/CHL1 from Arabidopsis, which is a dual-affinity nitrate transporter and nitrate sensor (Liu et al., 1999b; Ho et al., 2009). Resequencing NRT1.1 from wheat lines of the two panels identified sequence variation in 16 positions with a particularly high sequence variation in the N-terminal region (Figure 3.32). Comparing high-affinity nitrate uptake rates among different haplotype groups yielded one significant difference at position 439 in the C-terminus, where the V439I substitution in unadapted lines coincided with significantly higher uptake rates (Figure 3.33). Since NRT1.1 is a dual-affinity transporter that can contribute to high- or low-affinity nitrate transport according to its phosphorylation status (K.-H. Liu & Tsay, 2003), also low-affinity uptake rates were analysed. However, phenotypic variation in these could not be rated to single amino acid substitutions in haplotype groups (Figure 3.35).

4.5 Verifying expression levels of *AMT1.1*, *AMT1.2* and *NRT1.1* in roots as putative cause for differential ammonium or nitrate uptake rates

With the exception of the beta-sheet in AMT1.2, there were no other structural features or amino acid substitutions found to coincide with genotypic differences in ammonium uptake capacity. Hence, it was hypothesized that differential expression of *AMT1* transporter genes may have caused differences in ammonium uptake. For instance in rice roots, expression patterns of *OsAMT1;1*, *OsAMT1;2* and *OsAMT1;3* differ in response to N supply; transcript levels of *OsAMT1;1* and *OsAMT1;2* are upregulated by ammonium, while that of *OsAMT1;3* is downregulated by ammonium (Sonoda et al., 2003; Konishi & Ma, 2021). Opposite to rice, transcript levels of *AMT1.1* in wheat increased after preculture under low N, even though this increase was on average across all lines much less pronounced in unadapted than in adapted lines (Figure 3.35). Unexpectedly, transcript levels of *AMT1.2* even decreased in most of the lines or remained unchanged in both gene pools (Figure 3.37). This suggested a lacking responsiveness of *AMT1.2* to N deficiency and a higher responsiveness of *AMT1.1* gene expression in elite lines than in unadapted lines. Thus, the typical upregulation of *AMT1* gene expression under N deficiency as observed for orthologs from Arabidopsis or tomato (Gazzarrini et al., 1999; von Wirén et al., 2000) was only conserved for *AMT1.1* in elite lines of wheat, while in rice roots so far none of the *OsAMT1* genes has been found to be upregulated under N deficiency (Sonoda et al., 2003b; Konishi & Ma, 2021).

When correlating *AMT1.1* or *AMT1.2* transcript levels with ammonium uptake rates, the two measures had to be taken from different experiments, even though culture conditions in the two experiments remained exactly the same. The expectation that expression levels of the two genes may correlate with high-affinity uptake rates obtained from N-deficient cultures was not confirmed (Figure 3.36, Figure 3.38). Instead, transcript levels of both genes from elite lines correlated negatively with low-affinity uptake rates, suggesting *AMT1.1* and *AMT1.2* repression under N-adequate growth conditions. Thus, these two genes are concluded not being promising targets when breeding wheat for higher ammonium uptake efficiency.

Typically, NRT1.1 is upregulated under supply of nitrate (Wang et al., 1998). This transcriptional regulation remained conserved also in the contrasting wheat lines from the adapted panel, as most lines showed higher transcript levels under continuous N supply (Figure 3.39a, b). In the unadapted lines this regulation disappeared and an opposite trend was observed in some lines, i.e. upregulation of *NRT1.1* mRNA levels under low N (Figure 3.39c, d). However, none of these two contrasting observations was of direct relevance for the nitrate uptake capacity, as suggested from lacking correlations of *NRT1.1* transcript levels to nitrate uptake capacity (Figure 3.40). This is most likely due to fact that NRT1.1 acts as nitrate sensor controlling expression of high-affinity NRT2-type nitrate transporters and participates to high- or low-affinity nitrate transport in dependence of its own phosphorylation status (Liu & Tsay, 2003; Muños et al., 2004). To what extent this opposite transcriptional regulation of *NRT1.1* in response to N supply causes differential nitrate uptake efficiency in adapted and unadapted lines merits further investigations.

4.6 Effect of nitrogen deficiency on nitrogen uptake capacity in two contrasting lines of the adapted gene pool

Among the lines from the adapted gene pool, most consistent differences in N uptake rates were observed between Rockefeller and Tobak. This held true for growth conditions, under which uptake of double-labeled NH_4NO_3 or of single-labeled ammonium was measured in the high- and low-affinity range or of single-labeled nitrate only in the low-affinity range (Figure 3.4, Figure 3.7, Figure 3.9, Figure 3.13). Moreover, under most of these conditions, this genotypic difference was evident irrespective of whether plants were grown under low or high N. Since these genotypic differences were highly consistent, it was first decided to search for root traits that may favour higher N uptake capacities in Tobak. However, apart from a slight advantage of Tobak in the total number of lateral roots under low N, there were no significant differences found (Figure 3.16). Therefore, it was concluded that differential uptake capacities are caused by genotypic differences in the regulation or constitution of the major transport systems for ammonium and nitrate. To verify this conclusion, the uptake period was shortened from 60 min down to 6 min, i.e. conditions under which a regulatory feed-back of an altered N status caused by root uptake of N is unlikely to have set in (Jacquot et al., 2020; Lanquar et al., 2009), thus reflecting more directly the impact of N-dependent transcriptional regulation on the capacity of the transport systems. This direct comparison corroborated that the superior high-affinity uptake capacity determined in a time frame of 6 min in Tobak remained conserved for ammonium but not for nitrate (Figure 3.17), whereas the superior low-affinity transport capacities for either substrate were consistently higher in Tobak than in Rockefeller (Figure 3.18). Further confirmation of the consistency of this genotypic difference was found in an experiment designed to compare the impact of N deficiency on ammonium uptake in the two wheat lines. When plants were precultured under N deficiency for 2 and 4 days, the superior uptake capacity of Tobak for double-labeled ammonium nitrate remained consistent in the high- and low-affinity range (Figure 3.20). Since this genotypic difference remained rather constant under progressing N deficiency, both lines showed a similar responsiveness to N deficiency. When plants from the same experiment were assessed for short-term influx of ammonium, Tobak showed consistently in trend or significantly higher ammonium uptake rates in both affinity ranges (Figure 3.21), confirming that at least a part of the superior uptake capacity for N in Tobak was due to ammonium uptake. Notably, this advantage of Tobak was neither caused by an altered response of root or shoot biomass to N deficiency nor by an altered N nutritional status (Figure 3.19).

Structural differences in the major membrane transport systems that could explain superior uptake capacities in Tobak were not found. Although Tobak and Rockefeller differed in 5 amino acid substitutions in the AMT1.1 protein sequence (Figure 3.25), the derived protein structure was identical and could not explain superior ammonium uptake rates. By contrast, although both lines differed in only 2 amino acid substitutions in AMT1.2, the Tobak protein was predicted to form an additional beta-sheet that coincided with elevated ammonium uptake rates (Figure 3.30, Figure 3.31). Since such a beta-sheet was neither reported for the crystallized AMT/MEP proteins from E.coli and yeast (Khademi et al., 2004; van den Berg et al., 2016) nor found in AMT1.1 (Figure 3.29), further research into the impact of this structural domain may be worthwhile.

In a final attempt, the superior ammonium uptake capacity of Tobak was considered to be caused by differences in the expression level of *AMT1* transporter genes. As examined in an additional experiment, plant preculture under N deficiency had only a minor impact on transcript levels of *AMT1.1* and *AMT1.2*, as both of these dropped after 2 days of N deficiency and increased to the level of N-adequate plants after 4 days of N deficiency (Figure 3.22). Throughout progressing N deficiency, the two contrasting lines showed highly similar transcript levels of both genes, indicating that transcriptional regulation of *AMT1.1* and *AMT1.2* did not account for different uptake rates. Hence, expression analysis of AMT genes was expanded to AMT3 subfamily members, which so far have been involved in mycorrhizal N transfer (Koegel et al., 2017). In fact, in five graminaceous species other than wheat, *AMT3.1* was found to be upregulated by 20- to 60-fold in mycorrhized roots (Koegel et al., 2017). Together with the observation that also in poplar *AMT3.1* and *AMT3.2* were upregulated by ammonium treatment but not by N deficiency (Wu et al., 2015), AMT3-type transport genes were initially not considered of relevance for the ammonium uptake capacity under low N conditions. However, in roots of both wheat lines *AMT3.1* and *AMT3.2* showed a drastic upregulation under progressing N deficiency with a 10- to 20-fold increase in transcript levels after 4 days of N deficiency (Figure 3.22c, d). Remarkably, transcript levels in N-adequate roots of both lines were highly similar, whereas with progressing N deficiency upregulation of both genes was significantly higher in Tobak, indicating a higher responsiveness of the transcriptional regulation of *AMT3.1* and *AMT3.2* in Tobak. This was further supported by a steeper positive correlation of *AMT3.1* and *AMT3.2* transcript levels with ammonium uptake rates in Tobak (Figure 3.23), indicating that the two corresponding transporters likely contribute to its superior uptake capacity for ammonium under increasing N deficiency. Such a remarkable difference in the expression pattern of *AMT3.1* and *AMT3.2* between Tobak and Rockefeller may be linked to transcription factors involved in the N deficiency response, like those of the DOF or bHLH families (Curci et al., 2017; Yang et al., 2016). In wheat and rice, DOF transcription factors regulate certain *AMT* genes, which is related to elevated ammonium uptake capacities (Curci et al., 2017; Yanagisawa et al., 2004; Wu et al., 2017).

The adapted line Tobak has been considered as one of the most successful European wheat lines due to its high resistance against leaf rust and high yield potential. As shown here, the latter may be related to its elevated N uptake capacity. To what extent the N-responsive transcriptional regulation or possible structural differences in AMT3.1 and AMT3.2 or AMT1.2 are causative for the higher ammonium uptake capacity and the high yield potential requires more detailed investigations. With these characterized traits, the present findings contribute to an improved knowledge on genotypical differences in the N uptake capacity of adapted and unadapted wheat lines during vegetative development. They also indicate that there is potential in unadapted wheat lines with exceptionally high ammonium and nitrate uptake rates, such as in particular TRI_12804, to exploit allelic variation when breeding for N uptake efficiency. Uncovering the sequence variation responsible for these differences will provide important information for breeding wheat lines with high N uptake capacity to generate future plant production systems that require less N fertilizers and are more resource efficient.

5. References

Abbate, P. E., Andrade, F. H., Lázaro, L., Bariffi, J. H., Berardocco, H. G., Inza, V. H., & Marturano, F. (1998). Grain yield increase in recent argentine wheat cultivars. Crop Science, 38(5), 1203-1209.

Atkinson, J. A., Wingen, L. U., Griffiths, M., Pound, M. P., Gaju, O., Foulkes, M. J., le Gouis, J., Griffiths, S., Bennett, M. J., King, J., & Wells, D. M. (2015). Phenotyping pipeline reveals major seedling root growth QTL in hexaploid wheat. Journal of Experimental Botany, 66(8), 2283-2292.

Bai, C., Liang, Y., & Hawkesford, M. J. (2013). Identification of QTLs associated with seedling root traits and their correlation with plant height in wheat. Journal of Experimental Botany, 64(6), 1745-1753.

Bajgain, P., Russell, B., & Mohammadi, M. (2018). Phylogenetic analyses and in-seedling expression of ammonium and nitrate transporters in wheat. Scientific Reports, 8(1), 7082.

Barraclough, P. B., Howarth, J. R., Jones, J., Lopez-Bellido, R., Parmar, S., Shepherd, C. E., & Hawkesford, M. J. (2010). Nitrogen efficiency of wheat: Genotypic and environmental variation and prospects for improvement. European Journal of Agronomy, 33(1), 1-11.

Barraclough, P. B., Weir, A. H., & Kuhlmann, H. (1991). Factors affecting the growth and distribution of winter wheat roots under UK field conditions. Developments in agricultural and managed forest ecology 24: Plant roots and their environment, Elsevier Science Publishers, 410-417.

Bloom, A. J., Sukrapanna, S. S., & Warner, R. L. (1992). Root Respiration Associated with Ammonium and Nitrate Absorption and Assimilation by Barley. Plant Physiology, 99(4), 1294-1301.

Bowman, J. L., Eshed, Y., & Baum, S. F. (2002). Establishment of polarity in angiosperm lateral organs. Trends in Genetics, 18(3), 134-141.

Brady, D. J., Gregory, P. J., & Fillery, I. R. P. (1993). The Contribution of different regions of the seminal roots of wheat to uptake of nitrate from soil. In Plant Nutrition - from Genetic Engineering to Field Practice. Springer Netherlands, 169-172.

Brenner, W. G., Romanov, G. A., Köllmer, I., Bürkle, L., & Schmülling, T. (2005). Immediate-early and delayed cytokinin response genes of Arabidopsis thaliana identified by genome-wide expression profiling reveal novel cytokinin-sensitive processes and suggest cytokinin action through transcriptional cascades. The Plant Journal, 44(2), 314-333.

Brinton, J., Ramirez-Gonzalez, R. H., Simmonds, J., Wingen, L., Orford, S., Griffiths, S., Haberer, G., Spannagl, M., Walkowiak, S., Pozniak, C., & Uauy, C. (2020). A haplotype-led approach to increase the precision of wheat breeding. Communications Biology, 3(1), 712.

Cao, H., Qi, S., Sun, M., Li, Z., Yang, Y., Crawford, N. M., & Wang, Y. (2017). Overexpression of the Maize ZmNLP6 and ZmNLP8 Can Complement the Arabidopsis Nitrate Regulatory Mutant nlp7 by Restoring Nitrate Signaling and Assimilation. Frontiers in Plant Science, 8, 1703.

Chen, Y., Hou, M., Liu, L., Wu, S., Shen, Y., Ishiyama, K., Kobayashi, M., McCarty, D. R., & Tan, B.-C. (2014). The Maize DWARF1 Encodes a Gibberellin 3-Oxidase and Is Dual Localized to the Nucleus and Cytosol. Plant Physiology, 166(4), 2028-2039.

Crawford, N. M., & Glass, A. D. M. (1998). Molecular and physiological aspects of nitrate uptake in plants. Trends in Plant Science, 3(10), 389-395.

Curci, P. L., Aiese Cigliano, R., Zuluaga, D. L., Janni, M., Sanseverino, W., & Sonnante, G. (2017). Transcriptomic response of durum wheat to nitrogen starvation. Scientific Reports, 7(1), 1176.

Daniel-Vedele, F., Filleur, S., & Caboche, M. (1998). Nitrate transport: a key step in nitrate assimilation. Current Opinion in Plant Biology, 1(3), 235-239.

Dechorgnat, J., Nguyen, C. T., Armengaud, P., Jossier, M., Diatloff, E., Filleur, S., & Daniel-Vedele, F. (2011). From the soil to the seeds: the long journey of nitrate in plants. Journal of Experimental Botany, 62(4), 1349-1359.

Dong, J., Jones, R., & Mou, P. (2018). Relationships between Nutrient Heterogeneity, Root Growth, and Hormones: Evidence for Interspecific Variation. Plants, 7(1), 15.

Duan, F., Giehl, R. F. H., Geldner, N., Salt, D. E., & von Wirén, N. (2018). Root zone–specific localization of AMTs determines ammonium transport pathways and nitrogen allocation to shoots. PLOS Biology, 16(10), e2006024.

Ehdaie, B., Layne, A. P., & Waines, J. G. (2012). Root system plasticity to drought influences grain yield in bread wheat. Euphytica, 186(1), 219-232.

Eppley, R. W., Coatsworth, J. L., & Solórzano, L. (1969). Studies of nitrate reductase in marine phytoplankton1. Limnology and Oceanography, 14(2), 194-205.

FAO. (2016). World fertilizer trends and outlook to 2015 - 2019.

FAO. (2019). World fertilizer trends and outlook to 2019 - 2022.

Fiorani, F., & Schurr, U. (2013). Future Scenarios for Plant Phenotyping. Annual Review of Plant Biology, 64(1), 267-291.

Fischer, R. A. (2007). Understanding the physiological basis of yield potential in wheat. The Journal of Agricultural Science, 145(02), 99-113.

Fischer, R. A. (2011). Wheat physiology: a review of recent developments. Crop and Pasture Science, 62(2), 95-114.

Forde, B. G. (2000). Nitrate transporters in plants: structure, function and regulation. Biochimica et Biophysica Acta (BBA) - Biomembranes, 1465(1-2), 219-235.

Forde, B. G. (2002). Local and long-range signaling pathways regulating plant responses to nitrate. Annual Review of Plant Biology, 53(1), 203-224.

Foulkes, M. J., Slafer, G. A., Davies, W. J., Berry, P. M., Sylvester-Bradley, R., Martre, P., Calderini, D. F., Griffiths, S., & Reynolds, M. P. (2011a). Raising yield potential of wheat. III. Optimizing partitioning to grain while maintaining lodging resistance. Journal of Experimental Botany, 62(2), 469-486.

Foulkes, M. J., Snape, J. W., Shearman, V. J., Reynolds, M. P., Gaju, O., & Sylvester-Bradley, R. (2007). Genetic progress in yield potential in wheat: recent advances and future prospects. The Journal of Agricultural Science, 145(1), 17-29.

Fueki, N., Nakamura, R., Sawaguchi, A., Watanobe, K., Suzuki, T., Uchida, T., & Onodera, M. (2015). Prediction of nitrogen uptake by winter wheat (Triticum aestivum L.) by measurement of superior stem number and leaf color value, for decision-making regarding additional nitrogen fertilization. Soil Science and Plant Nutrition, 61(5), 769-774.

Gahoonia, T. S., Ali, R., Malhotra, R. S., Jahoor, A., & Rahman, M. M. (2007). Variation in Root Morphological and Physiological Traits and Nutrient Uptake of Chickpea Genotypes. Journal of Plant Nutrition, 30(6), 829-841.

Gansel, X., Muños, S., Tillard, P., & Gojon, A. (2001). Differential regulation of the NO3- and NH4+ transporter genes AtNrt2.1 and AtAmt1.1 in Arabidopsis: relation with long-distance and local controls by N status of the plant. The Plant Journal, 26(2), 143-155.

Ganz, P., Ijato, T., Porras-Murrilo, R., Stührwohldt, N., Ludewig, U., & Neuhäuser, B. (2020). A twin histidine motif is the core structure for high-affinity substrate selection in plant ammonium transporters. Journal of Biological Chemistry, 295(10), 3362-3370.

Garnett, T., Conn, V., & Kaiser, B. N. (2009). Root based approaches to improving nitrogen use efficiency in plants. Plant, Cell & Environment, 32(9), 1272-1283.

Garnett, T., Conn, V., Plett, D., Conn, S., Zanghellini, J., Mackenzie, N., Enju, A., Francis, K., Holtham, L., Roessner, U., Boughton, B., Bacic, A., Shirley, N., Rafalski, A., Dhugga, K., Tester, M., & Kaiser, B. N. (2013). The response of the maize nitrate transport system to nitrogen demand and supply across the lifecycle. New Phytologist, 198(1), 82-94.

Gazzarrini, S., Lejay, L., Gojon, A., Ninnemann, O., Frommer, W. B., & von Wirén, N. (1999). Three Functional Transporters for Constitutive, Diurnally Regulated, and Starvation-Induced Uptake of Ammonium into Arabidopsis Roots. The Plant Cell, 11(5), 937-947.

Giehl, R. F. H., Gruber, B. D., & von Wirén, N. (2014). It's time to make changes: modulation of root system architecture by nutrient signals. Journal of Experimental Botany, 65(3), 769-778

Giehl, R. F. H., Laginha, A. M., Duan, F., Rentsch, D., Yuan, L., & von Wirén, N. (2017). A Critical Role of AMT2;1 in Root-To-Shoot Translocation of Ammonium in Arabidopsis. Molecular Plant, 10(11), 1449-1460.

Giehl, R. F. H., & von Wiren, N. (2014). Root Nutrient Foraging. Plant Physiology, 166(2), 509-517.

Glass, A. D. M. (2002). The regulation of nitrate and ammonium transport systems in plants. Journal of Experimental Botany, 53(370), 855-864.

Gooding, M. J., Addisu, M., Uppal, R. K., Snape, J. W., & Jones, H. E. (2012). Effect of wheat dwarfing genes on nitrogen-use efficiency. The Journal of Agricultural Science, 150(1), 3-22.

Górny, A. G., Banaszak, Z., Ługowska, B., & Ratajczak, D. (2011). Inheritance of the efficiency of nitrogen uptake and utilization in winter wheat (Triticum aestivum L.) under diverse nutrition levels. Euphytica, 177(2), 191-206.

Gruber, B. D., Giehl, R. F. H., Friedel, S., & von Wirén, N. (2013). Plasticity of the Arabidopsis Root System under Nutrient Deficiencies. Plant Physiology, 163(1), 161-179.

Guo, F.-Q., Young, J., & Crawford, N. M. (2003). The Nitrate Transporter AtNRT1.1 (CHL1) Functions in Stomatal Opening and Contributes to Drought Susceptibility in Arabidopsis. The Plant Cell, 15(1), 107-117.

Hachiya, T., & Sakakibara, H. (2016). Interactions between nitrate and ammonium in their uptake, allocation, assimilation, and signaling in plants. Journal of Experimental Botany, erw449.

Haefele, S. M., Jabbar, S. M. A., Siopongco, J. D. L. C., Tirol-Padre, A., Amarante, S. T., Sta Cruz, P. C., & Cosico, W. C. (2008). Nitrogen use efficiency in selected rice (Oryza sativa L.) genotypes under different water regimes and nitrogen levels. Field Crops Research, 107(2), 137-146.

Han, M., Okamoto, M., Beatty, P. H., Rothstein, S. J., & Good, A. G. (2015). The Genetics of Nitrogen Use Efficiency in Crop Plants. Annual Review of Genetics, 49(1), 269-289.

Hao, D.-L., Zhou, J.-Y., Yang, S.-Y., Qi, W., Yang, K.-J., & Su, Y.-H. (2020). Function and Regulation of Ammonium Transporters in Plants. International Journal of Molecular Sciences, 21(10), 3557.

Hao, M., Zhang, L., Ning, S., Huang, L., Yuan, Z., Wu, B., Yan, Z., Dai, S., Jiang, B., Zheng, Y., & Liu, D. (2020). The Resurgence of Introgression Breeding, as Exemplified in Wheat Improvement. Frontiers in Plant Science, 11.

Harberd, N. P., Belfield, E., & Yasumura, Y. (2009). The Angiosperm Gibberellin-GID1-DELLA Growth Regulatory Mechanism: How an “Inhibitor of an Inhibitor” Enables Flexible Response to Fluctuating Environments. The Plant Cell, 21(5), 1328-1339.

Hawkesford, M. J. (2012). Improving Nutrient Use Efficiency in Crops. In eLS. Wiley.

Hawkesford, M. J. (2014). Reducing the reliance on nitrogen fertilizer for wheat production. Journal of Cereal Science, 59(3), 276-283.

Hawkesford, M. J. (2017). Genetic variation in traits for nitrogen use efficiency in wheat. Journal of Experimental Botany, 68(10).

Hedden, P. (2003). The genes of the Green Revolution. Trends in Genetics, 19(1), 5-9.

He, X., Qu, B., Li, W., Zhao, X., Teng, W., Ma, W., Ren, Y., Li, B., Li, Z., & Tong, Y. (2015). The nitrate inducible NAC transcription factor TaNAC2-5A controls nitrate response and increases wheat yield. Plant Physiology, 169(3), 1991-2005.

Ho, C.-H., Lin, S.-H., Hu, H.-C., & Tsay, Y.-F. (2009). CHL1 Functions as a Nitrate Sensor in Plants. Cell, 138(6), 1184-1194.

Hoopen, F. t., Cuin, T. A., Pedas, P., Hegelund, J. N., Shabala, S., Schjoerring, J. K., & Jahn, T. P. (2010). Competition between uptake of ammonium and potassium in barley and Arabidopsis roots: molecular mechanisms and physiological consequences. Journal of Experimental Botany, 61(9), 2303-2315.

Huang, N.-C., Liu, K.-H., Lo, H.-J., & Tsay, Y.-F. (1999). Cloning and Functional Characterization of an Arabidopsis Nitrate Transporter Gene That Encodes a Constitutive Component of Low-Affinity Uptake. The Plant Cell, 11(8), 1381-1392.

Huang, X. Q., Cöster, H., Ganal, M. W., & Röder, M. S. (2003). Advanced backcross QTL analysis for the identification of quantitative trait loci alleles from wild relatives of wheat (Triticum aestivum L.). Theoretical and Applied Genetics, 106(8), 1379–1389.

Huang, X. Q., Kempf, H., Ganal, M. W., & Röder, M. S. (2004). Advanced backcross QTL analysis in progenies derived from a cross between a German elite winter wheat variety and a synthetic wheat (Triticum aestivum L.). Theoretical and Applied Genetics, 109(5), 933-943.

Hu, B., Wang, W., Ou, S., Tang, J., Li, H., Che, R., Zhang, Z., Chai, X., Wang, H., Wang, Y., Liang, C., Liu, L., Piao, Z., Deng, Q., Deng, K., Xu, C., Liang, Y., Zhang, L., Li, L., & Chu, C. (2015). Variation in NRT1.1B contributes to nitrate-use divergence between rice subspecies. Nature Genetics, 47(7), 834-838.

Iqbal, A., Qiang, D., Alamzeb, M., Xiangru, W., Huiping, G., Hengheng, Z., Nianchang, P., Xiling, Z., & Meizhen, S. (2020). Untangling the molecular mechanisms and functions of nitrate to improve nitrogen use efficiency. Journal of the Science of Food and Agriculture, 100(3), 904-914.

Jacquot, A., Chaput, V., Mauries, A., Li, Z., Tillard, P., Fizames, C., Bonillo, P., Bellegarde, F., Laugier, E., Santoni, V., Hem, S., Martin, A., Gojon, A., Schulze, W., & Lejay, L. (2020). NRT2.1 C-terminus phosphorylation prevents root high affinity nitrate uptake activity in Arabidopsis thaliana. New Phytologist, 228(3), 1038-1054.

Jian, S., Liao, Q., Song, H., Liu, Q., Lepo, J. E., Guan, C., Zhang, J., Ismail, A. M., & Zhang, Z. (2018). NRT1.1-Related NH4+ Toxicity Is Associated with a Disturbed Balance between NH4+ Uptake and Assimilation. Plant Physiology, 178(4), 1473-1488.

Jia, Z., Giehl, R. F. H., Meyer, R. C., Altmann, T., & von Wirén, N. (2019). Natural variation of BSK3 tunes brassinosteroid signaling to regulate root foraging under low nitrogen. Nature Communications, 10(1), 2378.

Jia, Z., Giehl, R. F. H., & von Wirén, N. (2022). Nutrient–hormone relations: Driving root plasticity in plants. Molecular Plant, 15(1), 86-103.

Jung, J. K. H., & McCouch, S. (2013). Getting to the roots of it: Genetic and hormonal control of root architecture. Frontiers in Plant Science, 4, 186.

Kahiluoto, H., Kuisma, M., Kuokkanen, A., Mikkilä, M., & Linnanen, L. (2014). Taking planetary nutrient boundaries seriously: Can we feed the people? Global Food Security, 3(1), 16-21.

Katsura, K., Okami, M., Mizunuma, H., & Kato, Y. (2010). Radiation use efficiency, N accumulation and biomass production of high-yielding rice in aerobic culture. Field Crops Research, 117(1), 81-89.

Kelley, L. A., Mezulis, S., Yates, C. M., Wass, M. N., & Sternberg, M. J. E. (2015). The Phyre2 web portal for protein modeling, prediction and analysis. Nature Protocols, 10(6), 845-858.

Khademi, S., O'Connell, J., Remis, J., Robles-Colmenares, Y., Miercke, L. J. W., & Stroud, R. M. (2004). Mechanism of Ammonia Transport by Amt/MEP/Rh: Structure of AmtB at 1.35 Å. Science, 305(5690), 1587-1594.

Kiba, T., Feria-Bourrellier, A.-B., Lafouge, F., Lezhneva, L., Boutet-Mercey, S., Orsel, M., Bréhaut, V., Miller, A., Daniel-Vedele, F., Sakakibara, H., & Krapp, A. (2012). The arabidopsis nitrate transporter nrt2.4 plays a double role in roots and shoots of nitrogen-starved plants. The Plant Cell, 24(1), 245-258.

Kiba, T., Naitou, T., Koizumi, N., Yamashino, T., Sakakibara, H., & Mizuno, T. (2005). Combinatorial Microarray Analysis Revealing Arabidopsis Genes Implicated in Cytokinin Responses through the His→Asp Phosphorelay Circuitry. Plant and Cell Physiology, 46(2), 339-355.

Kichey, T., Hirel, B., Heumez, E., Dubois, F., & le Gouis, J. (2007). In winter wheat (Triticum aestivum L.), post-anthesis nitrogen uptake and remobilisation to the grain correlates with agronomic traits and nitrogen physiological markers. Field Crops Research, 102(1), 22-32.

Koegel, S., Mieulet, D., Baday, S., Chatagnier, O., Lehmann, M. F., Wiemken, A., Boller, T., Wipf, D., Bernèche, S., Guiderdoni, E., & Courty, P.-E. (2017). Phylogenetic, structural, and functional characterization of AMT3;1, an ammonium transporter induced by mycorrhization among model grasses. Mycorrhiza, 27(7), 695-708.

Konishi, N., & Ma, J. F. (2021). Three polarly localized ammonium transporter 1 members are cooperatively responsible for ammonium uptake in rice under low ammonium condition. New Phytologist, 232(4), 1778-1792.

Kronzucker, H. J., Siddiqi, M. Y., & Glass, ADM. (1996). Kinetics of NH4+ Influx in Spruce. Plant Physiology, 110(3), 773-779.

Krouk, G., Lacombe, B., Bielach, A., Perrine-Walker, F., Malinska, K., Mounier, E., Hoyerova, K., Tillard, P., Leon, S., Ljung, K., Zazimalova, E., Benkova, E., Nacry, P., & Gojon, A. (2010). Nitrate-Regulated Auxin Transport by NRT1.1 Defines a Mechanism for Nutrient Sensing in Plants. Developmental Cell, 18(6), 927-937.

Krouk, G., Ruffel, S., Gutiérrez, R. A., Gojon, A., Crawford, N. M., Coruzzi, G. M., & Lacombe, B. (2011). A framework integrating plant growth with hormones and nutrients. Trends in Plant Science, 16(4), 178-182.

Kumar, A., Silim, S. N., Okamoto, M., Siddiqi, M. Y., & Glass, A. D. M. (2003). Differential expression of three members of the AMT1 gene family encoding putative high-affinity NH4+ transporters in roots of Oryza sativa subspecies indica. Plant, Cell & Environment, 26(6), 907-914.

Kurai, T., Wakayama, M., Abiko, T., Yanagisawa, S., Aoki, N., & Ohsugi, R. (2011). Introduction of the ZmDof1 gene into rice enhances carbon and nitrogen assimilation under low-nitrogen conditions. Plant Biotechnology Journal, 9(8), 826-837.

Lammerts van Bueren, E. T., & Struik, P. C. (2017). Diverse concepts of breeding for nitrogen use efficiency. A review. Agronomy for Sustainable Development, 37(5), 50.

Lanquar, V., Loqué, D., Hörmann, F., Yuan, L., Bohner, A., Engelsberger, W. R., Lalonde, S., Schulze, W. X., von Wirén, N., & Frommer, W. B. (2009). Feedback Inhibition of Ammonium Uptake by a Phospho-Dependent Allosteric Mechanism in Arabidopsis. The Plant Cell, 21(11), 3610-3622.

le Gouis, J., Béghin, D., Heumez, E., & Pluchard, P. (2000). Genetic differences for nitrogen uptake and nitrogen utilisation efficiencies in winter wheat. European Journal of Agronomy, 12(3–4), 163-173.

le Marié, C. A., York, L. M., Strigens, A., Malosetti, M., Camp, K.-H., Giuliani, S., Lynch, J. P., & Hund, A. (2019). Shovelomics root traits assessed on the EURoot maize panel are highly heritable across environments but show low genotype-by-nitrogen interaction. Euphytica, 215(10), 173.

Lezhneva, L., Kiba, T., Feria-Bourrellier, A.-B., Lafouge, F., Boutet-Mercey, S., Zoufan, P., Sakakibara, H., Daniel-Vedele, F., & Krapp, A. (2014). The Arabidopsis nitrate transporter NRT2.5 plays a role in nitrate acquisition and remobilization in nitrogen-starved plants. The Plant Journal, 80(2), 230-241.

Liao, M., Fillery, I. R. P., & Palta, J. A. (2004). Early vigorous growth is a major factor influencing nitrogen uptake in wheat. Functional Plant Biology, 31(2), 121.

Lin, C.-M., Koh, S., Stacey, G., Yu, S.-M., Lin, T.-Y., & Tsay, Y.-F. (2000). Cloning and Functional Characterization of a Constitutively Expressed Nitrate Transporter Gene, OsNRT1, from Rice. Plant Physiology, 122(2), 379-388.

Li, Q., Wu, Y., Chen, W., Jin, R., Kong, F., Ke, Y., Shi, H., & Yuan, J. (2017). Cultivar Differences in Root Nitrogen Uptake Ability of Maize Hybrids. Frontiers in Plant Science, 8, 1060.

Li, T., Liao, K., Xu, X., Gao, Y., Wang, Z., Zhu, X., Jia, B., & Xuan, Y. (2017). Wheat Ammonium Transporter (AMT) Gene Family: Diversity and Possible Role in Host–Pathogen Interaction with Stem Rust. Frontiers in Plant Science, 8, 1637.

Liu, J., Chen, F., Olokhnuud, C., Glass, A. D. M., Tong, Y., Zhang, F., & Mi, G. (2009). Root size and nitrogen-uptake activity in two maize (Zea mays) inbred lines differing in nitrogen-use efficiency. Journal of Plant Nutrition and Soil Science, 172(2), 230-236.

Liu, K., He, A., Ye, C., Liu, S., Lu, J., Gao, M., Fan, Y., Lu, B., Tian, X., & Zhang, Y. (2018). Root Morphological Traits and Spatial Distribution under Different Nitrogen Treatments and Their Relationship with Grain Yield in Super Hybrid Rice. Scientific Reports, 8(1), 131.

Liu, K.-H., Huang, C.-Y., & Tsay, Y.-F. (1999a). CHL1 Is a Dual-Affinity Nitrate Transporter of Arabidopsis Involved in Multiple Phases of Nitrate Uptake. The Plant Cell, 11(5), 865-874.

Liu, K.-H., & Tsay, Y.-F. (2003). Switching between the two action modes of the dual-affinity nitrate transporter CHL1 by phosphorylation. The EMBO Journal, 22(5), 1005-1013.

Liu, S., Zhou, R., Dong, Y., Li, P., & Jia, J. (2006). Development, utilization of introgression lines using a synthetic wheat as donor. Theoretical and Applied Genetics, 112(7), 1360-1373.

Liu, Y., & von Wirén, N. (2017a). Ammonium as a signal for physiological and morphological responses in plants. Journal of Experimental Botany, 68(10), 2581-2592.

Loqué, D., Lalonde, S., Looger, L. L., von Wirén, N., & Frommer, W. B. (2007). A cytosolic trans-activation domain essential for ammonium uptake. Nature, 446(7132), 195-198.

Loqué, D., Mora, S. I., Andrade, S. L. A., Pantoja, O., & Frommer, W. B. (2009). Pore Mutations in Ammonium Transporter AMT1 with Increased Electrogenic Ammonium Transport Activity. Journal of Biological Chemistry, 284(37), 24988-24995.

Loque, D., & von Wiren, N. (2004). Regulatory levels for the transport of ammonium in plant roots. Journal of Experimental Botany, 55(401), 1293-1305.

Lynch, J. P., & Brown, K. M. (2012). New roots for agriculture: exploiting the root phenome. Philosophical Transactions of the Royal Society B: Biological Sciences, 367(1595), 1598-1604.

Ma, N., Dong, L., Lü, W., Lü, J., Meng, Q., & Liu, P. (2020). Transcriptome analysis of maize seedling roots in response to nitrogen-, phosphorus-, and potassium deficiency. Plant and Soil, 447(1–2), 637-658.

Masclaux-Daubresse, C., Daniel-Vedele, F., Dechorgnat, J., Chardon, F., Gaufichon, L., & Suzuki, A. (2010). Nitrogen uptake, assimilation and remobilization in plants: challenges for sustainable and productive agriculture. Annals of Botany, 105(7), 1141-1157.

Ma, W., Li, J., Qu, B., He, X., Zhao, X., Li, B., Fu, X., & Tong, Y. (2014). Auxin biosynthetic gene TAR2 is involved in low nitrogen-mediated reprogramming of root architecture in Arabidopsis. The Plant Journal, 78(1), 70-79.

McCarty, P. L. and S. C. N. (1978). Chemistry for environmental engineering. McGraw-Hill.

McGuire, A. M., Bryant, D. C., & Denison, R. F. (1998). Wheat Yields, Nitrogen Uptake, and Soil Moisture Following Winter Legume Cover Crop vs. Fallow. Agronomy Journal, 90(3), 404-410.

Moll, R. H., Kamprath, E. J., & Jackson, W. A. (1982). Analysis and Interpretation of Factors Which Contribute to Efficiency of Nitrogen Utilization[1]. Agronomy Journal, 74(3), 562-564.

M. Shahbandeh. (2021). Wheat - production volume worldwide 2011/2012-2020/21.

Muños, S., Cazettes, C., Fizames, C., Gaymard, F., Tillard, P., Lepetit, M., Lejay, L., & Gojon, A. (2004). Transcript Profiling in the chl1-5 Mutant of Arabidopsis Reveals a Role of the Nitrate Transporter NRT1.1 in the Regulation of Another Nitrate Transporter, NRT2.1[W]. The Plant Cell, 16(9), 2433-2447.

Muurinen, S., Slafer, G. A., & Peltonen-Sainio, P. (2006). Breeding Effects on Nitrogen Use Efficiency of Spring Cereals under Northern Conditions. Crop Science, 46(2), 561-568.

Neuhäuser, B., Dynowski, M., Mayer, M., & Ludewig, U. (2007). Regulation of NH4 + Transport by Essential Cross Talk between AMT Monomers through the Carboxyl Tails. Plant Physiology, 143(4), 1651-1659.

Ninnemann, O., Jauniaux, J. C., & Frommer, W. B. (1994). Identification of a high affinity NH4+ transporter from plants. The EMBO Journal, 13(15), 3464-3471.

Ohyama, T., Minagawa, R., Ishikawa, S., Yamamoto, M., Phi Hung, N. van, Ohtake, N., Sueyoshi, K., Sato, T., Nagumo, Y., & Takahashi, Y. (2013). Soybean Seed Production and Nitrogen Nutrition. In A Comprehensive Survey of International Soybean Research - Genetics, Physiology, Agronomy and Nitrogen Relationships. IntechOpen.

Okamoto, M., Vidmar, J. J., & Glass, A. D. M. (2003). Regulation of NRT1 and NRT2 Gene Families of Arabidopsis thaliana: Responses to Nitrate Provision. Plant and Cell Physiology, 44(3), 304-317.

Palta, J. A., & Yang, J. (2014). Crop root system behaviour and yield. Field Crops Research, 165, 1-4.

Pang, J., Milroy, S. P., Rebetzke, G. J., & Palta, J. A. (2015). The influence of shoot and root size on nitrogen uptake in wheat is affected by nitrate affinity in the roots during early growth. Functional Plant Biology, 42(12), 1179.

Peng, J., Richards, D. E., Hartley, N. M., Murphy, G. P., Devos, K. M., Flintham, J. E., Beales, J., Fish, L. J., Worland, A. J., Pelica, F., Sudhakar, D., Christou, P., Snape, J. W., Gale, M. D., & Harberd, N. P. (1999). 'Green revolution' genes encode mutant gibberellin response modulators. Nature, 400(6741), 256-261.

Plackett, A. R. G., Powers, S. J., Fernandez-Garcia, N., Urbanova, T., Takebayashi, Y., Seo, M., Jikumaru, Y., Benlloch, R., Nilsson, O., Ruiz-Rivero, O., Phillips, A. L., Wilson, Z. A., Thomas, S. G., & Hedden, P. (2012). Analysis of the Developmental Roles of the Arabidopsis Gibberellin 20-Oxidases Demonstrates That GA20ox1, -2 , and -3 Are the Dominant Paralogs. The Plant Cell, 24(3), 941-960.

Plett, D., Toubia, J., Garnett, T., Tester, M., Kaiser, B. N., & Baumann, U. (2010). Dichotomy in the NRT Gene Families of Dicots and Grass Species. PLoS ONE, 5(12), e15289.

Ranathunge, K., El-kereamy, A., Gidda, S., Bi, Y.-M., & Rothstein, S. J. (2014). AMT1;1 transgenic rice plants with enhanced NH4+ permeability show superior growth and higher yield under optimal and suboptimal NH4+ conditions. Journal of Experimental Botany, 65(4), 965-979.

Raun, W. R., & Johnson, G. v. (1999). Improving Nitrogen Use Efficiency for Cereal Production. Agronomy Journal, 91(3), 357-363.

Reynolds, M. P., Lewis, J. M., Ammar, K., Basnet, B. R., Crespo-Herrera, L., Crossa, J., Dhugga, K. S., Dreisigacker, S., Juliana, P., Karwat, H., Kishii, M., Krause, M. R., Langridge, P., Lashkari, A., Mondal, S., Payne, T., Pequeno, D., Pinto, F., Sansaloni, C., Braun, H. J. (2021). Harnessing translational research in wheat for climate resilience. Journal of Experimental Botany, 72(14), 5134-5157.

Rockström, J., (2009). Planetary boundaries exploring the safe operating space for humanity. Ecology and Society.

Ruffel, S., Krouk, G., Ristova, D., Shasha, D., Birnbaum, K. D., & Coruzzi, G. M. (2011). Nitrogen economics of root foraging: Transitive closure of the nitrate–cytokinin relay and distinct systemic signaling for N supply vs. demand. Proceedings of the National Academy of Sciences, 108(45), 18524-18529.

Sakakibara, H., Takei, K., & Hirose, N. (2006). Interactions between nitrogen and cytokinin in the regulation of metabolism and development. Trends in Plant Science, 11(9), 440-448.

Saville, R. J., Gosman, N., Burt, C. J., Makepeace, J., Steed, A., Corbitt, M., Chandler, E., Brown, J. K. M., Boulton, M. I., & Nicholson, P. (2012). The “Green Revolution” dwarfing genes play a role in disease resistance in Triticum aestivum and Hordeum vulgare. Journal of Experimental Botany, 63(3), 1271-1283.

Schjoerring, J. K., Husted, S., Mäck, G., & Mattsson, M. (2002). The regulation of ammonium translocation in plants. Journal of Experimental Botany, 53(370), 883-890.

Shao, A., Ma, W., Zhao, X., Hu, M., He, X., Teng, W., Li, H., & Tong, Y. (2017). The Auxin Biosynthetic tryptophan aminotransferase related TaTAR2.1-3A Increases Grain Yield of Wheat. Plant Physiology, 174(4), 2274-2288.

Sharma, S., Bhat, P. R., Ehdaie, B., Close, T. J., Lukaszewski, A. J., & Waines, J. G. (2009). Integrated genetic map and genetic analysis of a region associated with root traits on the short arm of rye chromosome 1 in bread wheat. Theoretical and Applied Genetics, 119(5), 783-793.

Shen, Y., Li, S., & Shao, M. (2013). Effects of spatial coupling of water and fertilizer applications on root growth characteristics and water use of winter wheat. Journal of Plant Nutrition, 36(4), 515-528.

Shorinola, O., Kaye, R., Golan, G., Peleg, Z., Kepinski, S., & Uauy, C. (2019). Genetic Screening for Mutants with Altered Seminal Root Numbers in Hexaploid Wheat Using a High-Throughput Root Phenotyping Platform. G3 Genes|Genomes|Genetics, 9(9), 2799-2809.

Søgaard, R., Alsterfjord, M., MacAulay, N., & Zeuthen, T. (2009). Ammonium ion transport by the AMT/Rh homolog TaAMT1;1 is stimulated by acidic pH. Pflügers Archiv - European Journal of Physiology, 458(4), 733-743.

Sohlenkamp, C., Shelden, M., Howitt, S., & Udvardi, M. (2000). Characterization of Arabidopsis AtAMT2, a novel ammonium transporter in plants. FEBS Letters, 467(2–3), 273-278.

Sohlenkamp, C., Wood, C. C., Roeb, G. W., & Udvardi, M. K. (2002). Characterization of Arabidopsis AtAMT2, a High-Affinity Ammonium Transporter of the Plasma Membrane. Plant Physiology, 130(4), 1788-1796.

Sonoda, Y., Ikeda, A., Saiki, S., Wirén, N. von, Yamaya, T., & Yamaguchi, J. (2003). Distinct Expression and Function of Three Ammonium Transporter Genes (OsAMT1;1 – 1;3) in Rice. Plant and Cell Physiology, 44(7), 726-734.

Sonoda, Y., Ikeda, A., Saiki, S., Yamaya, T., & Yamaguchi, J. (2003a). Feedback Regulation of the Ammonium Transporter Gene Family AMT1 by Glutamine in Rice. Plant and Cell Physiology, 44(12), 1396-1402.

Straub, T., Ludewig, U., & Neuhäuser, B. (2017). The Kinase CIPK23 Inhibits Ammonium Transport in Arabidopsis thaliana. The Plant Cell, 29(2), 409-422.

Sun, J., & Zheng, N. (2015). Molecular Mechanism Underlying the Plant NRT1.1 Dual-Affinity Nitrate Transporter. Frontiers in Physiology, 6, 386.

Swarbreck, S. M., Wang, M., Wang, Y., Kindred, D., Sylvester-Bradley, R., Shi, W., Varinderpal-Singh, Bentley, A. R., & Griffiths, H. (2019). A Roadmap for Lowering Crop Nitrogen Requirement. Trends in Plant Science, 24(10), 892-904.

Tanksley, S. D., Grandillo, S., Fulton, T. M., Zamir, D., Eshed, Y., Petiard, V., Lopez, J., & Beck-Bunn, T. (1996). Advanced backcross QTL analysis in a cross between an elite processing line of tomato and its wild relative L. pimpinellifolium. Theoretical and Applied Genetics, 92(2), 213-224.

Thornton, B. (2004). Inhibition of nitrate influx by glutamine in Lolium perenne depends upon the contribution of the HATS to the total influx. Journal of Experimental Botany, 55(397), 761-769.

Tian, Y., Fan, M., Qin, Z., Lv, H., Wang, M., Zhang, Z., Zhou, W., Zhao, N., Li, X., Han, C., Ding, Z., Wang, W., Wang, Z.-Y., & Bai, M.-Y. (2018). Hydrogen peroxide positively regulates brassinosteroid signaling through oxidation of the brassinazole-resistant1 transcription factor. Nature Communications, 9(1), 1063.

Trachsel, S., Kaeppler, S. M., Brown, K. M., & Lynch, J. P. (2011). Shovelomics: high throughput phenotyping of maize (Zea mays L.) root architecture in the field. Plant and Soil, 341(1–2), 75-87.

Tsay, Y.-F., Chiu, C.-C., Tsai, C.-B., Ho, C.-H., & Hsu, P.-K. (2007). Nitrate transporters and peptide transporters. FEBS Letters, 581(12), 2290-2300.

van den Berg, B., Chembath, A., Jefferies, D., Basle, A., Khalid, S., & Rutherford, J. C. (2016). Structural basis for Mep2 ammonium transceptor activation by phosphorylation. Nature Communications, 7(1), 11337.

Vidal, E. A., Alvarez, J. M., Araus, V., Riveras, E., Brooks, M. D., Krouk, G., Ruffel, S., Lejay, L., Crawford, N. M., Coruzzi, G. M., & Gutiérrez, R. A. (2020). Nitrate in 2020: Thirty Years from Transport to Signaling Networks. The Plant Cell, 32(7), 2094-2119.

von Wirén, N., Gazzarrini, S., Gojon, A., & Frommer, W. B. (2000). The molecular physiology of ammonium uptake and retrieval. Current Opinion in Plant Biology, 3(3), 254-261.

Voss-Fels, K. P., Stahl, A., & Hickey, L. T. (2019). Q&A: modern crop breeding for future food security. BMC Biology, 17(1), 18.

Walkowiak, S., Gao, L., Monat, C., Haberer, G., Kassa, M. T., Brinton, J., Ramirez-Gonzalez, R. H., Kolodziej, M. C., Delorean, E., Thambugala, D., Klymiuk, V., Byrns, B., Gundlach, H., Bandi, V., Siri, J. N., Nilsen, K., Aquino, C., Himmelbach, A., Copetti, D., Pozniak, C. J. (2020). Multiple wheat genomes reveal global variation in modern breeding. Nature, 588(7837), 277-283.

Wang, P., Wang, Z., Cai, R., Li, Y., Chen, X., & Yin, Y. (2011). Physiological and Molecular Response of Wheat Roots to Nitrate Supply in Seedling Stage. Agricultural Sciences in China, 10(5), 695-704.

Wang, R., Liu, D., & Crawford, N. M. (1998). The Arabidopsis CHL1 protein plays a major role in high-affinity nitrate uptake. Proceedings of the National Academy of Sciences, 95(25), 15134-15139.

Wang, Y.-Y., Hsu, P.-K., & Tsay, Y.-F. (2012). Uptake, allocation and signaling of nitrate. Trends in Plant Science, 17(8), 458-467.

Waterhouse, A., Bertoni, M., Bienert, S., Studer, G., Tauriello, G., Gumienny, R., Heer, F. T., de Beer, T. A. P., Rempfer, C., Bordoli, L., Lepore, R., & Schwede, T. (2018). SWISS-MODEL: homology modelling of protein structures and complexes. Nucleic Acids Research, 46(W1), W296-W303.

Weih, M., Hamnér, K., & Pourazari, F. (2018). Analyzing plant nutrient uptake and utilization efficiencies: comparison between crops and approaches. Plant and Soil, 430(1–2), 7-21.

Williams, L., & Miller, A. (2001). Transporters responsible for the uptake and partitioning of nitrogenous solutes. Annual Review of Plant Physiology and Plant Molecular Biology, 52(1), 659-688.

Wu, X., Yang, H., Qu, C., Xu, Z., Li, W., Hao, B., Yang, C., Sun, G., & Liu, G. (2015). Sequence and expression analysis of the AMT gene family in poplar. Frontiers in Plant Science, 6.

Xiao, J., Li, J., Grandillo, S., Ahn, S. N., Yuan, L., Tanksley, S. D., & McCouch, S. R. (1998). Identification of Trait-Improving Quantitative Trait Loci Alleles from a Wild Rice Relative, Oryza rufipogon. Genetics, 150(2), 899-909.

Xuan, W., Beeckman, T., & Xu, G. (2017). Plant nitrogen nutrition: sensing and signaling. Current Opinion in Plant Biology, 39, 57-65.

Xu, G., Fan, X., & Miller, A. J. (2012). Plant Nitrogen Assimilation and Use Efficiency. Annual Review of Plant Biology, 63(1), 153-182.

Yanagisawa, S., Akiyama, A., Kisaka, H., Uchimiya, H., & Miwa, T. (2004). Metabolic engineering with Dof1 transcription factor in plants: Improved nitrogen assimilation and growth under low-nitrogen conditions. Proceedings of the National Academy of Sciences, 101(20), 7833-7838.

Yang, T., Hao, L., Yao, S., Zhao, Y., Lu, W., & Xiao, K. (2016). TabHLH1, a bHLH-type transcription factor gene in wheat, improves plant tolerance to Pi and N deprivation via regulation of nutrient transporter gene transcription and ROS homeostasis. Plant Physiology and Biochemistry, 104, 99-113.

Yin, L.-P., Li, P., Wen, B., Taylor, D., & Berry, J. O. (2007). Characterization and expression of a high-affinity nitrate system transporter gene (TaNRT2.1) from wheat roots, and its evolutionary relationship to other NTR2 genes. Plant Science, 172(3), 621-631.

Yokoyama, A., Yamashino, T., Amano, Y.-I., Tajima, Y., Imamura, A., Sakakibara, H., & Mizuno, T. (2006). Type-B ARR Transcription Factors, ARR10 and ARR12, are

Implicated in Cytokinin-Mediated Regulation of Protoxylem Differentiation in Roots of Arabidopsis thaliana. Plant and Cell Physiology, 48(1), 84-96.

Yuan, L., Graff, L., Loqué, D., Kojima, S., Tsuchiya, Y. N., Takahashi, H., & von Wirén, N. (2009). AtAMT1;4, a Pollen-Specific High-Affinity Ammonium Transporter of the Plasma Membrane in Arabidopsis. Plant and Cell Physiology, 50(1), 13-25.

Yuan, L., Loqué, D., Kojima, S., Rauch, S., Ishiyama, K., Inoue, E., Takahashi, H., & von Wirén, N. (2007). The Organization of High-Affinity Ammonium Uptake in Arabidopsis Roots Depends on the Spatial Arrangement and Biochemical Properties of AMT1-Type Transporters. The Plant Cell, 19(8), 2636-2652.

Yuan, L., Loqué, D., Ye, F., Frommer, W. B., & von Wirén, N. (2007). Nitrogen-Dependent Posttranscriptional Regulation of the Ammonium Transporter AtAMT1;1. Plant Physiology, 143(2), 732-744.

Yunfei Wu, W. Y. J. W. H. Y. G. A. (2017). Transcription Factor OsDOF18 Controls Ammonium Uptake by Inducing Ammonium Transporters in Rice Roots. Molecules and Cells, 40(3), 178-185.

Zadoks, J. C., Chang, T. T., & Konzak, C. F. (1974). A decimal code for the growth stages of cereals. Weed Research, 14(6), 415-421.

Zetzsche, H., Friedt, W., & Ordon, F. (2020). Breeding progress for pathogen resistance is a second major driver for yield increase in German winter wheat at contrasting N levels. Scientific Reports, 10(1), 20374.

Zhang, L., Zhao, G., Jia, J., Liu, X., & Kong, X. (2012). Molecular characterization of 60 isolated wheat MYB genes and analysis of their expression during abiotic stress. Journal of Experimental Botany, 63(1), 203-214.

Zörb, C., Ludewig, U., & Hawkesford, M. J. (2018). Perspective on Wheat Yield and Quality with Reduced Nitrogen Supply. Trends in Plant Science, 23(11), 1029-1037.

6. Supplementary Figure and Table

Supplementary figure 1: Multiple sequence alignment of the AMT1.1 from adapted and unadapted lines with contrasting nitrogen uptake capacity. Multiple sequence alignment was performed by ClustalW from re-sequenced data. Black boxes indicate amino acid substitutions in more than 2 lines.

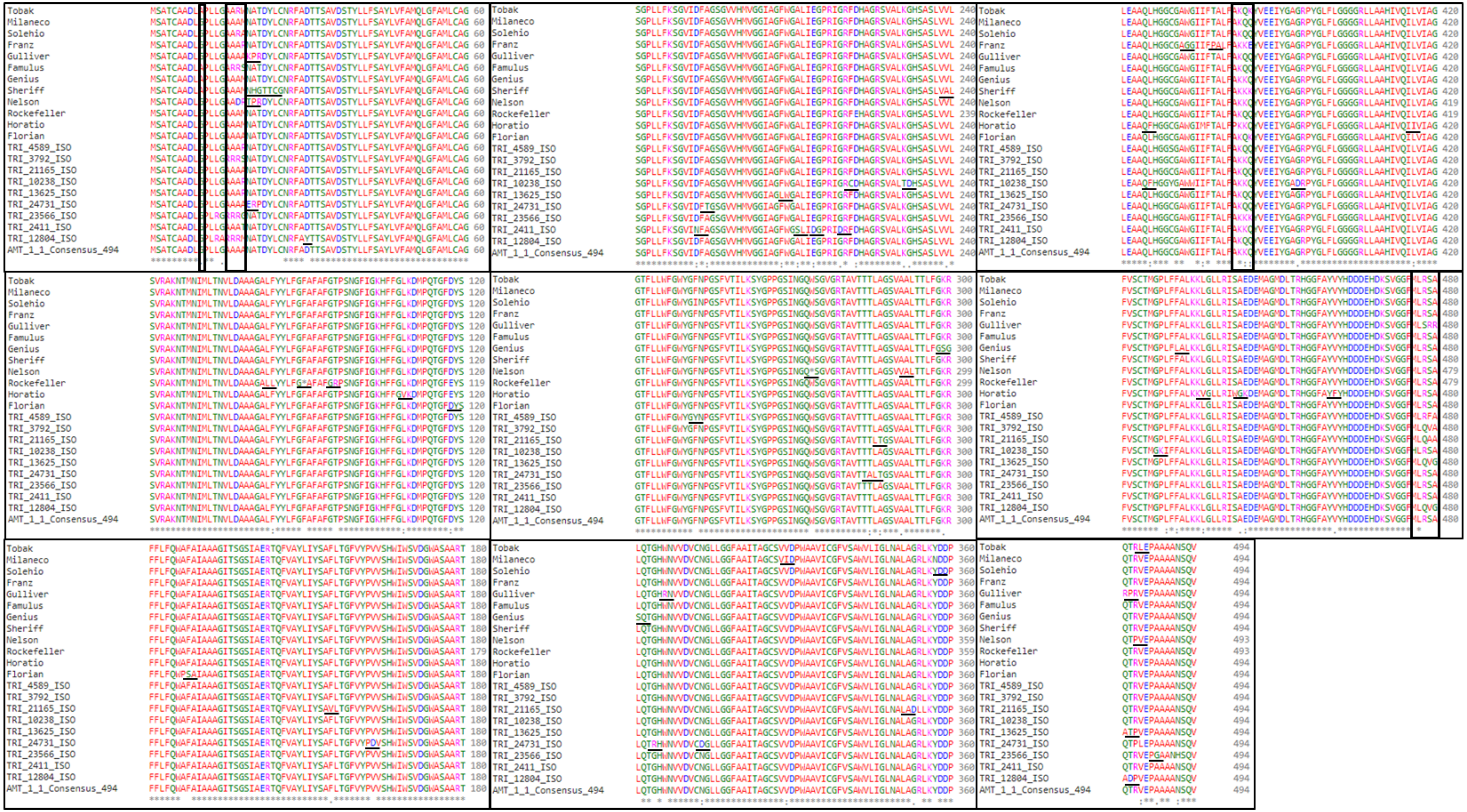

Supplementary figure 2*:* Multiple sequence alignment of the AMT1.2 from adapted and unadapted lines with contrasting nitrogen uptake capacity. Multiple sequence alignment was performed by ClustalW from re-sequenced data. Black boxes indicate amino acid substitutions in more than 2 lines.

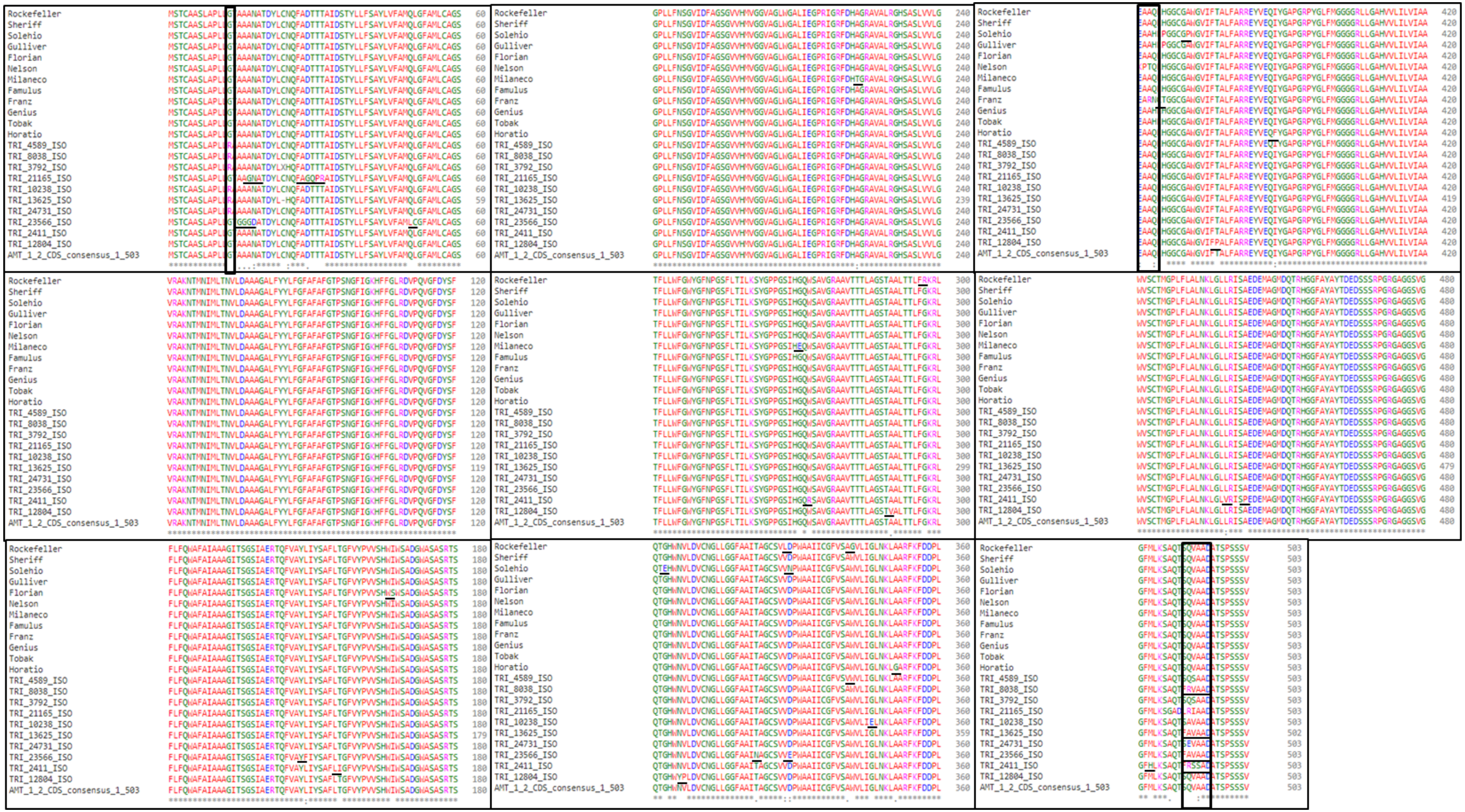

Supplementary figure 3: Multiple sequence alignment of the NRT1.1 from adapted and unadapted lines with contrasting nitrogen uptake capacity. Multiple sequence alignment was performed by ClustalW from re-sequenced data. Black boxes indicate amino acid substitutions in more than 2 lines.

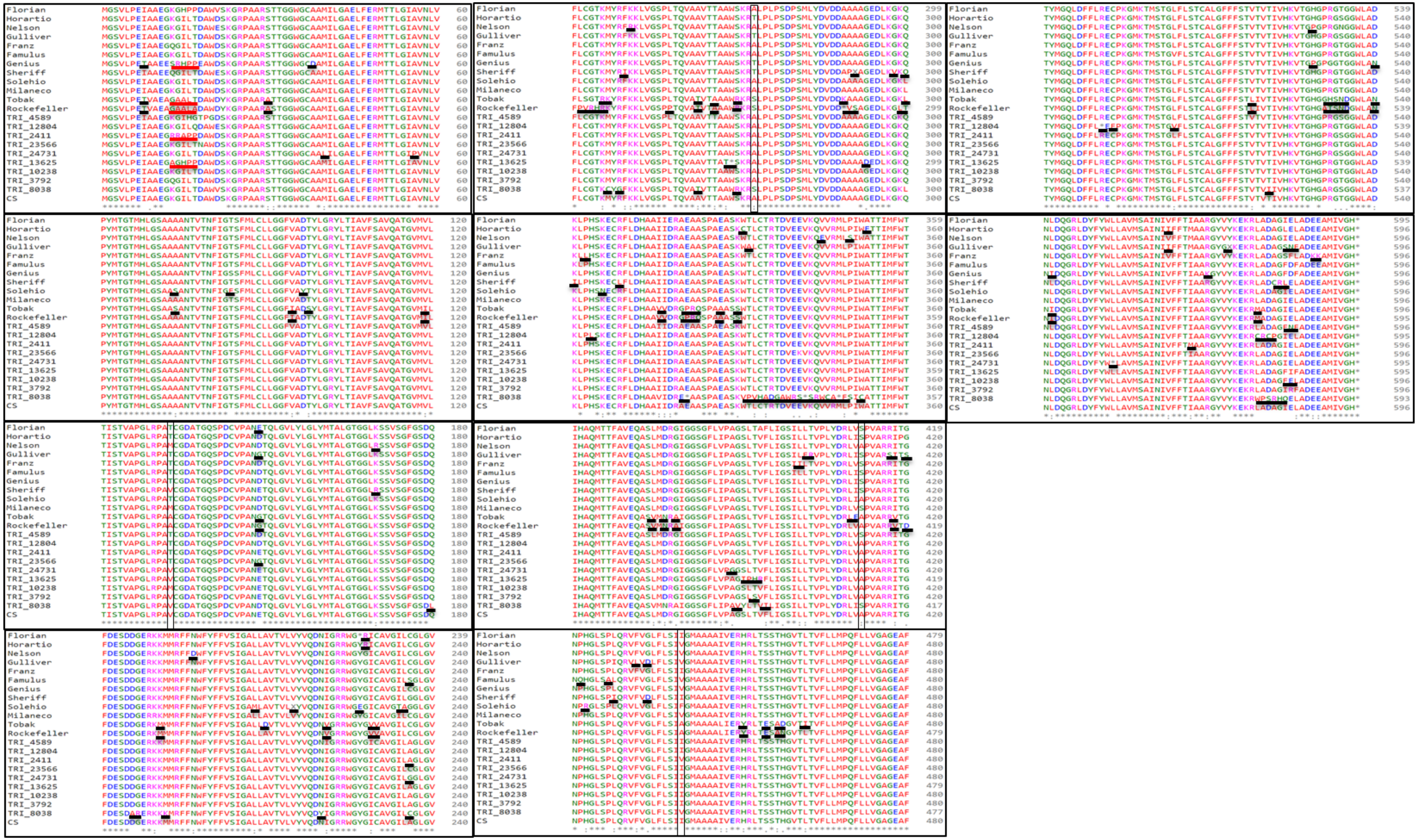

Supplementary figure 4: Multiple sequence alignment of AMT3.1 from two adapted lines with contrasting nitrogen uptake capacity (Rockefeller with low and Tobak with high capacity). Multiple sequence alignment was performed by ClustalW from PCR-generated amplicons. Black boxes indicate amino acid substitutions in more than 2 lines.

```
CS_TraesCS3A01G381600.1    MSTAADYNMSVGYSPNGIVVPPWLNKGDNAWQMIAATLVGLQSMPGLVILYGSIVKKKWA    60
CS_TraesCS3D01G374800.1    MSTAADYNMSVGYSPNGIVVPPWLNKGDNAWQMIAATLVGLQSMPGLVILYGSIVKKKWA    60
Rockefeller_AMT_3_1        MSTAADYNMSVGYSPNGIVVPPWLNKGDNAWQMIAATLVGLQSMPGLVILYGSIVKKKWA    60
Tobak_AMT_3_1              MSTAADYNMSVGYSPNGIVVPPWLNKGDNAWQMIAATLVGLQSMPGLVILYGSIVKKKWA    60
                           ************************************************************

CS_TraesCS3A01G381600.1    VNSAFMALYAFAAVWLCWVTWGYNMSFGHQLLPFWGKARPALGQKFLLMQAVLPESTHFF    120
CS_TraesCS3D01G374800.1    VNAAFMALYAFAAVWLCWVTWGYNMSFGHQLLPFWGKARPALGQKFLLMQAVLPESTHFF    120
Rockefeller_AMT_3_1        VNSAFMALYAFAAVWLCWVTWGYNMSFGHQLLPFWGKARPALGQKFLLMQAVLPESTHFF    120
Tobak_AMT_3_1              VNSAFMALYAFAAVWLCWVTWGYNMSFGHQLLPFWGKARPALGQKFLLMQAVLPESTHFF    120
                           **:*********************************************************

CS_TraesCS3A01G381600.1    KDGSQETAWINPNYPMATMVYFQCVFAAITLILLAGSLLGRMNIRAWMIFVPLWLTFSYT    180
CS_TraesCS3D01G374800.1    KDGSQETAWINPNYPMATMVYFQCVFAAITLILLAGSLLGRMNIRAWMIFVPLWLTFSYT    180
Rockefeller_AMT_3_1        KDGSQETAWINPNYPMATMVYFQCVFAAITLILLAGSLLGRMNIRAWMIFVPLWLTFSYT    180
Tobak_AMT_3_1              KDGSQETAWINPNYPMATMVYFQCVFAAITLILLAGSLLGRMNIRAWMIFVPLWLTFSYT    180
                           ************************************************************

CS_TraesCS3A01G381600.1    IGAFSLWGGGFLFQWGVMDYSGGYVIHLSSGIAGFTAAYWVGPRSTKDRERFPPNNVLLM    240
CS_TraesCS3D01G374800.1    IGAFSLWGGGFLFQWGVMDYSGGYVIHLSSGIAGFTAAYWVGPRSTKDRERFPPNNVLLM    240
Rockefeller_AMT_3_1        IGAFSLWGGGFLFQWGVMDYSGGYVIHLSSGIAGFTAAYWVGPRSTKDRERFPPNNVLLM    240
Tobak_AMT_3_1              IGAFSLWGGGFLFQWGVMDYSGGYVIHLSSGIAGFTAAYWVGPRSTKDRERFPPNNVLLM    240
                           ************************************************************

CS_TraesCS3A01G381600.1    LAGAGILWMGWAGFNGGDPYAANLDSSIAVLNTNICAATSLLVWTSLDVIFFKKPSVIGA    300
CS_TraesCS3D01G374800.1    LAGAGILWMGWAGFNGGDPYAANLDSSIAVLNTNICAATSLLVWTSLDVIFFKKPSVIGA    300
Rockefeller_AMT_3_1        LAGAGILWMGWAGFNGGDPYAANLDSSIAVLNTNICAATSLLVWTSLDVIFFKKPSVIGA    300
Tobak_AMT_3_1              LAGAGILWMGWAGFNGGDPYAANLDSSIAVLNTNICAATSLLVWTSLDVIFFKKPSVIGA    300
                           ************************************************************

CS_TraesCS3A01G381600.1    VQGMITGLVCITPGAGLVQGWAAIVMGVLSGSIPWFTMMVVHKRSKLLQRVDDTLGVFHT    360
CS_TraesCS3D01G374800.1    VQGMITGLVCITPGAGLVQGWAAIVMGILSGSIPWFTMMVVHKRSKLLQRVDDTLGVFHT    360
Rockefeller_AMT_3_1        VQGMITGLVCITPGAGLGQGWAAIVMGVLSGSIPWFTMMVVHKRSKLLQRVDDTLGVFHT    360
Tobak_AMT_3_1              VQGMITGLVCITPGAGLVQGWAAIVMGVLSGSIPWFTMMVVHKRSKLLQRVDDTLGVFHT    360
                           ***************** *********:********************************

CS_TraesCS3A01G381600.1    HAVAGFLGGVTTGLFAEPTLCSMFVPVTNSRGAFYGGSSGGMQLLKQVVGALFIVGWNVV    420
CS_TraesCS3D01G374800.1    HAVAGFLGGVTTGLFAEPTLCSMFVPVTNSRGAFYGGS-GGMQLLKQVVGALFIVGWNVV    419
Rockefeller_AMT_3_1        HAVAGFLGGVTTGLFAEPTLCSMFVPVTNSRGAFYGGSSGGMQLLKQVVGALFIVGWNVV    420
Tobak_AMT_3_1              HAVAGFLGGVTTGLFAEPTLCSMFVPVTNSRGAFYGGSSGGMQLLKQVVGALFIVGWNVV    420
                           ************************************** *********************

CS_TraesCS3A01G381600.1    VTSIICLVVRLIVPLRMPEEELVIGDDAVHGEEAYALWGDGEKYDSSKHGWYSDNETNQP    480
CS_TraesCS3D01G374800.1    VTSIICLVVRLIVPLRMPEEELVIGDDAVHGEEAYALWGDGEKYDSSKHGWYSDNETNQP    479
Rockefeller_AMT_3_1        VTSIICLVVRLIVPLRMPEEELVIGDDAVHGEEAYALWGDGEKYDSSKHGWYSDNETNQP    480
Tobak_AMT_3_1              VTSIICLVVRLIVPLRMPEEELVIGDDAVHGEEAYALWGDGEKYDSSKHGWYSDNETNQP    480
                           ************************************************************

CS_TraesCS3A01G381600.1    RNRAPSGVTQDV    492
CS_TraesCS3D01G374800.1    RNRAPSGVTQDV    491
Rockefeller_AMT_3_1        RNRAPSGVTQDV    492
Tobak_AMT_3_1              RNRAPSGVTQDV    492
                           ************
```

Supplementary figure 5: Multiple sequence alignment of AMT3.2 from two adapted lines with contrasting nitrogen uptake capacity (Rockefeller with low and Tobak with high capacity). Multiple sequence alignment was performed by ClustalW from PCR-generated amplicons. Black boxes indicate amino acid substitutions in more than 2 lines.

```
CS_TraesCS4A01G352900.1      MSVPVAYQGNTSAAVADWLNKGDNAWQLTASTLVGLMSVPGMVVLYGGVVKKKWAVNSAF    60
Rockefeller_AMT_3_2          MSVPVAYQGNTSAAVADWLNKGDNAWQLTASTLVGLMSVPGMVVLYGGVVKKKWAVNSAF    60
Tobak_AMT_3_2                MSVPVAYQGNTSAAVADWLNKGDNAWQLTASTLVGLMSVPGMVVLYGGVVKKKWAVNSAF    60
                             ************************************************************

CS_TraesCS4A01G352900.1      MALYAFAAVWICWVVWAYNMSFGEELLPFWGKAGPALDQAFLVGRASLPATAHYRADGSL    120
Rockefeller_AMT_3_2          MALYAFAAVWICWVVWAYNMSFGEELLPFWGKAGPALDQAFLVGRASLPATAHYRADGSL    120
Tobak_AMT_3_2                MALYAFAAVWICWVVWAYNMSFGEELLPFWGKAGPALDQAFLVGRASLPATAHYRADGSL    120
                             ************************************************************

CS_TraesCS4A01G352900.1      ETAMVEPYFPMATVVYFQCVFAAITLILVAGSLLGRMSFLAWMLFVPLWLTFSYTVGAFS    180
Rockefeller_AMT_3_2          ETAMVEPYFPMATVVYFQCVFAAITLILVAGSLLGRMSFLAWMLFVPLWLTFSYTVGAFS    180
Tobak_AMT_3_2                ETAMVEPYFPMATVVYFQCVFAAITLILVAGSLLGRMSFLAWMLFVPLWLTFSYTVGAFS    180
                             ************************************************************

CS_TraesCS4A01G352900.1      VWGGGFLFHWGVIDYCGGYVIHIPAGVAGFTAAYWVGPRTKKDRESFPPNNILFALTGAG    240
Rockefeller_AMT_3_2          VWGGGFLFHWGVIDYCGGYVIHIPAGVAGFTAAYWVGPRTKKDRESFPPNNILFALTGAG    240
Tobak_AMT_3_2                VWGVGFLFHWGVIDYCGGYVIHIPAGVAGFTAAYWVGPRTKKDRESFPPNNILFALTGAG    240
                             *** ********************************************************

CS_TraesCS4A01G352900.1      LLWMGWAGFNGGGPYAANVDSSMAILNTNICTAASLIVWTCLDAVFFKKPSVVGAVQAVI    300
Rockefeller_AMT_3_2          LLWMGWAGFNGGGPYAANVDSSMAILNTNICTAASLIVWTCLDAVFFKKPSVVGAVQAVI    300
Tobak_AMT_3_2                LLWMGWAGFNGGGPYAANVDSSMAILNTNICTAASLIVWTCLDAVFFKKPSVVGAVQAVI    300
                             ************************************************************

CS_TraesCS4A01G352900.1      TGLVCITPGAGVVQGWAALVMGVLAGSVPWYTMMVLHKRSKLLQRVDDTLGVIHTHGVAG    360
Rockefeller_AMT_3_2          TGLVCITPGAGVVQGWAALVMGVLAGSVPWYTMMVLHKRSKLLQRVDETLGVIHTHGVAG    360
Tobak_AMT_3_2                TGLVCITPGAGVVQGWAALVMGVLAGSVPWYTMMVLHKRSKLLQRVDDTLGVINTHGVAG    360
                             ***********************************************:*****:******

CS_TraesCS4A01G352900.1      LLGGVLTGLFAEPNLCNLFLPVTNSRGAFYGGNGGAQLGKQIAGALFVIGWNVVVTSIIC    420
Rockefeller_AMT_3_2          LLGGVLTGLFAEPNLCNLFLPVTNSRGAFYGGNGGAQLGKQIAGALFVIGWNVVVTSIIC    420
Tobak_AMT_3_2                LLGGVLTGLFAEPNLCNLFLPVTNSRGAFYGGNGGAQLGKQIAGALFVIGWNVVVTSIIC    420
                             ************************************************************

CS_TraesCS4A01G352900.1      VVIRLVVPLRMSEEKLAIGDDAVHGEEAYALWGDGEHYDDTKHGAAVVPV 470
Rockefeller_AMT_3_2          VVIRLVVPLRMSEEKLAIGDDAVHGEEAYALWGDGEHYDDTKHGAAVVPV 470
Tobak_AMT_3_2                VVIRLVVPLRMSEEKLAIGDDAVHGEEAYALWGDGEHYDDTKHGAAVVPV 470
                             **************************************************
```

Supplementary Table 1: GeneBank 2.0 project (website) 200 winter wheat (*Triticum aestivum* L.) lines acquisition date and country of origin.

Before the "Green Revolution lines" (Unadapted)					Elite (Adapted) lines			
Material	**ACQDATE**	**ORIGCTY**	**Rht1/Rht2**		**Material**	**ACQDATE**	**ORIGCTY**	**Rht1/Rht2**
TRI_316	1946	YUG	no		**Cellule**	2013	Hun	
TRI_355	1946	AUT	no		**Apache**	1998	Fra	
TRI_344	1946	AUT	no		**CF_99007**	NA	NA	
TRI_319	1946	GER	no		**Arezzo**	2007	Fra	
TRI_1340	1947	GER	no		**SUR_99934**	NA	NA	
TRI_1020	1947	GER	no		**Elixer**	2012	Deu	
TRI_2411	1950	AFG	no		**Franz**	1972	Fra	
TRI_5288	1957	CHN	no		**RGTReform**	2012	Fra	
TRI_4742	1957	CSK	no		**Tabasco**	2006	Deu	
TRI_1635	1946	GRC	no		**Buenno**	2007	Fra	
TRI_2422	1946	CHN	no		**Famulus**	1982	Aut	
TRI_1389	1946	USA	no		**Rumor**	2013	Deu	
TRI_233	1946	GER	no		**Patras**	2012	Deu	
TRI_1601	1947	GER	no		**Tuerkis**	2004	Deu	
TRI_2287	1947	GER	no		**JBAsano**	2008	Deu	
TRI_1156	1947	GER	no		**Glaucus**	2012	Deu	
TRI_1370	1947	POL	no		**KWSFerrum**	2010	Deu	
TRI_3393	1950	ALB	no		**Hermann**	2004	Deu	
TRI_3819	1951	GER	no		**Henrik**	2006	Fra	
TRI_4268	1951	ITA	no		**Genius**	2011	Deu	
TRI_4179	1953	NPL	no		**Mulan**	2007	Deu	
TRI_4822	1957	FRA	no		**Bonanza**	1969	USA	
TRI_7018	1957	CSK	no		**Benchmark**	2014	DNK	
TRI_5201	1960	AUT	no		**KWSMilaneco**	2010	Deu	
TRI_5095	1961	BGR	no		**Fidelius**	2008	Aut	
TRI_5085	1961	SUN	no		**Balaton**	2006	Aut	
TRI_5082	1961	SUN	no		**Tobak**	2011	Deu	
TRI_7004	1962	FRA	no		**Desamo**	2013	Deu	
TRI_6876	1962	FRA	no		**Johnny**	2014	Fra	
TRI_6747	1963	SUN	no		**Ponticus**	1993	USA	
TRI_6811	1963	CSK	no		**Meister**	2008	Fra	
TRI_7415	1964	NLD	no		**Atomic**	2012	Deu	
TRI_7707	1965	DEU	no		**KWSSalix**	2010	Deu	
TRI_7689	1965	DEU	no		**Horatio**	2012	GBR	
TRI_7706	1965	DEU	no		**Mescal**	NA	NA	
TRI_3792	1949	FRA	no		**Odyssee**	1998	GBR	
TRI_4526	1957	CHN	no		**Oakley**	2008	GBR	
TRI_4589	1959	URY	no		**Einstein**	2007	GBR	
TRI_5191	1960	EST	no		**Dialog**	1987	Rus	
TRI_7399	1964	JPN	no		**Bussard**	1990	Deu	
TRI_7711	1965	SUN	no		**Piko**	1994	Deu	
TRI_7887	1965	FRA	no		**KWSMontana**	2010	Deu	
TRI_8137	1966	YUG	no		**Produzent**	2015	Deu	
TRI_8134	1966	YUG	no		**Smaragd**	2007	Deu	
TRI_8070	1966	CHN	no		**PilgrimPZO**	2003	Deu	
TRI_8130	1966	DEU	no		**Solehio**	2008	Ita	
TRI_7861	1966	BGR	no		**Altigo**	2007	Fra	
TRI_8038	1966	CSK	no		**Ambello**	2010	Fra	
TRI_7874	1966	BGR	no		**Barok**	2009	Fra	
TRI_9361	1969	GER	no		**Boregar**	2007	Fra	

TRI_9798	1970	ROU	no		**Midas**	2008	Aut	
TRI_10699	1973	GRC	no		**Premio**	2007	Fra	
TRI_10924	1973	NPL	no		**Rubisko**	2011	Fra	
TRI_11221	1975	SVK	no		**Faustus**	1998	Deu	
TRI_11191	1975	SVK	no		**Norin**	2011	Deu	
TRI_12038	1978	SVK	no		**Partner**	2015	Deu	
TRI_12804	1980	POL	no		**Porthus**	2016	Deu	
TRI_13066	1981	ITA	no		**Zeppelin**	2011	Deu	
TRI_13326	1983	SVK	no		**Folklor**	2010	Fra	
TRI_13519	1983	ITA	no		**Kerubino**	2007	Deu	
TRI_13692	1983	AUT	no		**KWSBarny**	2010	Deu	
TRI_13625	1983	AUT	no		**KWSMaddox**	2010	Deu	
TRI_13672	1983	AUT	no		**Manitou**	1965	Deu	
TRI_14068	1984	ITA	no		**Sheriff**	2015	DNK	
TRI_13024	1984	ITA	no		**Apian**	2013	Deu	
TRI_14297	1984		no		**Bosporus**	2016	Deu	
TRI_14913	1985	POL	no		**Capone**	2013	Deu	
TRI_14887	1985	POL	no		**Dichter**	2014	Deu	
TRI_16434	1987	ITA	no		**Rockefeller**	2010	DNK	
TRI_16498	1987	ITA	no		**Toras**	2004	Deu	
TRI_17391	1994		no		**Julius**	2008	Deu	
TRI_19521	NA	SWE	no		**Adler**	1965	Deu	
TRI_19607	NA	USA	no		**Arktis**	2010	Deu	
TRI_19547	NA	AUT	no		**Chevalier**	2011	Deu	
TRI_19860	NA	USA	no		**Discus**	2007	Deu	
TRI_19818	NA		no		**Edgar**	2011	Deu	
TRI_20004	NA	IRN	no		**Florian**	1985	Fra	
TRI_19897	NA	AUT	no		**KWSLoft**	2012	Deu	
TRI_21059	NA	DEU	no		**KWSPius**	2010	Deu	
TRI_21165	NA		no		**Lear**	2007	GBR	
TRI_21125	NA		no		**Linus**	2011	Fra	
TRI_21181	NA	POL	no		**Manager**	2006	Fra	
TRI_21092	NA	PRT	no		**Matrix**	2007	Deu	
TRI_21395	NA		no		**Nelson**	2011	Deu	
TRI_21330	NA		no		**Orcas**	2002	Pol	
TRI_21352	NA	DEU	no		**Oxal**	2010	Deu	
TRI_22527	NA	DEU	no		**Pionier**	2013	Deu	
TRI_23428	NA	HUN	no		**Potenzial**	2006	Deu	
TRI_23525	NA	USA	no		**Primus**	2007	Deu	
TRI_23566	NA	TUR	no		**Sailor**	2010	Deu	
TRI_23572	NA	USA	no		**Schamane**	2005	Deu	
TRI_23924	NA	FRA	no		**Skagen**	2008	DNK	
TRI_24071	NA		no		**Sokrates**	1984	Deu	
TRI_24731	NA		no		**Sophytra**	2008	Deu	
TRI_25050	NA	DEU	no		**Tommi**	2002	Deu	
TRI_25079	NA	DEU	no		**Tuareg**	2005	Deu	
TRI_9806	1971	ROU	no		**Winnetou**	1972	Deu	
TRI_10238	1972	USA	no		**Slejpner**	1986	SWE	
TRI_25134	NA	DEU	no		**Gladiator**	2005	GBR	
TRI_28624	NA		no		**Gulliver**	2006	GBR	

Acknowledgements

First of all, special thanks go to Prof. Dr. Nicolaus von Wirén for giving me the opportunity to do my PhD thesis at his institute.

Thanks to Prof. Dr. Edgar Peiter and Prof. Dr. Gerd Patrick Bienert for accepting to evaluate my thesis.

Thanks to Prof. Dr. Jochen C. Reif and Dr. Albert Schulthess for providing the wheat seeds and the team member of Genbank2.0 framework.

Thanks to Dr. Britt Leps for her friendly nature and continuous help to solve all queries related to international documentation and many more.

I also thank Mrs. Barbara Kettig for always managing and continuous support to measure ^{15}N samples in time.

Of course very special thanks go to the lab people and their friendly nature and keeping the good atmosphere where I always enjoyed the work in the institute. Thanks to the technician: Annett, Jacqueline, Elis, Heike, Dagmar, Christina, Andrea. And Thanks to the PhDs and Postdoc of Molecular Plant Nutrition Lab for lively discussion over the scientific topic: Dr. Ricardo Giehl, Dr. Ying Liu, Dr. Zhaojun Liu, Dr. Zhongtao Jia, Dr. Markus Meier, Dr. Anja Hartmann, Dr. Desiree Bienert, Dr. Mohammad Hajirezaei, Dr. Sara Naseri Rad, Dr. Vanessa Paffrath, Esin, Geeisy, Nagarjuna, Mikel Rivero.

I also thank Elmarie secretary of my PhD supervisor, who always help us to solve the office related queries.

Eidesstattliche Erklärung/Declaration on oath

Hiermit versichere, dass ich die vorliegende Arbeit selbstständig verfasst habe, dass ich keine anderen Quellen und Hilfsmittel als die angegebenen benutzt habe und dass ich die Stellen der Arbeit, dieh ich anderen Werken - auch elektronischen Medien - dem Wortlaut oder Sinn nach entnommen habe, in jedem Fall unter Angabe der Quelle als Entlehnung kenntlich gemacht habe. Die Arbeit wurde bisher in gleicher oder ähnlicher Form keiner anderen Institution vorgelegt.

hereby declare that I have written the submitted thesis independently and without illicit assistance of third parties. I have not used any other reference and sources than those listed in the thesis or engaged any plagiarism. All references and sources used in the presented work are properly cited and acknowledged. Further, I declare that the presented work has not been previously submitted for the purpose of academic examination, either in its original or similar form, anywhere else.

Ort/Place. Datum/Date Unterschrift/Signature

Erklärung über bestehende Vorstrafen und anhängige Ermittlungsverfahren/Declaration concerning Criminal Record and Pending Investigations

Hiermit erkläre ich, dass ich weder vorbestraft bin, noch dass gegen mich Ermittlungsverfahren anhängig sind.

I hereby declare that I have no criminal record and that no preliminary investigations are pending against me.

Ort/Place, Datum/Date Unterschrift/Signature

Curriculum vitae

Bijal Krushnakant Thakkar

Date of Birth: 06.08.1988 in Kadi, India

Nationality: Indian

Education

2017 – 2021	PhD student at the Leibniz institute of plant genetics and crop research (IPK) Gatersleben. Enrolled at the Martin-Luther University Halle/Wittenberg, Germany, Institute of Biology Title of the PhD thesis: “Using genetic resources to identify favourable alleles for ammonium and nitrate transporter genes that contribute to nitrogen uptake efficiency in wheat”, Research group: Plant Molecular Nutrition, Supervised by Prof. Dr. Nicolaus von Wirén.
2010 – 2012	Master of Science - Bioinformatics, The Maharaja Sayaji Rao University of Baroda Title of Master thesis: “De novo hybrid genome assembly and annotation of a filamentous fungus (*Grosmannia clavigera*) using various NGS platform data.
2008 – 2010	Bachelor of Science – Biotechnology, Hemchandracharya North Gujarat University
2005 – 2007	Diploma in Pharmacy, Gujarat University

Work experience

2022 – till date	Bioinformatician (Postdoc) at University Ghent
2021 – 2022	Wissenschaftler Mitarbeiter (Bioinformatician) at Martin Luther University
2015 – 2017	Bioinformatician at Reliance Industries Limited, Mumbai, India.
2013 – 2015	Junior Research Fellow (Bioinformatics) at National Institute of Plant Genome Research (NIPGR), Applied Genomics Lab. New Delhi, India.
2012 -2013	Bioinformatician trainee at Xcelris Genomics Labs Pvt. Ltd. Ahmedabad, India.

Languages and Computer Skills

Languages	English, German (A2)

Computer Skills	MS Office (Word, Excel, Power Point), Adobe programs (Photoshop, Illustrater, Acrobate), statistical data analysing tools (SigmaStat, R)

Congresses, Supervising, and Fellowship awardee

- Poster presentation at German Conference on Bioinformatics 2021 (GCB), Sept – 2021.
- Poster presentation at Plant Science Student Conference 2019 Leibniz Institute of Plant Biochemistry (IPB) in Halle (Saale), Saxony-Anhalt.
- Poster presentation at PLANT 2030 Status Seminar meeting in Potsdam March-2019.
- Poster presentation at Plant Science Student Conference 2018 Leibniz Institute of Plant Genetics and Crop Plant Research in Gatersleben, Saxony-Anhalt.
- Supervising Master thesis experiments on Impact of nitrogen nutrition on root architectural traits and phytohormone levels in roots of modern wheat cultivars.
- Bioinformatics industrial training program organized by Biotechnology consortium India limited (BCIL - Fellowship awardee) duration of 6 months to conduct research at Xcelris Genomics Labs Pvt. Ltd, Ahmedabad, India.

Publications

- Nagesh Kancharla, Saakshi Jalali, J.V. Narasimham, Vinod Nair, Vijay Yepuri, Bijal Thakkar, VB Reddy, Boney Kuriakose, Neeta Madan, Arockiasamy S. De Novo Sequencing and Hybrid Assembly of the Biofuel Crop Jatropha curcas L.: Identification of Quantitative Trait Loci for Geminivirus Resistance (https://www.mdpi.com/2073-4425/10/1/69)
- Rohini Garg, Rama Shankar, Bijal Thakkar, Himabindu Kudapa, Lakshmanan Krishnamurthy, Nitin Mantri, Rajeev K. Varshney, Sabhyata Bhatia, Mukesh Jain. Transcriptome analyses reveal genotype and developmental stage-specific molecular responses to drought and salinity stresses in chickpea. (http://www.nature.com/articles/srep19228)
- Rohini Garg, Jyoti Agrawal, Bijal Thakkar. Genome wide discovery of G-quadruplex structures and their prevalence in distinct transcription factor binding sites in plant. (http://www.nature.com/articles/srep28211)

Bijal Thakkar